



Publicly Accessible Penn Dissertations

---


1-1-2016

# Caspase-8 in Cell Death and Inflammation

Naomi Hannah Philip

University of Pennsylvania, naomihp@gmail.com

Follow this and additional works at: <http://repository.upenn.edu/edissertations>

 Part of the [Allergy and Immunology Commons](#), [Immunology and Infectious Disease Commons](#), and the [Medical Immunology Commons](#)

---

## Recommended Citation

Philip, Naomi Hannah, "Caspase-8 in Cell Death and Inflammation" (2016). *Publicly Accessible Penn Dissertations*. 1945.  
<http://repository.upenn.edu/edissertations/1945>

This paper is posted at ScholarlyCommons. <http://repository.upenn.edu/edissertations/1945>  
For more information, please contact [libraryrepository@pobox.upenn.edu](mailto:libraryrepository@pobox.upenn.edu).

---

# Caspase-8 in Cell Death and Inflammation

## **Abstract**

Pathogenic organisms express virulence factors that can inhibit immune signaling pathways. Thus, the immune system is faced with the challenge of eliciting an effective inflammatory response to pathogens that actively suppress inflammation. The mechanisms that regulate this response are largely undefined. Here, I used the gram-negative extracellular bacterial pathogen *Yersinia pseudotuberculosis* to investigate anti-pathogen responses, as the *Yersinia* virulence factor YopJ blocks NF- $\kappa$ B and MAPK signaling, resulting in reduced cytokine production and target cell death. I set out to first, determine the molecular mechanism of *Yersinia*-mediated cell death and second, examine the impact of cell death on immune responses in vivo. Multiple caspases are activated during *Yersinia* infection, including caspase-1, which regulates pyroptosis, and caspase-3 and -8, which elicit apoptosis. I found that caspase-8 and receptor-interacting protein kinase-3 (RIPK3), RIPK1 and FADD are required for *Yersinia*-induced cell death. My studies also showed that caspase-8 is required for the activation of caspase-1 and -3 during *Yersinia* infection. Interestingly, mice lacking caspase-8 were severely susceptible to *Yersinia* infection and had defective pro-inflammatory cytokine production. These findings highlight a possible mechanism of immune defense that can overcome pathogen inhibition of cell-intrinsic pro-inflammatory immune responses.

Caspases are proteases that are best characterized for their abilities to regulate apoptotic or pyroptotic cell death programs, both of which are critical for the proper operation of the mammalian immune system. Within this family of proteins is caspase-8, which is unusual as it can promote both cell death, and inflammatory gene expression induced by Toll-like Receptors. How these two dichotomous outcomes occur independently of the other, is mysterious. Using mice that specifically ablate caspase-8 auto-processing, I have demonstrated that caspase-8 enzymatic, but not autoprocessing activity, mediates induction of inflammatory cytokines by a wide variety of TLR stimuli. Since uncleaved caspase-8 functions together with its homolog, cFLIP, our findings implicate the activity of a caspase-8/cFLIP heterodimer in control of inflammatory cytokines during microbial infection, and provide new mechanistic insight into how caspase-8 regulates gene expression.

## **Degree Type**

Dissertation

## **Degree Name**

Doctor of Philosophy (PhD)

## **Graduate Group**

Immunology

## **First Advisor**

Igor E. Brodsky

## **Keywords**

caspase-1, caspase-8, cell death, cytokines, TLR, *Yersinia*

---

**Subject Categories**

Allergy and Immunology | Immunology and Infectious Disease | Medical Immunology

# CASPASE-8 IN CELL DEATH AND INFLAMMATION

Naomi H. Philip

A DISSERTATION in  
Immunology

Presented to the Faculties of the University of Pennsylvania  
In Partial Fulfillment of the Requirements for the Degree of Doctor of Philosophy  
2016

Supervisor of Dissertation:

---

Igor E. Brodsky, Ph.D.  
Assistant Professor of Pathobiology

Graduate Group Chairperson:

---

David Michael Allman, Ph.D.  
Professor of Pathology and Laboratory Medicine

Dissertation Committee:

Taku Kambayashi, M.D., Ph.D., Assistant Professor of Pathology and Laboratory  
Medicine (Committee Chair)

Terri Marilyn Laufer, M.D., Associate Professor of Medicine

Jorge Henao-Mejia, M.D., Ph.D., Assistant Professor of Pathology and Laboratory  
Medicine

Michael J. May, Ph.D., Associate Professor of Biomedical Sciences

## **DEDICATION**

I would like to dedicate this work to my parents, Annie and Philip John, for encouraging me to pursue my interests, regardless of what they are, and giving me the opportunities to do so.

## ACKNOWLEDGEMENTS

I would like to acknowledge the following people for their contributions to this work:

Igor Brodsky, for his mentorship, sharing his enthusiasm for science, and constant advice and support.

My thesis committee: Taku Kambayashi, my committee chair, Michael May, Terri Laufer and Jorge Henao-Mejia for their continued guidance and support.

My labmates, Meghan Wynosky-Dolfi, Lance Peterson and Annelise Snyder for their incredibly helpful hands during long experiment days, friendship and for showing me the larger picture. Erin Zwack, Baofeng Hu, Alexandra DeLaney and Elisabet Bjanes for their feedback, energy and cheer.

Members of the Shin lab, especially Sunny Shin, Alan Copenhaver and Cierra Casson, for valuable feedback and discussions.

All members of the Hunter, Scott, Lopez, Beiting and Povelones labs for the many opportunities to talk about science, critical feedback on my research, and providing reagents and technical advice.

Our collaborators Christopher Dillon, Andrew Oberst and Doug Green for bones from knock-out mice, plasmids and scientific discussions that were central to one co-authored published paper and another manuscript in review.

Jorge Henao-Mejia and Sam McCright for helping design and generate two lines of knock-in mice using CRISPR/Cas9 that were essential for these studies.

Daniel Beiting, for teaching me the bioinformatics skills necessary to analyze and interpret my RNA-seq data.

The animal care technicians at Hill Pavilion, for looking after my mice.

The IGG program, for making graduate school a transformative experience.

Mary Taylor for her attention to details and exceptional organization skills.

My friends and family for their patience, understanding and encouragement.

Jonathan DeLong, for helping me clarify my thoughts, his enthusiasm and words of reason.

# ABSTRACT

## CASPASE-8 IN CELL DEATH AND INFLAMMATION

Naomi H. Philip

Igor E. Brodsky

Pathogenic organisms express virulence factors that can inhibit immune signaling pathways. Thus, the immune system is faced with the challenge of eliciting an effective inflammatory response to pathogens that actively suppress inflammation. The mechanisms that regulate this response are largely undefined. Here, I used the gram-negative extracellular bacterial pathogen *Yersinia pseudotuberculosis* to investigate anti-pathogen responses, as the *Yersinia* virulence factor YopJ blocks NF- $\kappa$ B and MAPK signaling, resulting in reduced cytokine production and target cell death. I set out to first, determine the molecular mechanism of *Yersinia*-mediated cell death and second, examine the impact of cell death on immune responses *in vivo*. Multiple caspases are activated during *Yersinia* infection, including caspase-1, which regulates pyroptosis, and caspase-3 and -8, which elicit apoptosis. I found that caspase-8 and receptor-interacting protein kinase-3 (RIPK3), RIPK1 and FADD are required for *Yersinia*-induced cell death. My studies also showed that caspase-8 is required for the activation of caspase-1 and -3 during *Yersinia* infection. Interestingly, mice lacking caspase-8 were severely susceptible to *Yersinia* infection and had defective pro-inflammatory cytokine production. These findings highlight a possible mechanism of immune defense that can overcome pathogen inhibition of cell-intrinsic pro-inflammatory immune responses.

Caspases are proteases that are best characterized for their abilities to regulate apoptotic or pyroptotic cell death programs, both of which are critical for the proper operation of the mammalian immune system. Within this family of proteins is caspase-8, which is unusual as it can promote both cell death, and inflammatory gene expression

induced by Toll-like Receptors. How these two dichotomous outcomes occur independently of the other, is mysterious. Using mice that specifically ablate caspase-8 auto-processing, I have demonstrated that caspase-8 enzymatic, but not autoprocessing activity, mediates induction of inflammatory cytokines by a wide variety of TLR stimuli. Since uncleaved caspase-8 functions together with its homolog, cFLIP, our findings implicate the activity of a caspase-8/cFLIP heterodimer in control of inflammatory cytokines during microbial infection, and provide new mechanistic insight into how caspase-8 regulates gene expression.



# TABLE OF CONTENTS

I. INTRODUCTION	1
Innate Immunity and Pattern Recognition	1
Pathways of cell death downstream of Pattern Recognition Receptors	3
<i>In vivo</i> consequences of cell death on inflammation	8
<i>Yersinia</i> as a useful model to study the mechanisms and role of death	10
Mechanisms of <i>Yersinia</i> -induced cell death	12
The role of YopJ-induced death in vivo	15
Caspase-8 and its homolog cFLIP	19
Regulation of caspase-8 activation	20
cFLIP is a key regulator of caspase-8 activation	22
Non-apoptotic roles for caspase-8 and cFLIP	23
II. MATERIALS AND METHODS	26
Mice	26
Generation of <i>Casp8</i> <sup>DA/DA</sup> mice	27
Animal Infections	27
Histopathology	28
Detection of germline single nucleotide variations (SNVs) and small insertion/ deletion (indels)	28
Flow cytometry	29
Cell Culture and Infection Conditions	30
Generation of immortalized cell line	32

Viral transductions	32
Western Blotting	32
Immunoprecipitations	33
Nuclear Extractions	33
Cell Death Assays	34
Caspase-8 Activity Assay	35
ELISAs and Luminex	35
RT-qPCR	36
Chromatin Immunoprecipitation	37
RNA-seq	38
Statistics	38
III. CASPASE-8 MEDIATES CASPASE-1 PROCESSING AND INNATE IMMUNE DEFENSE IN RESPONSE TO BACTERIAL BLOCKADE OF NF- $\kappa$ B AND MAPK SIGNALING	39
Background	39
Results	40
Discussion	47
IV. CELL-INTRINSIC ACTIVITY OF UNCLEAVED CASPASE-8 CONTROLS EXPRESSION OF TLR-INDUCED INFLAMMATORY RESPONSES	68
Background	68
Results	70

Discussion	80
V. CONCLUDING REMARKS	100
VI. APPENDIX I SUPPLEMENTARY CODE	117
VIII. BIBLIOGRAPHY	133

## LIST OF ILLUSTRATIONS

Figure 1. Different types of cell death have distinct impacts on inflammation	3
Figure 2. Mechanisms of cell death	5
Figure 3. Paradoxical roles for <i>Yersinia</i> YopJ/P in bacterial pathogenesis	17
Figure 4. Caspase-8 and cFLIP are homologs and mediate cell death and survival	20
Figure 5: Caspase-1 contributes to <i>Yersinia</i> -induced cell death and neither ASC, NLRC4, NLRP3, nor IFNAR are required for <i>Yersinia</i> -induced death	50
Figure 6. RIPK1 is required for <i>Yersinia</i> -induced caspase-1 processing and cell death	51
Figure 7. YopJ induces caspase-1 activation and cell death during <i>Yersinia</i> infection is TRIF-dependent and reduced cytokine production during <i>Yersinia</i> infection is not due to cell death	53
Figure 8. Caspase-1 activation and IL-18 secretion in response to <i>Yersinia</i> infection require caspase-8	54
Figure 9. Caspase-8, cFLIP and RIPK3 loci are identical in B6 and 129 mice	56
Figure 10. YopJ-dependent caspase-1 processing requires caspase-8	57
Figure 11. Active caspase-8 is required for <i>Yersinia</i> -induced caspase-1 processing	58
Figure 12. YopJ-deficient <i>Yersinia</i> -induces caspase-8-dependent caspase-1 processing in the presence of NF- $\kappa$ B and MAPK inhibitors	59
Figure 13. FADD is required for <i>Yersinia</i> -induced caspase-1 processing and cell death in the absence of RIPK3	60
Figure 14. <i>Ripk3<sup>-/-</sup>Casp8<sup>-/-</sup></i> and <i>Ripk3<sup>-/-</sup>Fadd<sup>-/-</sup></i> BMDMs have a defect in LPS priming	61
Figure 15. RIPK3/caspase-8-deficient mice are highly susceptible to <i>Yersinia</i> infection and have dysregulated cytokine production	62
Figure 16. RIPK3-deficient mice are not more susceptible to <i>Yersinia</i> infection and exhibit wild-type levels of IFN $\gamma$ production from adaptive cells	63
Figure 17. RIPK3/caspase-8-deficient mice experience faster bacterial dissemination and dysregulated cytokine production even at early time points during <i>Yersinia</i> infection	64
Figure 18. RIPK3/caspase-8-deficient mice survive $\Delta$ YopJ infection and partially recover intracellular cytokine production	66

Figure 19. <i>Yersinia</i> YopJ induces caspase-8/RIPK1/FADD dependent caspase-1 processing and cell death via inhibition of NF- $\kappa$ B and MAPK	67
Figure 20. <i>Ripk3<sup>-/-</sup>Casp8<sup>-/-</sup></i> inflammatory monocytes and neutrophils have a cell-intrinsic defect in IL-6 and TNF production	86
Figure 21. Caspase-8 plays a cell-intrinsic role in inflammatory cytokine production during bacterial infection <i>in vivo</i>	88
Figure 22. <i>Ripk3<sup>-/-</sup>Casp8<sup>-/-</sup></i> bone marrow-derived macrophages are defective in both MyD88 and TRIF-dependent cytokine production	89
Figure 23. Caspase-8 is not required for induction of NF- $\kappa$ B and MAPK signaling or p65 recruitment to inflammatory gene promoters	90
Figure 24. Caspase-8 deficiency does not impact the stability of caspase-8-dependent mRNAs	91
Figure 25. Caspase-8 regulates a functionally important subset of LPS-induced genes	92
Figure 26. Caspase-8-deficient cells exhibit wild-type levels of intracellular bacterial killing and responsiveness to TNF	93
Figure 27. Caspase-8 is not required for cytokine production in response to Sendai virus infection	94
Figure 28. Caspase-8 is required for optimal cytokine production in RIPK3-sufficient cells	95
Figure 29. Caspase-8 catalytic activity is required for maximal TLR-induced cytokine production	96
Figure 30. The control of TLR-induced gene expression by caspase-8 is independent of caspase-3 and -7	97
Figure 31. Caspase-8 self-cleavage is necessary for apoptosis but not cytokine responses	98
Figure 32. Cell-intrinsic activity of uncleaved caspase-8 controls TLR-induced gene expression	99
Figure 33. Inhibition of NF- $\kappa$ B signaling activates inflammatory caspase-8-dependent cell death	103
Figure 34. A model for cell-type specific requirements for caspase-8 self-processing activity in apoptosis and gene expression	112
Figure 35. Biological networks show properties of scale-free networks	116

# I. INTRODUCTION<sup>1</sup>

## Innate Immunity and Pattern Recognition

The innate immune system forms the first line of defense against non-self or pathogenic organisms. Cells of the myeloid lineage including macrophages, dendritic cells (DCs) and neutrophils express germline-encoded receptors, called pattern recognition receptors (PRRs) that recognize a vast range of ligands including lipoproteins, polysaccharides, nucleic acids, conserved microbial proteins and carbohydrate structures (2). PRR signaling can induce a vast array of changes in the cell from activating gene expression of pro-survival and inflammatory proteins to eliciting cell death. Toll-like receptors (TLRs) and C-type lectin receptors (CLRs) are membrane-bound receptors and are situated on the plasma membrane or on endosomes, enabling detection of extracellular organisms and microbes that are internalized or shuttled to endocytic compartments. The cytoplasm is patrolled by nucleotide-binding domain and leucine rich repeat containing proteins (NLRs), AIM-2 like receptors (ALRs) and RIG-I-like receptors (RLRs). RLRs recognize nucleic acids and NLRs sense a range of factors including microbial products as well as disturbances in cytosolic homeostasis (NLRs are discussed in more detail in the cell death section). There are a number of mechanisms that allow for preferential detection of microbial versus host-derived PRR ligands, including sub-cellular localization and cleavage of TLR ectodomains for activation.

TLR, RLR and CLR ligation trigger MAPK, NF- $\kappa$ B and IRF signaling that activate anti-microbial programs and initiate adaptive immune responses (3). There are 13 mammalian TLRs (10 in humans and 12 in mice) that are composed of an

---

<sup>1</sup> This section contains excerpts from 1. Philip NH & Brodsky IE (2012) Cell death programs in *Yersinia* immunity and pathogenesis. *Front Cell Infect Microbiol* 2:149.

ectodomain, containing leucine-rich repeats, and a cytosolic Toll-IL-1 receptor (TIR) domain (4). Sub-cellular localization of TLRs by sorting adaptors, regulates signaling outcomes. For instance, when TLR4 binds lipopolysaccharide (LPS), TLR4 is shuttled to lipid rafts by the sorting adaptor CD14 and this initiates signaling through the adaptor MyD88. Likewise, CD14-mediated endocytosis is necessary to activate the second TLR4 signaling pathway, via the adaptor TRIF (5). When MyD88 is recruited to TLR4, IL-1R1-associated protein kinase 4 (IRAK4), IRAK2 and IRAK1 form a complex termed the myddosome (6, 7). The myddosome induces TNFR-associated factor 6 (TRAF6) to activate the TAK1 complex, which phosphorylates I $\kappa$ B kinase- $\beta$  (IKK $\beta$ ) and MAPKs. The IKK $\beta$  complex phosphorylates I $\kappa$ B $\alpha$ , triggering proteasomal degradation of I $\kappa$ B $\alpha$ , which mobilizes NF- $\kappa$ B to the nucleus. MAPK kinases (MKKs) phosphorylate p38 kinases, Jun kinases (JNK) and extracellular signal related kinases (ERK), resulting in nuclear translocation and gene expression. Along with contributing to late-phase NF- $\kappa$ B and MAPK activation, TRIF recruits TRAF3, which activates the phosphorylation of IRF3 through TANK-binding kinase 1 (TBK1) and IKKi, inducing type I IFN. TLR signaling modulates the expression of many genes, including those involved in cell survival, pro-inflammatory cytokine and anti-microbial peptide production. In this way, innate immune signaling pathways induce important changes in the host cell that are essential for activating anti-pathogen responses.

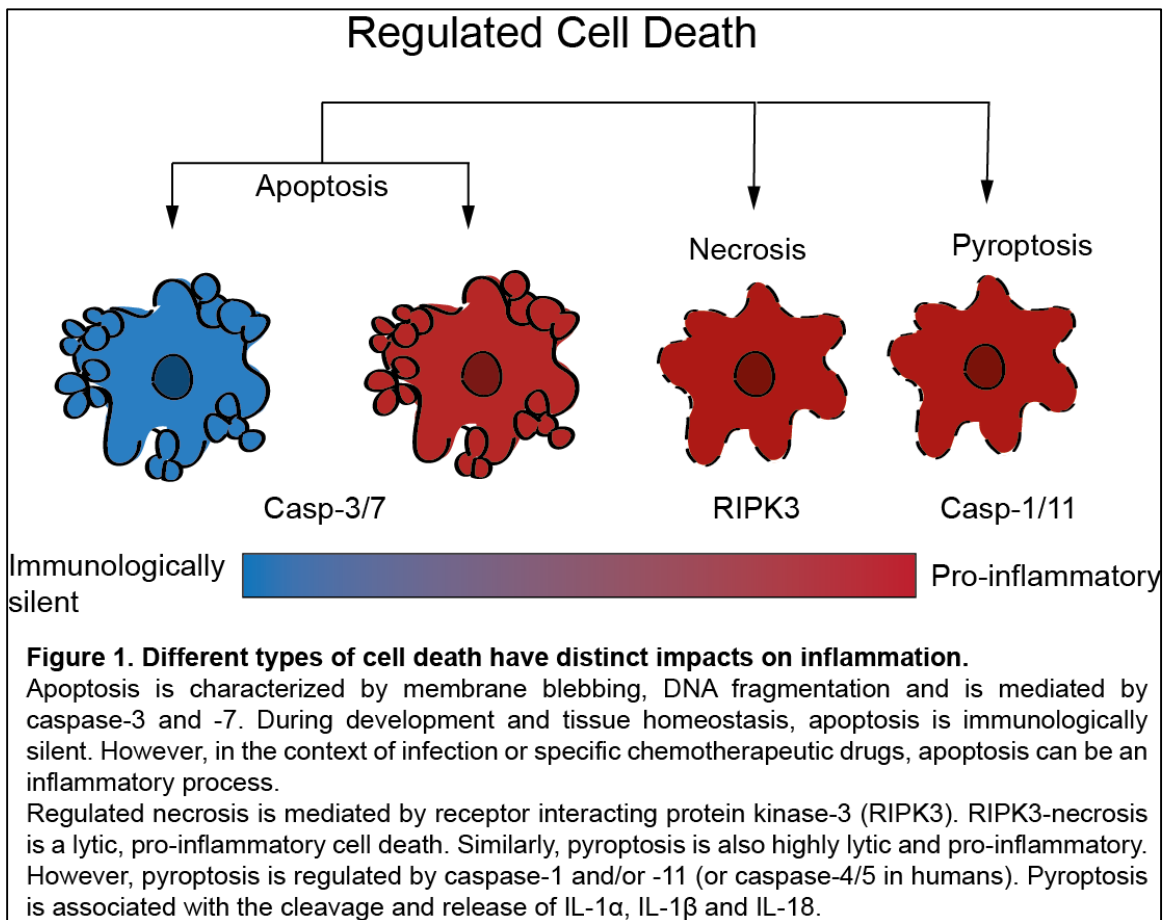
Cell survival, proliferation and gene expression are important anti-pathogen responses. However, regulated cell death is an alternative outcome that can be either pathologic or protective to the host. The next sections will highlight key pathways of cell death and the impact of cell death on the immune response.

## Pathways of cell death downstream of Pattern Recognition Receptors

From plants to mammals, cell death is an evolutionarily conserved host cell response to pathogens. Here, I discuss the three major types of cell death that are activated in mammalian cells, apoptosis, necroptosis and pyroptosis.

Cell death plays a key role in maintaining tissue homeostasis by eliminating stressed, damaged, and infected cells. Distinct cell death pathways that result in distinct downstream outcomes are induced under different circumstances (8-11) (Figure 1).

Apoptosis is traditionally viewed as an immunomodulatory form of cell death



characterized by cell shrinkage, while necrosis and pyroptosis are pro-inflammatory forms of death associated with rapid loss of membrane integrity and release of intracellular contents. While apoptosis during development is anti-inflammatory,



apoptotic cell death during infection has been associated with inflammation (12). How these distinct cell death pathways contribute to host defense responses remains an important unanswered question.

There are two major pathways that mediate apoptosis, intrinsic and extrinsic (Figure 2). Intrinsic apoptosis is mediated by caspase-9, which is activated upon release of cytochrome c and other apoptotic factors from the mitochondria. Bid and Bax, members of the Bcl-2 family of proteins, form pores in the mitochondria, which compromises its permeability. Caspase-9 is activated in a complex, termed the apoptosome resulting in activation of caspase-3 and -7 (13). Receptors of the TNFR, Fas and TLR families, also called death receptors, regulate extrinsic apoptosis and pro-survival signaling. Extrinsic cell death programs that are activated through TNFR1/2 are most well-characterized and have informed much of the work in the field. Here, I will focus on the pathways of cell death that are activated downstream of TLRs. TLR3 and TLR4 engage extrinsic cell death in the presence of pharmacological or microbial inhibitors of NF- $\kappa$ B (14-16). TLR3- or TLR4-dependent apoptosis requires caspase-8 or caspase-10, members of the cysteine protease family of caspases. Upon receptor ligation, caspase-8 is recruited to TRIF by RIPK1 via RIP homotypic interaction motifs (RHIM) (17). RIPK1 can bind FADD through shared death domains (DD) and FADD can engage caspase-8 via their respective death effector domains (DED), resulting in assembly of a RIPK1-FADD-caspase-8 Death Inducing Signaling Complex (DISC) or Complex II (18, 19). In this complex, caspase-8 undergoes dimerization and autoprocessing, which stabilizes the active enzyme and activates its apoptotic function (20). Since Bid is also a target of caspase-8, there are some cells where intrinsic and extrinsic apoptosis are linked (21).

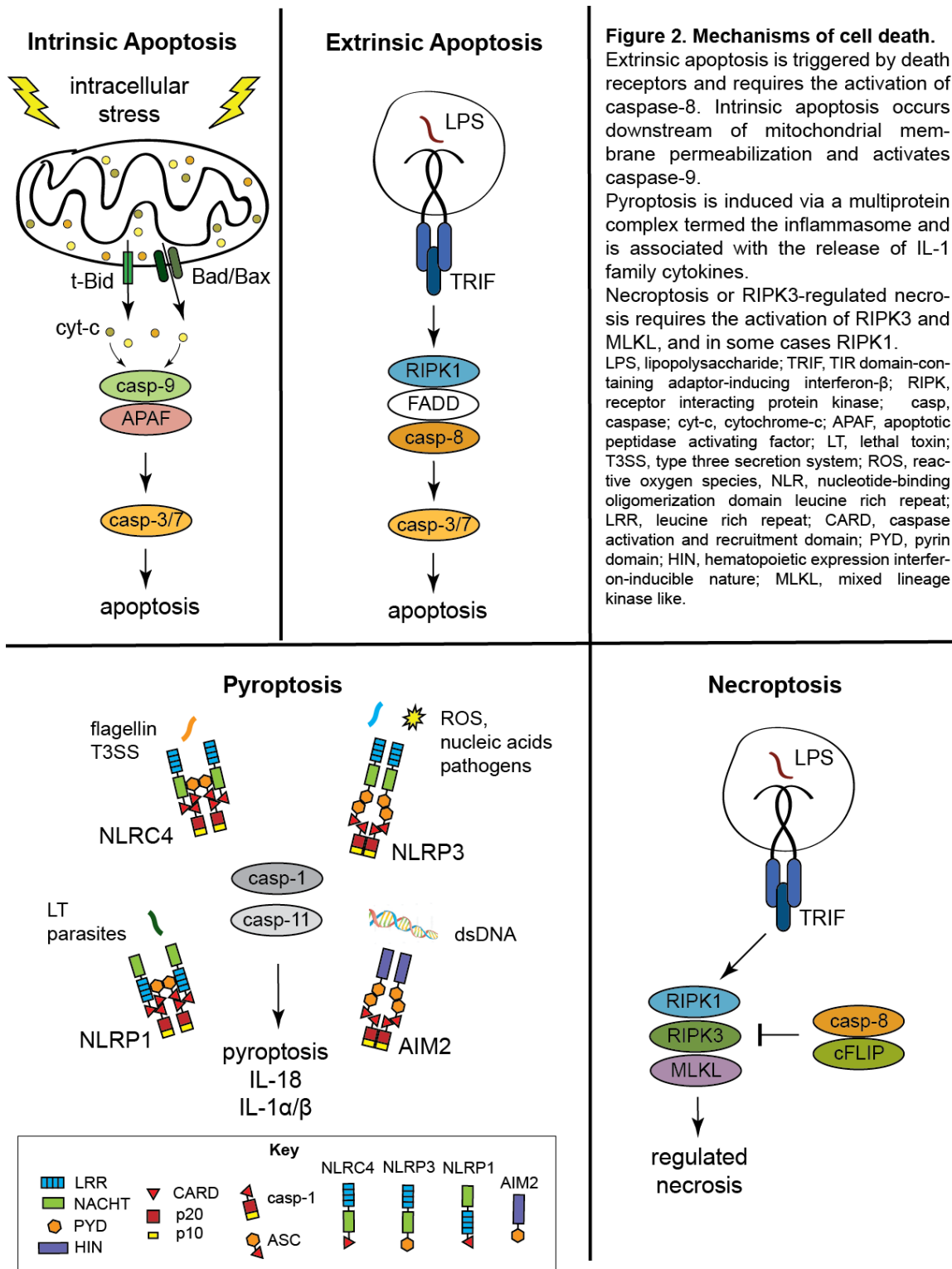


**Figure 2. Mechanisms of cell death.** Extrinsic apoptosis is triggered by death receptors and requires the activation of caspase-8. Intrinsic apoptosis occurs downstream of mitochondrial membrane permeabilization and activates caspase-9. Pyroptosis is induced via a multiprotein complex termed the inflammasome and is associated with the release of IL-1 family cytokines. Necroptosis or RIPK3-regulated necrosis requires the activation of RIPK3 and MLKL, and in some cases RIPK1. LPS, lipopolysaccharide; TRIF, TIR domain-containing adaptor-inducing interferon-β; RIPK, receptor interacting protein kinase; casp, caspase; cyt-c, cytochrome-c; APAF, apoptotic peptidase activating factor; LT, lethal toxin; T3SS, type three secretion system; ROS, reactive oxygen species, NLR, nucleotide-binding oligomerization domain leucine rich repeat; LRR, leucine rich repeat; CARD, caspase activation and recruitment domain; PYD, pyrin domain; HIN, hematopoietic expression interferon-inducible nature; MLKL, mixed lineage kinase like.

TLR3 and -4 can also mediate a caspase-independent cell death pathway, termed receptor-interacting serine/threonine protein kinase-3 (RIPK3)-dependent necroptosis (22-24) (Figure 2). During homeostasis, the pro-survival activity of caspase-8, mediated by heterodimers of caspase-8 and its catalytically inactive homologue, cFLIP represses RIPK3. However, inhibition of caspase-8 activity or deletion of caspase-8 derepresses RIPK3-dependent necroptosis (25, 26). Consistent with this, caspase-8- and FADD-deficient mice are embryonic lethal, due to activation of RIPK3-dependent necrosis during development and are protected by RIPK3 deficiency (27) (28) (25, 26, 29-32). RIPK3-regulated necrosis requires the pseudokinase Mixed Lineage Kinase Like (MLKL) (33-35), and with RIPK1 and RIPK3 forms a complex termed the necrosome. RIPK3 phosphorylates MLKL, which causes plasma membrane permeability. Current studies offer two models: the first model suggests that MLKL binds negatively-charged phosphatidylinositol groups on the plasma membrane inducing pore formation (36-38), and the second model proposes that MLKL localization to the plasma membrane regulates ion channels, resulting in osmolysis (39, 40).

Pyroptosis is a caspase-dependent pathway of pro-inflammatory cell death that requires the formation of a multiprotein complex, termed the inflammasome (41, 42) (Figure 2). The assembly of NLRs that contain a leucine-rich-repeat (LRR) sensor domain, a nucleotide-binding oligomerization domain (NOD), and a pyrin domain- (PYD) or caspase activation and recruitment domain- (CARD) containing signaling domain (43), with caspase-1 or -11 (caspase-4 and -5 in humans) and an adaptor protein such as ASC that bridges the NLR with the caspase creates the inflammasome structure. Inflammasomes form a platform for the autoprocessing and activation of the cysteine proteases caspase-1 and caspase-11, resulting in caspase-dependent secretion of IL-1 $\alpha$ , IL-1 $\beta$  and IL-18, and a caspase-1/11-dependent cell death termed pyroptosis (41,

44-48). Inflammasome activation is thought to require two signals, the first signal induces the expression of certain inflammasome components and cytokines of the IL-1 family, and the second signal activates assembly of the multiprotein complex (41, 42). The precise structural changes that occur during oligomerization and caspase activation are not fully elucidated, but studies suggest the process is similar to the proximity-induced cleavage model of caspase-8/9 activation.

Inflammasomes are characterized by the class of NLR or sensor and the type of signal. They are generally classified as the canonical caspase-1 inflammasome and non-canonical caspase-11 inflammasome. The NLRP3, NLRC4 (NLR family, CARD containing 4) and AIM2 (absent in melanoma 2) inflammasomes are most well characterized. NLRC4, together with NAIPs (NLR family, apoptosis inhibitory proteins) responds to intracellular flagellin, and components of type III and IV secretion systems of gram-negative bacteria (49-52). Interestingly, NLRP3 has a wide range of agonists including bacterial, fungal and viral proteins or nucleic acids that gain access to the cytosol, protein aggregates, DAMPs such as ATP, pore-forming toxins, as well as crystals (41). As there is no unifying set of signals or outcomes associated with the NLRP3 inflammasome, multiple hypotheses have been proposed for the mechanism of NLRP3 activation (41). Similarly, the NLRP1 inflammasome does not appear to be activated via a ligand-receptor mode (53). Murine NLRP1b is required for detecting *Bacillus anthracis* lethal toxin (54) and *Toxoplasma gondii* (55). Since inflammasome activation results in IL-18 and IL-1 release, inflammasomes indirectly mediate IFN $\gamma$  production from lymphocytes. For instance, AIM2, which senses double-stranded DNA, contributes to NK-cell-dependent IFN $\gamma$  production against the DNA virus, cytomegalovirus (CMV) (56). Finally, the NLRP6 and NLRP12 inflammasomes, which are among the least well-defined, are implicated in intestinal disease and anti-microbial

defense respectively, but the precise stimuli that activate them are unknown (57-61). Despite differences in the biochemical mechanisms of activation, NLR-dependent inflammasomes induce caspase-1/11-mediated pyroptosis and release of the IL-1 family of cytokines.

The mechanism of pyroptosis and precise contributions of caspase-1 and caspase-11 to caspase-1/11 inflammasome activation are not clear. However, it is now appreciated that caspase-1 and -11 have stimulus-dependent contributions to pyroptosis and IL-1 release. For gram-negative pathogens such as *Escherichia coli*, *Vibrio cholera* and *Citrobacter rodentium*, pyroptosis requires caspase-11, and IL-1 $\beta$  and IL-18 release require caspase-1 (46, 62). Furthermore, caspase-11, but not caspase-1, IL-1 $\beta$  or IL-18, is a crucial mediator of endotoxic shock, providing further evidence for individual roles for these caspases (46, 63). Caspase-11 was subsequently shown to be a sensor for the hexa-acylated lipid A portion of LPS (64, 65), which explains prior studies that implicated caspase-11 in inflammasome-dependent responses to gram-negative bacteria that access the host cytosol (44, 62, 66-69).

### ***In vivo* consequences of cell death on inflammation**

Every second, millions of cells undergo cell death and are removed in a manner that generates minimal inflammation. Conversely, cell death in the context of infection or certain cancer therapeutics can be highly inflammatory. For sessile organisms lacking circulatory systems, such as plants, cell death provides a cell-autonomous host defense response (70). In mammalian cells, immunogenic cell death is characterized by certain hallmarks, such as the release of damage-associated molecular patterns (DAMPs), which include HMGB1 (high mobility group box 1), IL-33 and ATP. Cell death has also been proposed to enhance cross-presentation, whereby extracellular antigens are

phagocytosed and presented on major histocompatibility complex I (MHC I) to T cells. But how cell death affects cross presentation is poorly understood. Moreover, the precise requirements for individual DAMPs in inflammatory responses are not known. Finally, the factors that determine whether cell death is beneficial or pathological to the host are not well-defined.

Apoptotic cell death is generally viewed as non-inflammatory or immunosuppressive. While this is true during development and tissue homeostasis, apoptotic cell death can also promote immune responses. For example, anthracyclin treatment of tumor cells causes apoptosis that leads to exposure of calreticulin on the surface, which acts as a signal to induce phagocytosis and promote anti-tumor T cell responses *in vivo* (71, 72). Similarly, the dendritic cell C-type lectin receptor, DNGR-1, can promote cross-presentation of apoptotic cell antigens by CD8 $\alpha^+$  DCs to CD8 $^+$  T cells in both non-infectious and infectious settings (73, 74). HMGB1 release by dying tumor cells is recognized by TLR4 on DCs and enhances antigen presentation (75). Finally, DCs that phagocytose bacterially-infected apoptotic cells produce both the immunoregulatory cytokine TGF $\beta$ , and the inflammatory cytokine IL-6, which together promote the differentiation of naïve CD4 $^+$  T cells into T<sub>H</sub>17 cells (12). These cells play a critical role in anti-bacterial immunity and pathological inflammatory responses at mucosal barrier surfaces (76-78). Together, these studies argue that under specific circumstances, namely microbial infection or stimuli that promote DAMP release, apoptosis can be immunostimulatory (Figure 1).

Caspase-1/11-mediated pyroptosis is inherently lytic, but is also associated with the release of pro-inflammatory cytokines. Therefore, recent work in the field has stressed the importance of distinguishing the role of cell death on inflammation independently of inflammatory gene expression. Indeed, caspase-1-dependent

pyroptosis can promote antibacterial responses against intracellular pathogens independent of production of the caspase-1 dependent cytokines IL-1 $\beta$  and IL-18 (79). Consistently, caspase-1-deficient mice are resistant to LPS-induced septic shock, while IL-1-deficient mice are still susceptible, suggesting that pyroptosis is a major driver of inflammatory disease (46). In murine models of spontaneous cryopyrin-associated periodic syndromes (CAPS), where missense mutations in NLRP3 induce high systemic levels of IL-1 $\beta$  and IL-18, deficiency in IL-1R and IL-18 did not completely abrogate disease (80). However, mice lacking caspase-1 were protected from CAPS, suggesting a role for cytokine-independent, likely pyroptosis-mediated pathology.

RIPK3-regulated necrosis is also lytic in nature, implying necroptosis can generate local and systemic inflammation. In fact, RIPK3-dependent necrosis promotes control of *Vaccinia* and CMV viral infections (81). Furthermore, pyroptosis and programmed necrosis may promote pathologies that are not directly associated with microbial infections, such as gout, experimental autoimmune encephalomyelitis and intestinal barrier function (32, 48, 82). Using a reductionist approach, Yatim and colleagues utilized a drug-inducible cell death system, to trigger cell death in the absence of any other source of inflammation (81, 83). The authors demonstrated that RIPK3/RIPK1-dependent death, activated RIPK1 signaling within necroptotic cells, which was necessary for cross-priming CD8<sup>+</sup> T cells. However, how different cell death pathways contribute to inflammation, and orchestrate activation of innate and adaptive cells during bacterial infections remains a major unresolved question for understanding of anti-bacterial immunity.

### ***Yersinia* as a useful model to study the mechanisms and role of death**

Cell death is an evolutionarily conserved immune response to microbial infection, as it prevents pathogen replication and can provide pro-inflammatory signals necessary

for an effective immune response. Infection with the pathogenic *Yersinia* species elicits host cell death. There are three pathogenic species of *Yersinia*; *Y. pestis*, *Y. pseudotuberculosis*, and *Y. enterocolitica* share a virulence plasmid encoding a conserved Type Three Secretion System (T3SS) and virulence factors, known as *Yersinia* outer proteins (Yops) (84). T3SS-mediated injection of Yops into infected cells enables *Yersinia* to modulate host signaling pathways and suppress innate and adaptive immunity (85). YopJ of *Y. pestis* and *Y. pseudotuberculosis*, termed YopP in *Y. enterocolitica*, blocks NF- $\kappa$ B and MAPK signaling, thereby inhibiting cytokine production and triggering death of *Yersinia*-infected cells (86-88). Among the sequenced strains of pathogenic *Yersinia*, YopJ and YopP share 95-98% identity across the full length of the protein sequence, but key polymorphisms have been identified that impact both enzymatic activity and translocation of the protein, which affect the outcome of *Yersinia* infection (89-92).

Interestingly, *Yersinia*-infected cells can exhibit features of apoptosis, pyroptosis, or necrosis, depending on the relative amounts of host cell death regulators and *Yersinia* virulence factors (87, 88, 93-96). However, whether *Yersinia*-induced cell death promotes host defense or bacterial virulence during infection *in vivo* remains unclear. A number of studies have revealed key players in cell death pathways during *Yersinia* infection, providing some insight into mechanisms of *Yersinia*-induced cell death, but very little is known about the nature and role of *Yersinia* death *in vivo*. *Yersinia* is thought to primarily replicate as an extracellular pathogen that evades phagocytosis by neutrophils and monocytic cells in lymphoid tissues. Cell death has therefore been viewed as a strategy for *Yersinia* to eliminate host phagocytes (97). However, several studies suggest that host cell death during *Yersinia* infection may promote anti-*Yersinia* immunity, although the precise mechanisms are poorly understood (89, 98, 99). An



alternative possibility is that if *Yersinia* are capable of intracellular replication *in vivo*, host cell death may eliminate a replicative niche (100). Since cell death is a characteristic feature of *Yersinia* infection both *in vitro* and *in vivo*, and because *Yersinia* is genetically tractable, it is a powerful tool to study the mechanisms and consequences of cell death.

### **Mechanisms of *Yersinia*-induced cell death**

Early studies observed that macrophages and dendritic cells infected by *Yersinia* exhibit characteristics of apoptotic cells, specifically membrane blebbing, nuclear condensation, DNA fragmentation, and formation of large cytoplasmic vacuoles (87, 95). Apoptosis has been viewed as immunologically silent, but growing evidence suggests that during infection, apoptosis may promote inflammatory responses (8, 12). Furthermore, apoptotic cells can be phagocytosed, and their associated microbial antigens used to prime CD8<sup>+</sup> T cell responses (101). Therefore, while cell death during *Yersinia* infection is thought to be apoptotic, it may not be immunologically silent. Below, I discuss the nature of *Yersinia*-induced cell death and its contribution to bacterial virulence or host defense.

The cysteine protease YopJ induces cell death during *Yersinia* infection (86, 87, 97). YopJ is a potent inhibitor of MAPK and NF- $\kappa$ B signaling, and blocks proinflammatory cytokine production by infected cells (88, 94, 102, 103) (Figure 3). YopJ has been reported to function as a ubiquitin-like protein protease (102), and as a deubiquitinase (104, 105). YopJ is also reported to be an acyl transferase that acetylates serine residues in the activation loop of MKK family proteins and prevents their activation (106, 107). The sensitivity of NF- $\kappa$ B signaling pathways to YopJ-mediated inhibition occurs at the level of TAK1 and is evolutionarily conserved from *Drosophila* to mammalian cells (108).

Macrophages stimulated with LPS in the presence of inhibitors of protein synthesis or components of NF- $\kappa$ B signaling undergo cell death (15, 109). Consistent with this, *Tlr4*<sup>-/-</sup> macrophages are resistant to YopJ-dependent apoptosis, as are cells deficient in the TLR3/4 adaptor TRIF, but not MyD88 (14-16). Moreover, infection of dendritic cells with *Yersinia* leads to the formation of a FADD/caspase-8/RIP1 complex and caspase-8 activation (110). Cytochrome-c release and caspase-9 cleavage were observed downstream of *Yersinia*-induced cleavage of the pro-apoptotic Bid protein (111). Additionally, treatment with broad-spectrum caspase inhibitors reduced the number of TUNEL<sup>+</sup> cells during *Yersinia* infection, suggesting *Yersinia* induces caspase-dependent cell death (97, 111). Whether these proteins are required for *Yersinia*-induced cell death is unclear. Interestingly, *Yersinia* infection of dendritic cells exposed to a pan-caspase inhibitor still induced a cell death that is presumably caspase-independent and exhibited morphological features of necrosis (112), likely RIPK3-regulated necrosis. But how this pathway functions during *Yersinia* infection and the link between programmed necrosis and other forms of *Yersinia*-induced death is not known.

Pathogens express pore-forming toxins and virulence proteins that disrupt membrane integrity and modulate signaling networks (113). Consequently, mammalian hosts have evolved mechanisms that detect these virulence activities, such as the activation of a multiprotein complex called the inflammasome (114). *Yersinia* expresses a conserved T3SS that activates the NLRP3 and NLRC4 inflammasomes, triggering pyroptosis (115). However, the virulence factor YopK prevents this inflammasome activation, and promotes bacterial replication and dissemination *in vivo* (115). In the presence of YopJ, YopK-sufficient bacteria still induce cell death. Thus, a key question is how these two seemingly contradictory outcomes are controlled during *Yersinia* infection. *Yersinia* expressing YopK but lacking YopJ, do not induce T3SS-dependent

inflammasome activation or cell death. Thus, YopK likely limits inflammasome activation under conditions where YopJ expression or translocation is reduced, as may happen during infection of systemic sites (discussed further below). Thus, specific Yops, such as YopJ and YopK, can control the mechanisms of host cell death. However, the activation state of host cells is also an important factor in the cell death response. Previous encounter with a pathogen or PAMP is most relevant *in vivo*, where PAMPs such as LPS are shed by bacteria.

Macrophages that are treated with LPS prior to infection, also called “primed”, respond to pathogens, such as *Yersinia*, differently than unprimed or naïve macrophages. LPS priming upregulates an array of pro-survival proteins and inflammasome components, such as NLRP3 (116), and may set the threshold for Yop-dependent cell death. For instance, macrophages primed by inflammatory stimuli undergo pyroptosis in response to YopJ-deficient *Yersinia* infection (93), which is greatly enhanced in the additional absence of YopK or YopM (115, 117, 118). Interestingly, YopM inhibits caspase-1 and inflammasome activation in LPS-primed macrophages, by preventing the association of pro-caspase-1 with ASC (119, 120). These studies demonstrate how prior exposure to PAMPs sensitizes macrophages to YopJ-independent cell death. Nevertheless, naïve macrophages undergo cell death that requires YopJ.

Interestingly, YopJ-dependent apoptosis is also associated with caspase-1 activation (92, 115, 121), and the extent of YopJ-mediated NF- $\kappa$ B inhibition correlates with the degree of caspase-1 activation (92), consistent with the finding that deletion of IKK $\beta$  in macrophages induces spontaneous inflammasome activation (122). Although NLRP3 and the adaptor ASC are required for YopJ-dependent secretion of IL-1 $\beta$  and IL-18 (92), the mechanism by which YopJ activates caspase-1 is unclear, as caspase-1

processing and YopJ-dependent cell death still occur in cells lacking ASC, NLRC4, or NLRP3 (115, 123, 124) (Figure 2). Distinct inflammasome complexes with different functions have been identified, and could potentially account for these observations. Caspase-1 could be recruited to an NLRP3/ASC complex that regulates IL-1 $\beta$  and IL-18 production, and to a separate complex that activates cell death. Indeed, during *Salmonella* infection, a complex containing catalytically active caspase-1, but not ASC triggers cell death but not cytokine secretion, while a distinct ASC-containing focus mediates caspase-1 processing and cytokine secretion (125). NLRP12 was also recently found to induce inflammasome activation in response to *Y. pestis* infection, and both NLRP3 and NLRP12 contributed to host defense against *Yersinia*, presumably via induction of caspase-1-dependent IL-1 $\beta$  and IL-18. (60). YopJ may activate an NLRP12 inflammasome, although this remains to be demonstrated. Finally, a non-canonical inflammasome pathway involving caspase-11, TRIF, and type I IFN signaling has been described that responds to gram-negative intracellular bacteria independently of T3SS activity (46, 66, 68, 69, 126). Whether this pathway contributes to anti-*Yersinia* host defense remains unknown.

### **The role of YopJ-induced death in vivo**

A number of studies indicate that YopJ/P promotes *Yersinia* virulence. Oral infection with *Y. pseudotuberculosis* and *Y. enterocolitica* demonstrate that YopJ/P contributes to systemic disease and barrier dysfunction (97, 127, 128). YopJ is dispensable for colonization of the Peyer's patches (PPs) and mesenteric lymph nodes (mLNs), especially at higher infectious doses; however, YopJ-deficient *Yersinia* had significantly reduced levels of spleen colonization after oral infection (97). Spleens and mLNs from mice infected with YopJ-sufficient bacteria had a higher percentage of Mac1<sup>+</sup> TUNEL<sup>+</sup> and total TUNEL<sup>+</sup> cells compared to YopJ-deficient bacteria, consistent with the

role of YopJ in apoptosis *in vivo*. Furthermore, in competitive index experiments, YopJ-deficient *Yersinia* showed colonization defects in PPs, mLNs and spleen. YopJ-deficient *Yersinia* were not defective for splenic replication following intraperitoneal infection, indicating that YopJ primarily regulates dissemination from mucosal tissues, rather than replication at systemic sites (97). Consistently, YopJ-deficient *Y. pestis* are still able to cause systemic infection in an intradermal rat model of bubonic plague, despite a defect in induction of apoptosis and higher levels of TNF compared to wild type *Y. pestis* infection (129). These findings imply that apoptosis may be utilized by *Yersinia* to eliminate immune cells at mucosal surfaces resulting in barrier dysfunction and dissemination. An alternative explanation is that YopJ-dependent cytokine suppression weakens barrier integrity and promotes bacterial spread. Thus, it is important that future studies distinguish the roles of cell death versus cytokine expression on disease progression.

Paradoxically, ectopic expression of a hypercytotoxic YopP from *Y. enterocolitica* in *Y. pseudotuberculosis* results in its attenuation in oral mouse infection (89) (Figure 3). While both *Y. pseudotuberculosis* and *Y. enterocolitica* cause cell death in cultured macrophages and infected tissues, infection with YopP-expressing *Y. pseudotuberculosis* showed a significant increase in TUNEL<sup>+</sup> CD11b<sup>+</sup>, CD11c<sup>+</sup> and B220<sup>+</sup> cells in mLNs relative to mice infected with the YopP-expressing strain (89). Similarly, *Y. pestis* strains expressing YopP had higher cytotoxic potency than strains expressing YopJ, both *in vitro* and in tissues of infected mice; furthermore, expression of YopP in *Y. pestis* also resulted in lower virulence following subcutaneous, but not intranasal or intravenous routes of infection (99). Interestingly, subcutaneous administration of *Y. pestis* expressing YopP protected against infection with virulent *Y. pestis*, regardless of the route of challenge. These observations suggest that YopJ

contributes to dissemination of *Yersinia* from barrier surfaces, but may be less important once bacteria have spread to systemic sites. Whether YopJ or additional

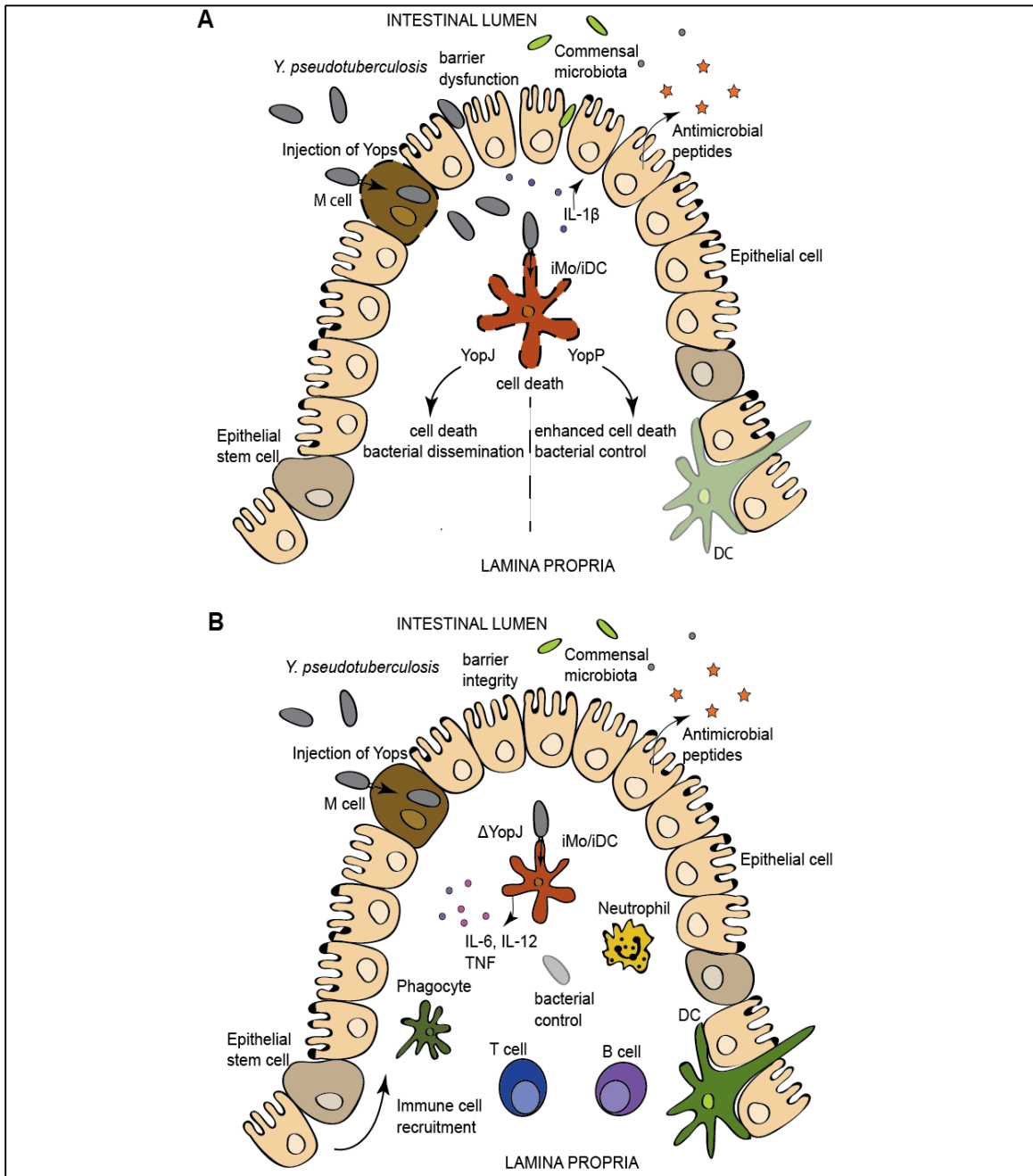


**Figure 3. Paradoxical roles for YopJ/P in bacterial pathogenesis.** (A) Injection of YopJ/P activates caspase-1 and the release of the IL-1 family of cytokines. However, the hypercytotoxic YopP-expressing *Y. pseudotuberculosis* induces enhanced levels of cell death and promotes bacterial control, relative to infection with YopJ-expressing *Y. pseudotuberculosis* (B) Conversely infection with YopJ-deficient *Y. pseudotuberculosis* results in robust cytokine production, intact barrier function and control of bacteremia. Abbreviations: DC, dendritic cell, iMo/iDC, intestinal macrophage/intestinal DC

immunosuppressive virulence mechanisms play a role in dampening the early inflammatory response to *Yersinia* infection in pneumonic plague (130) also remains to be determined.

Consistent with observations that YopJ promotes systemic dissemination following oral infection, YopJ contributes to gut barrier disruption (127, 128). Specifically, YopJ can induce TLR2-dependent IL-1 $\beta$  secretion in PPs, which was associated with increased barrier permeability, suggesting that TLR2 signaling mediates YopJ-dependent gut disruption (127). Conversely, TLR2-deficient mice have been reported to be more susceptible to oral infection by *Yersinia pseudotuberculosis*, due to a loss of TLR2-dependent Reg3 $\beta$  expression in the gut epithelium (131). Thus, the precise role of TLR2 in *Yersinia* infection remains to be further dissected. Notably, IL-1 $\alpha$  is associated with pathological intestinal inflammation and increased dissemination of *Yersinia enterocolitica* (132), but the role of YopP or TLR2 in this context has not been examined.

In contrast to cell death induced by the activity of a bacterial virulence factor, CD8<sup>+</sup> cytotoxic T cells also induce death of *Yersinia*-infected cells, and are important for control of *Yersinia* infection, as demonstrated by the more severe disease in infected  $\beta 2m^{-/-}$ , anti-CD8 $\alpha$ -treated, or perforin-deficient mice (98). CD8<sup>+</sup> T cell-mediated killing of bacteria-associated cells targeted them for phagocytosis by uninfected macrophages, and could bypass the anti-phagocytic activity of *Yersinia* Yops (98). Notably, CD8<sup>+</sup> T cells were not responsible for resistance to YopP-expressing *Y. pestis*, (99). The more cytotoxic YopP may bypass the requirement for CD8<sup>+</sup> T cell-mediated killing due to the elevated cytotoxicity induced by the bacteria. These studies collectively suggest that regulation of cytotoxicity during *Yersinia* infection impacts virulence, and that a balance between the cytokine-blocking and death-inducing functions of YopJ is required for optimal virulence. Specifically, absence of YopJ results in failure of *Yersinia* to suppress

cytokine production or induce cell death and causes a defect in dissemination. However, *Y. pseudotuberculosis* expressing YopP, which enables stronger inhibition of cytokine production and elevated levels of cell death, are also significantly attenuated *in vivo*. Thus, while the relative contributions of bacteria-induced and T cell-induced cell death during *Yersinia* infection *in vivo* are not yet defined, activation of cell death *in vivo* either in response to YopJ activity, or as a consequence of T-cell-mediated cytotoxicity likely promotes immune responses against *Yersinia*. Finally, the precise pathways of cell death that may be activated in a cell type specific manner *in vivo*, is still unclear.

### **Caspase-8 and its homolog cFLIP**

Caspases belong to a family of cysteine proteases that recognize four contiguous amino acids and cleave their substrates after an aspartate residue. Apoptotic caspases can be segregated into initiator caspases, caspase-2, -8, -9 and -10, and executioner caspases, caspase-3, -6, and -7. Most caspases are inactive zymogens that need to undergo cleavage, either by initiator caspases or by themselves, to be activated. Although the first caspase, IL-1beta converting enzyme (ICE), now called caspase-1, was identified in humans (133, 134), the critical studies that uncovered the role of caspases in apoptosis were performed in the nematode worm, *Caenorhabditis elegans* (135). Since then, 14 caspases have been identified in mammals and 11 in humans. The homologs caspase-8 and -10 are executioner caspases that are activated by proximity-induced dimerization and cleavage. Caspase-8 and -10 are considered to have branched-off from their ancestor caspase-8/10 sometime after the split between fish and tetrapods, but the gene for caspase-10 is lost in rodents, suggesting overlapping functions (136) (137). Although caspase-8 and caspase-10 share substrate specificity (138), whether they have similar roles in non-apoptotic pathways remains to be discovered. Interestingly, another member of this family, caspase-18, is suggested to



have originated from a duplication event of caspase-8 or -10 in the split of the amphibians from the amniotes. As such, caspase-18 is conserved among birds, prototherian (egg-laying) and metatherian (marsupials) mammals, but appears to be lost among eutherian (placental) mammals (137). As I have used murine models to examine the role caspase-8 in immunity, this section will focus on caspase-8.

### Regulation of caspase-8 activation

The current model for caspase-8 activation describes two cleavage steps (139). For human caspase-8, which has been studied in more depth, caspase-8 first undergoes self-cleavage between the large and small catalytic subunits at Asp384 (or Asp387 in mice). Then, a second cleavage event takes place between the second DED and large subunit, at Asp210, Asp216, or Asp223, and just downstream the large subunit at Asp374, releasing the active p18<sub>2</sub>-p10<sub>2</sub> heterotetramer (Figure 4).

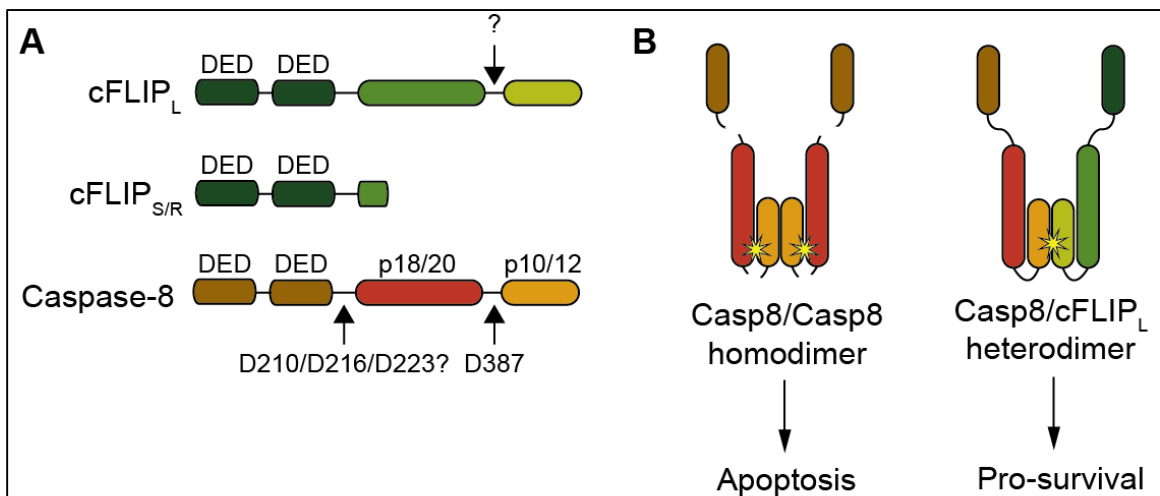


**Figure 4. Caspase-8 and cFLIP are homologs and mediate cell death and survival.**

(A) Caspase-8 and cFLIP<sub>L</sub> contain two death effector domains (DED) and one caspase domain. cFLIP is a homolog of caspase-8, but has no catalytic activity. Murine caspase-8 is cleaved between the large (p20) and small (p10) subunit at D387. Human caspase-8 is cleaved at D201, D216 and D223, but whether murine caspase-8 is also cleaved at precisely those residues is not known. Human cFLIP<sub>L</sub> is also processed within the caspase domain, but whether this is conserved in mice has not been determined. cFLIP<sub>s</sub> in humans and cFLIP<sub>R</sub> in mice is an isoform of cFLIP<sub>L</sub> that lacks part of the caspase domain.

(B) Caspase-8 undergoes homodimerization and self processing resulting in tetramers of p10/p20, which have two active sites, denoted by yellow stars, that mediate apoptosis. Caspase-8/cFLIP heterodimers prevent cell death, where cFLIP<sub>L</sub>/caspase-8 (with one active site) heterodimers block RIPK3-necrosis and cFLIP<sub>s</sub>/caspase-8 heterodimers inhibit apoptosis.

In mice, the equivalent cleavage at Asp374 is not thought to occur, suggesting potential differences in substrate specificity between human and mouse caspase-8. Additionally, the cleavage at one site does not affect self-processing at another site (140), implying different cleavage products may have distinct functions. The precise roles of caspase-8 cleavage and dimerization in its activation will be discussed below.

*In vitro* experiments with recombinant proteins have shown that non-cleavable caspase-8 undergoes dimerization in high salt solutions and can hydrolyse substrates (139, 141, 142). Since cleavage alone was insufficient to activate caspase-8 *in vitro* (142), these studies proposed an early model, whereby caspase-8 cleavage stabilizes the dimer but is not necessary for activation. However, other experiments suggested that when caspase-8 is cleaved by Granzyme B or upon addition of cytochrome c/ATP, as is the case during intrinsic apoptosis, dimerization in the context of the DISC is not necessary for caspase-8-mediated substrate processing (143, 144) (145, 146). Therefore, whether dimerization and cleavage was necessary for caspase-8 activation remained unresolved.

Subsequent work demonstrated that dimerization of non-cleavable caspase-8, using modified caspase-8 expressing drug-inducible dimerizable domains, is insufficient for caspase-8 activation in cellular conditions (20, 147, 148). Interestingly, addition of non-physiological levels of sodium citrate overcomes the requirement for self-cleavage, consistent with the findings above (148). Therefore, noncleavable caspase-8 homodimers can be active under certain conditions, but whether this occurs *in vivo* is not clear. The requirement for caspase-8 homodimerization and subsequent self-cleavage for activation may be a cell-type specific phenomenon, that depends on the relative abundance of caspase-8, its homolog cFLIP and other components of the DISC.

## **cFLIP is a key regulator of caspase-8 activation**

FLIPs (Fas-associated death domain-like IL-1 $\beta$ -converting enzyme inhibitory proteins) are cellular (cFLIP) and viral (vFLIP) proteins that are homologs of caspase-8, but possess no enzymatic activity on their own (149-157). There are many splice variants of cFLIP: the long isoform cFLIP<sub>L</sub>/cFLIP $\alpha$  expresses the two DEDs and caspase-like domain of caspase-8, the short isoform cFLIP<sub>S</sub>/cFLIP $\delta$  (cFLIP<sub>R</sub> in mice) consists of the two caspase-8 DEDs, and cFLIP $\beta$  and cFLIP $\gamma$  express two DEDs and part of the caspase-like domain. The DEDs of cFLIP<sub>S</sub> engage the DEDs of caspase-8, thereby preventing caspase-8 homodimerization and apoptosis via a dominant negative fashion (150, 154). Viral FLIPs, which are analogous to cFLIP<sub>S</sub>, are nonessential viral genes that are expressed in pox viruses and lymphotropic gamma-herpes viruses and also block caspase-8-dependent apoptosis (149, 157). In addition, cFLIP<sub>L</sub> has a prosurvival role, as cFLIP<sub>L</sub>-deficient mice are embryonic lethal and suffer from cardiac developmental defects at E10.5 similar to caspase-8 and FADD-deficient mice (27, 158, 159). cFLIP represses apoptosis and necrosis: the caspase-8/cFLIP/FADD complex inhibits RIPK3-regulated necrosis and caspase-8/cFLIP blocks caspase-8-dependent apoptosis (26, 160) (161).

The function and activity of cFLIP has been examined in the context of caspase-8. Paradoxically, experiments using kosmotropic salts to force dimerization between cFLIP and non-cleavable or wild type caspase-8 demonstrate that cFLIP<sub>L</sub> can activate caspase-8 under these cell-free conditions (162). The caspase-8/cFLIP heterodimer has one catalytic site, while caspase-8 homodimers have two sites. One plausible explanation is that cFLIP/caspase-8 heterodimers at superphysiological concentrations contain the sufficient number of active sites necessary for apoptotic substrate cleavage (147). Nevertheless, upon Fas ligation, caspase-8/cFLIP<sub>L</sub> heterodimers undergo

proteolytic processing between the small and large subunits, producing 43 kDa active subunits (163). Additionally, *in vitro* studies suggest that processing of cFLIP<sub>L</sub> occurs in the caspase-8/cFLIP<sub>L</sub> heterodimer and not as a consequence of caspase-8 homodimer activity (164). The cFLIP/caspase-8 p43 subunit does not mediate any known apoptotic functions of caspase-8, however p43 caspase-8/cFLIP<sub>L</sub> may control non-apoptotic signaling.

### **Non-apoptotic roles for caspase-8 and cFLIP**

In the *Drosophila immune deficiency (imd)* pathway, the caspase-8 homolog, Dredd, activates Relish, the p100/105 NF- $\kappa$ B homolog in *Drosophila* via cleavage between its I $\kappa$ B and Rel homology domains (165). However, the roles of caspase-8 and cFLIP on NF- $\kappa$ B signaling in mammalian cells, is under debate. There is a sizeable literature suggesting that caspase-8 and cFLIP control NF- $\kappa$ B and MAPK signaling (166-172), but there are also studies showing no connection between these pathways (173-175). As caspase-8 represses RIPK3-necrosis, caspase-8 inhibition may have released the break on necroptosis, confounding the interpretation that caspase-8 affects NF- $\kappa$ B independently of cell death. It is also possible that certain conditions *in vitro* may promote interactions between caspase-8, cFLIP and NF- $\kappa$ B. Future studies will need to examine this interaction in a cell-, stimulus- and dose-specific manner to shed more light on these mechanisms.

In addition to their well-described roles in regulating cell death, caspases (especially caspase-3 and -9) are also implicated in regulating non-apoptotic functions in glial cell development, erythroid maturation and skeletal muscle differentiation (176-178). Recent studies have implicated a role for caspase-8 in anti-microbial responses, but the

extent and mechanisms of this regulation remain poorly defined (123, 124, 173, 179-182).

Caspases regulate cell death and survival during homeostasis and disease. How cells die, and how neighboring cells respond to dying cells are critical factors that control the pathogenesis of disease. Cell death can be beneficial under some circumstances and pathological under others. Therefore, understanding the mechanisms of cell death and how cell death impacts immune responses will shed light on how the balance between protective and pathological inflammation is regulated. In this work, using *Yersinia* as a model, I will investigate the molecular requirements of cell death during *Yersinia* infection. Once I have identified the mechanisms by which host cells undergo *Yersinia*-induced cell death, I will study the role of cell death during *Yersinia* infection on the immune response. These findings will aid in the development of novel therapeutics that modulate inflammation during infection, cancer and autoimmunity.

Appropriate regulation of innate and adaptive immune responses is necessary when the host encounters potentially dangerous stimuli. PRRs are a family of innate immune receptors that sense conserved microbial features activating innate and consequently adaptive immune responses. Modulating gene expression is a critical outcome of PRR signaling. Since the initial discovery of TLRs, many of the factors that are necessary for PRR signaling are now well-characterized. However, TLR signaling is not a bimodal switch. The concentration of input can control the magnitude of the output, suggesting that signal strength is an important factor that can modulate outcome. Furthermore, signaling networks consisting of core regulators and fine-tuners that define the nature, magnitude and specificity of the response. But, the precise cell-intrinsic circuits that modulate the specificity of signaling outcomes are poorly defined. Here, I will examine the role of caspase-8 in TLR signaling and in host defense against bacterial

and viral infections. Understanding the factors that control TLR signaling will provide rational targets that can be hyperactivated or repressed to manipulate disease outcomes in autoimmunity, infection, vaccines and cancer.

## II. MATERIALS AND METHODS

### Mice

C57BL/6.SJL mice were obtained from Jackson Laboratories. *Ripk3*<sup>-/-</sup> mice were provided by Vishva M. Dixit (Genentech) and are N7 and N10 generation backcrossed. The *Ripk3*<sup>-/-</sup>*Casp8*<sup>-/-</sup> mice were provided by Doug Green (St. Jude Children's Research Hospital). *Casp8*<sup>fl/-</sup> mice were provided by Rasq Hakem (University Health Network), *Fadd*<sup>-/-</sup> mice were provided by Tak W. Mak (University Health Network), *Ripk1*<sup>-/-</sup> mice were provided by Michele Kelliher (University of Massachusetts), and *Mkl1*<sup>-/-</sup> mice were provided by Warren Alexander (The Walter and Eliza Hall Institute of Medical Research). *Casp8*<sup>+/-</sup> mice that were used to generate the *Mkl1*<sup>-/-</sup>*Casp8*<sup>-/-</sup> mice were provided by Steve Hedrick (UCSD). *Ripk3*<sup>-/-</sup>*Casp8*<sup>-/-</sup> mice in these studies were backcrossed 6-10 times and a detailed SNP analysis of *Ripk3*<sup>-/-</sup>*Fadd*<sup>-/-</sup> mice indicated that 90-94% of loci are B6 in any given mouse. Bones from *Casp3*<sup>-/-</sup> and *Casp7*<sup>-/-</sup> mice were provided by T. Devi-Kanneganti (St. Jude Children's Research Hospital) or purchased from Jackson Laboratories. Bones from *Trif*<sup>-/-</sup> mice were provided by Sankar Ghosh (Columbia University) and bones from *MyD88*<sup>-/-</sup> mice were provided by Ruslan Medzhitov (Yale University). *Casp8*<sup>fl/fl</sup>*xLysM-Cre* bones were provided by Stephen Hedrick (UCSD). *Casp3*<sup>fl/fl</sup>*Tie2-Cre*<sup>+</sup> and *Casp7*<sup>-/-</sup> mice were previously described (183, 184). Six- to eight-week-old C57BL/6.SJL mice were lethally irradiated with 1100 rads and 2-5 x 10<sup>6</sup> *Ripk3*<sup>-/-</sup>, *Ripk3*<sup>+/-</sup>*Casp8*<sup>+/-</sup>, *Ripk3*<sup>+/-</sup>*Casp8*<sup>-/-</sup>, *Ripk3*<sup>-/-</sup>*Casp8*<sup>-/-</sup> or C57BL/6 (Jackson Laboratories) congenic bone marrow (BM) cells were transferred i.v. BM chimeras were allowed to reconstitute for eight to ten weeks. For other animal experiments, age- and sex-matched six-to-eight-week old mice were used. All experiments were performed under Institutional Animal Care and Use Committee (IACUC) approved protocols and in accordance with the guidelines of the IACUC of the University of Pennsylvania.

## Generation of *Casp8*<sup>DA/DA</sup> mice

*Casp8*<sup>DA/DA</sup> mice were generated using the reagents and protocol described by Henao-Mejia and colleagues (185). Briefly, single guide RNA (gRNA:ACAGAACCACACTTTAGAAAGGTTTTAGAGCTAGAAATAGCAAGTTAAAATAA GGCTAGTCCGTTATCAACTTGAAAAAGTGGCACCGAGTCGGTGCTTTTTT) and Cas9 RNA were in vitro transcribed, purified and injected into B6xSJL F1 embryos with repair oligoDNA containing 50 base pairs of flanking regions on each side (TTGCCATCATCTCACAAAGAACTATATTCCGGATGAGGCAGAT). The complementary gRNA sequence is in blue, mutated base pairs are in red, and codon changes for D387A are highlighted in green. Embryos were transferred to pseudopregnant females and pups were screened for mutagenesis using Surveyor Mutation Detection Kit (IDT). Founders were identified by cloning PCR products of tail DNA (primer F: TTCACTGGTTCAAAGTGCCC, primer R: ACTTTGCCAGAGCCTGAGGG) according to manufacturer's instructions (M13 primers, TOPO TA Cloning Kit for Sequencing, ThermoFisher), followed by sequencing using T3 and T7 primers. Mice were backcrossed onto C57BL/6J for 5 generations until a minimum of 95% B6 was achieved by SNP analysis (Jax Genome Scanning Service). *Casp8*<sup>DA/+</sup> x *Casp8*<sup>DA/+</sup> mice were crossed and littermates were used for experiments.

## Animal Infections

For *Yersinia* infections, mice were fasted for 12-16 hours and infected orally with 1-4 x 10<sup>8</sup> *Yersinia* (32777). Mice were sacrificed and tissues were harvested on days 3, 5, 6 and 7 post-infection, as indicated. Tissues were processed and plated on LB plates containing irgasan (2 µg/mL) to determine bacterial loads (CFU/g). Levels of serum cytokines were assayed by Luminex. Cells from spleens and mesenteric lymph nodes



were cultured in the presence of BFA and monensin for 5 hrs, stained for surface and intracellular cytokines and analyzed by flow cytometry as described below. Spleen and liver sections were fixed and stained for H&E. For *in vivo* Sendai virus infections, mice were anaesthetized using ketamine and infected with  $10^4$  of SeV strain 52 (low defective viral genomes) per mouse (186). Mice were weighed every one to two days. On days 3 and 10, lungs were harvested and homogenized in Trizol for RT-qPCR analysis.

## Histopathology

Spleens and livers were fixed and stained for haematoxylin and eosin. Sections were quantified by a blinded pathologist (Louise Fitzgerald, PennVet) according to the metric in Table S1.

**Table S1. Histopathology scoring scheme.** Rubric that describes scoring scale for lesion size and number of lesions in spleens and livers of mice.

<b>Score</b>	<b># Lesions</b>	<b>Size of Lesions</b>	<b>Bacterial Colonies</b>
<b>0</b>	None	None	None
<b>1</b>	0 – 9	Small	Rare, small
<b>2</b>	10 – 19	Medium	Infrequent, small to medium
<b>3</b>	20 – 30	Medium to large, infrequent confluence	Frequent, small to medium
<b>4</b>	>30 or marked confluence	Medium to large, frequent confluence	Frequent, large or coalescing

## Detection of germline single nucleotide variations (SNVs) and small insertion/ deletion (indels)

We downloaded Whole-genome sequencing (WGS) data from the Mouse Genomes Project of WELLCOME TRUST SANGER INSTITUTE (187). Using a pipeline that was initially developed for detecting somatic mutations using paired tumor/normal sample, we identified the germline single nucleotide variations (SNVs) of the three 129 strains (129P2, 129S1, 129S5) by running a paired SNV analysis using C57B6 as the reference sample. The initial variant calls were generated using variation detection module of

Bambino (188) with the following parameters: -min-flanking-quality 15 -min-alt-allele-count 2 -min-minor-frequency 0 -broad-min-quality 10 -mmf-max-hq-mismatches 15 -mmf-min-quality 15 -mmf-max-any-mismatches 20 -unique-filter-coverage 2 -min-mapq 1. A post-process pipeline filters SNVs in regions with low quality regions, re-maps (using the program BLAT) and re-aligns (using the program SIM) the reads harbouring variant allele to the mouse mm10 genome to remove additional false calls. The validation rate for human cancer genome analysis is about 95% (189) while that of a mouse exome sequencing data is ~ 90% (190).

### **Flow cytometry**

For animal studies, mesenteric lymph nodes were isolated and plated in complete-DMEM containing brefeldin A (Sigma) and monensin (BD) in a 37°C humidified incubator for 5 hrs. For BMDMs, cells were plated in 48- or 12-well suspension dishes and pre-treated with zVAD-fmk (100 µM) for 1 hr prior to PAMP stimulation, where indicated. BFA and monensin were added 1 hr later and samples were harvested for analysis 4-5 hrs later. BMDMs were harvested using PBS with EDTA (2mM) prior to staining. Cells were washed with PBS, stained for viability (Zombie Yellow, BioLegend or Aqua Live Dead, Invitrogen) and then stained with the following antibodies from BioLegend: Ly6G (clone 1A-8 PE-Cy7), IL-6 (MP5-20F3 APC/FITC), F4/80 (clone BM8 Pacific Blue), CD3ε (clone 17A2 AF700), NK1.1 (clone PK136, Pacific Blue), BD Biosciences: CD45.1 (clone A20 APC-Cy7), CD45.2 (clone 104 FITC), MHCII (clone M5/114 BV650), B220 (clone RA3-6B2 PETexasRed), NK1.1 ThermoFisher: CD11b (clone M1/70.15 PE-Texas Red), eBioscience: Ly6C (clone HK1.4 PerCPCy5.5), CD11c (clone N418 AF700), F480 (clone BM8 APC-eF780), TNF (clone MP6-XT22 eF450), IL-12p40 (clone C17.8 PE), proIL-1β (clone NJTEN3 APC/FITC), CD19 (clone MB19-1 APC), IFNγ (clone XMG1.2

AF700/APC) or cleaved caspase-3 (Asp 175, Cell Signaling Technologies). Inflammatory monocytes and neutrophils were gated as follows live CD45.1<sup>2+</sup>/CD45.2<sup>+</sup>, CD11c<sup>-</sup>, CD11b<sup>hi</sup>, Ly6C<sup>hi</sup> or Ly6G<sup>+</sup>. BMDMs were gated on Live/dead<sup>-</sup>, singlets, and in Figure 7 also CD11b<sup>+</sup>F480<sup>+</sup>. Resident peritoneal exudate cells (PECs) were isolated from naïve six- to eight-week-old sex-matched mice with cold PBS. PECs were incubated with LPS (10 ng/mL), BFA and monensin for 4hrs and large peritoneal macrophage responses were examined based on gating strategy as published by Ghosn et al. (191). Surface staining was performed in FACS buffer (PBS with 1% BSA, 2mM EDTA) and sample fixation and permeabilization prior to intracellular staining were all performed according to manufacturer's instructions (BD). Samples were run on an LSRFortessa and analyzed using FlowJo Treestar software.

### **Cell Culture and Infection Conditions**

Bone marrow-derived macrophages (BMDMs) were grown as previously described (115) in a 37°C humidified incubator in DMEM supplemented with 10% FBS, HEPES, sodium pyruvate (complete-DMEM) and 30% L929 supernatant for 7-9 days. Fetal liver-derived macrophages (FLDMs) were grown from E12-14 livers in complete-DMEM and 50% L929 supernatant for 7-9 days. 16-20 hrs prior to infection cells were re-plated into 96-, 48-, 24- or 12-well dishes in complete-DMEM containing 10% L929 supernatant. Necrostatin-1, zVAD-fmk, QVD-oph and GSK'872 were added 1-3 hours prior to infection or treatment with PAMPs (30 µM or 60 µM Necrostatin-1 Calbiochem, 100 µM zVAD-fmk-001 R & D Systems or SMBiochemicals, 3µM GSK'872 Calbiochem, 0.5 µg/mL Cytochalasin-D Sigma, 25 mM N-acetylcysteine Sigma). IKKβ and p38 inhibitors were added 1 hr prior to infection (BMS 345541, SB202190 Millipore).

Bacterial and viral infections: Bacterial strains are described in Table S2. *Yersinia* were grown overnight with aeration in 2xYT broth at 26°C. The bacteria were diluted into fresh

2xYT containing 20 mM sodium oxalate and 20 mM MgCl<sub>2</sub> (inducing media). Bacteria were grown with aeration for 1 hr at 26°C followed by 2 hrs at 37°C. *Salmonella* were grown overnight in LB medium at 37°C with aeration, diluted into fresh LB containing 300 mM NaCl, and grown standing at 37°C for 3 hrs. Bacteria were washed three times with pre-warmed DMEM, added to the cells at an MOI of 20:1 unless otherwise indicated, and spun onto the cells at 1000 rpm for 5 min. Cells were incubated at 37°C for 1 hr post-infection followed by addition of 100 µg/mL gentamicin. For *in vitro* Sendai virus infections, cells were washed twice with warm PBS, and infected with Sendai virus Cantell (high defective viral genomes) in a low volume of serum-free media as previously described (192).

4-OHT treatment: 4-OHT (50 nM, 98% pure Z-form, Sigma) was added on day 3 and day 5 to indicated BMDMs in complete-DMEM supplemented with 30% L929 supernatant. Cells were replated on day 7 and infections were performed as described above on day 8.

**Table S2. Bacterial strains used in this work. A description of strain name or genotype, abbreviations and source or reference information for all strains used.**

Strain name or genotype	Description	Source or Reference
IP2666 (Yp)	Wild type <i>Yersinia pseudotuberculosis</i> serogroup O:3 strain	(193)
IP26 (ΔYopJ)	IP2666 YopJ-deficient strain	(121)
32777	Wild type <i>Yersinia pseudotuberculosis</i> serogroup O:1 strain (previously known as IP2777)	(194) Provided by Jim Bliska.
327	YopJ-deficient <i>Yersinia pseudotuberculosis</i> serogroup O:1 strain	This work.
YopJC172A	32777 mutant YopJ C172A	(195)
T3SS/mCD1	Yp cured of virulence plasmid, reconstituted with modified virulence plasmid from <i>Y. pestis</i> lacking all known effectors but expressing function type III secretion system	(115)
8081 (Ye)	Wild type <i>Yersinia enterocolitica</i> serogroup O:8	(196)

8081c- (YeP-)	8081 virulence plasmid cured	(89, 196)
SL1344	Wild type <i>Salmonella enterica</i> serovar Typhimurium	(197)

### Generation of immortalized cell line

Freshly isolated *Ripk3<sup>-/-</sup>Casp8<sup>-/-</sup>* bone marrow was infected with the v-myc/v-raf expressing J2-Cre retrovirus (198) and differentiated in 15% L929 supernatant. After 20 days in culture macrophages were weaned off L929 and passaged in complete-DMEM.

### Viral transductions

WT C8 expression was accomplished by cloning full-length murine caspase-8 into the pBabe-Puro retroviral vector upstream of the T2A ribosomal skipping sequence followed by enhanced GFP. Mutations in murine D3A C8 were inserted at D387A, D397A and D400A using the QuikChange Site Directed Mutagenesis kit (Agilent). D3A C8 was cloned into the pRRL-Puro lentiviral vector upstream of the T2A ribosomal skipping sequence followed by enhanced GFP. Stable expression was achieved by retro- or lentiviral transduction of *iR3<sup>-/-</sup>C8<sup>-/-</sup>* cells followed by two rounds of sorting by FACS to enrich for GFP<sup>+</sup> cells. Plasmids were a kind gift from Andrew Oberst (University of Washington, Seattle).

### Western Blotting

All *Yersinia* infections, unless otherwise indicated were performed with IP2666 (Yp) or IP26 ( $\Delta$ YopJ). Whole cell lysate western blotting was adapted from (115). Briefly, cells were lysed in 20 mM HEPES, 150 mM NaCl, 10% glycerol, 1% Triton X-100, 1 mM EDTA, 1mM NaF, 1mM activated Na<sub>3</sub>VO<sub>4</sub> and protease inhibitors. Lysates were mixed with protein loading buffer, boiled, centrifuged, and 20% of the total cell lysate loaded onto 4%–12% NuPAGE gels (Invitrogen). Proteins were transferred to PVDF membrane

(Millipore) and blotted with rabbit anti-mouse caspase-1 antibody (sc-514, Santa Cruz Biotechnology), rabbit anti-mouse MAPK and phospho-MAPK antibodies (all from Cell Signaling Technologies), rat anti-mouse caspase-8 (clone 1G12, ALX 804-447-C100, Enzo Life Sciences), mouse anti-mouse  $\beta$ -actin (Sigma), mouse anti-mouse  $\beta$ -tubulin (Sigma), anti-IRAK2 (ProSci 3595 rabbit anti-mouse), anti-HDAC1 (Cell Signaling Technologies). Secondary antibodies were goat anti-rabbit, goat anti-rat (Jackson ImmunoResearch) or horse anti-mouse HRP (Cell Signaling Technology).

### **Immunoprecipitations**

Myddosome isolation assays were adapted from (Bonham et al., 2014). Briefly, BMDMs were treated with LPS (100 ng/mL) and harvested in cold PBS.  $4 \times 10^6$  cells were used per IP condition. Cells were lysed in 1% NP-40 (IGEPAL<sup>®</sup> CA-630 Sigma), 50 mM Tris-HCl (pH 7.4), 150 mM NaCl, 10% glycerol, and protease/phosphatase inhibitors (Roche) for 20 minutes on ice and spun at high speed for 20 minutes. 1/7 of lysates was aliquoted for inputs, the remaining lysate was incubated at 4°C with 1  $\mu$ g anti-MyD88 (R&D LifeSciences, AF3109 goat anti-mouse) or control goat IgG (R&D Normal Goat IgG Control, AB-108-C). The following day, 50  $\mu$ l of protein G Dynabeads (ThermoFisher) was added for 1 hr at 4°C. Beads were washed 3 times with lysis buffer, proteins were extracted by adding Laemmli buffer, boiled, electrophoresed, and immunoblotted with the indicated antibodies using standard conditions.

### **Nuclear Extractions**

$5 \times 10^6$  cells per condition were treated as described and harvested with cold PBS. Pellets were resuspended in 100  $\mu$ l cold NAR A (10 mM HEPES pH 7.9, 10 mM KCl, 0.1 mM EDTA pH 8, protease/phosphatase inhibitors, 1mM DTT, 1mM  $\beta$ -glycerophosphate and 1mM NaF) and incubated on ice for 20 minutes. 10  $\mu$ l 1% NP-40 was added and

lysates were incubated at room temperature for 2-5 minutes. Lysates were vortexed for 10-30 seconds, centrifuged for 1.5 min at 6000 rpm. Supernatants containing the crude cytoplasmic extract were transferred to new microcentrifuge tubes. Cytoplasmic extracts were spun for 60 minutes at full speed at 4°C and supernatants containing purified cytoplasmic extracts were recovered. Nuclear pellets from first wash were washed four times in 100 µl cold NAR A. Pellets were resuspended in 50 µl NAR C (20 mM HEPES pH 7.9, 0.4 M NaCl pH 8, 1 mM EDTA pH 8, protease/phosphatase inhibitors, 1mM DTT, 1mM β-glycerophosphate and 1mM NaF). Tubes were vortexed at 4°C for 1 hr at full speed. Supernatants containing nuclear extracts were recovered after max speed spin for 20 minutes. All lysates were quantified, run on SDS-PAGE and analyzed by western blotting.

### **Cell Death Assays**

Lactate dehydrogenase (LDH) release: All *Yersinia* infections, unless otherwise indicated (as in Figure 1g, S. Figure 1b and Extended Data Fig. 6) were performed with IP2666 (Yp) or IP26 (ΔYopJ). BMDMs were seeded into 96-well plates at a density of  $7 \times 10^4$  cells/well in complete-DMEM containing 10% L929 supernatant. Cells were infected as described above and supernatants harvested at indicated times post-infection. LDH release was quantified using the Cytotox96 Assay Kit (Promega) according to the manufacturer's instructions. Cytotoxicity was normalized to Triton (100%) and LDH release from uninfected/untreated cells was used for background subtraction.

Propidium iodide (PI) uptake was analyzed by flow cytometry and confocal microscopy:

Cells were seeded in 12-well suspension dishes at a density of  $5 \times 10^5$  cells/well 16-20 hrs prior to infection. Cells were harvested with cold PBS at indicated times, washed twice with PBS, and stained with PI (Calbiochem), washed twice with PBS, run on an LSR Fortessa and analyzed using FlowJo Treestar software.

Kinetics of PI uptake was analyzed by time-lapse confocal microscopy as follows: 12-well chamber slides (IBIDI) were coated with 1 mg/mL poly-L-lysine (Sigma) at 4°C, 1 day prior to seeding cells. Cells were seeded at a density of  $8-10 \times 10^4$  cells/well, 16-20 hrs prior to infection. 4 hours prior to infection, cells were loaded with Cell Tracker Green (Invitrogen) according to manufacturer's instructions, washed once and replenished with fresh media. At time of infection, PI was added and PI uptake was analyzed using the inverted Leica DMI4000 based Yokagawa CSUX-1 spinning disk confocal microscope in a 37°C humidified chamber (Penn Vet Imaging Core) over indicated time points.

### **Caspase-8 Activity Assay**

BMDMs were seeded into 96-well white-walled plates at a density of  $7 \times 10^4$  cells/well in complete-DMEM containing 10% L929 supernatant. Cells were infected as described above with Ye or YeP- for 2 hrs. Media was aspirated and a 1:1 mix of PBS and Caspase-Glo 8 reagent+buffer (Promega) was added as per the manufacturer's protocol. Plates were allowed to shake at 300rpm for 40 minutes before luminescence was read.

### **ELISAs and Luminex**

BMDMs were pretreated with 50 ng/mL *E. coli* LPS (Sigma) for 3 hr prior to bacterial infection as described above, and supernatants were harvested 4 hrs post-infection. In experiments without bacterial infections, BMDMs were treated with 100 ng/mL *E. coli* LPS (Sigma), 1 µg/mL Pam3CSK4 (Invivogen), 1 µg/mL CpG (Invivogen), or 50 µg/mL HMW Poly(I:C) (Invivogen). Release of proinflammatory cytokines was measured by enzyme-linked immunosorbent assay (ELISA) using capture and detection antibodies against IL-6 (BD), IL-12p40 (BD), IL-1α (BD Pharmingen), IL-1β (e-Bioscience) or or TNFα (BioLegend). To detect IL-18 by ELISA (MBL International) from *Yersinia*-infected



cells, BMDMs were infected (with LPS priming where indicated) and supernatants were harvested 4 hrs post-infection. Magnetic 20-plex Luminex (Invitrogen) was performed at the University of Pennsylvania Human Immunology Core to quantify cytokines and chemokines in mouse serum.

## RT-qPCR

1x10<sup>6</sup> BMDMs/well were plated in 6-well tissue culture-treated dishes 16 hrs before the experiment. Cells were treated with 10 ng/mL mTNF $\alpha$  (BioLegend) for 6hrs. For RNA stability experiments, BMDMs were stimulated with LPS (100 ng/mL) for 2 hrs, and then treated with Actinomycin D (Sigma, 5  $\mu$ g/mL). Samples were lysed in Trizol Reagent (Invitrogen/ThermoFisher) and RNA was extracted using phenol/chloroform method. RNA was resuspended in RNase-free water and cDNA synthesis was performed using High Capacity RNA to cDNA kit (ThermoFisher) as per manufacturer's instructions. qPCR was run using Power Sybr Green Master Mix (ThermoFisher) on a QuantStudio Flex6000 (ThermoFisher). Primer sequences used are listed in Table S3.

**Table S3: Primer sequences for ChIP and RT-qPCR.** A description of gene and primer names, primer sequences, assay conducted and reference information of all primers used in this work.

Gene	Primer Name	Primer Sequence	Type	Reference
<i>Gapdh</i>	GapdF	GGTCCAAAGAGAGGGAGGAG	ChIP	(199)
<i>Gapdh</i>	GapdR	GCCCTGCTTATCCAGTCCTA	ChIP	(199)
<i>Cxcl2</i>	Cxcl2F	GGGCTCTGTGCTTCCTGAT	ChIP	(199)
<i>Cxcl2</i>	Cxcl2R	TCCCGAGAGCTCCTTTTATG	ChIP	(199)
<i>Il1beta</i>	Il1betaF	CCCACCCTTCAGTTTTGTTG	ChIP	(199)
<i>Il1beta</i>	Il1betaR	CTTGTTTTCCCTCCCTTGTTT	ChIP	(199)
<i>Ccl5</i>	Ccl5F	CTGCTACCCTGGCTCCCTAT	ChIP	(199)
<i>Ccl5</i>	Ccl5R	TGGGAGATGCATGTGCTGT	ChIP	(199)
<i>Il6</i>	Il6F	AATGTGGGATTTTCCCATGA	ChIP	(199)
<i>Il6</i>	Il6FR	GCTCCAGAGCAGAATGAGCTA	ChIP	(199)
<i>Tnf</i>	TnfF	GATTCCTTGATGCCTGGGTGTC	ChIP	(199)
<i>Tnf</i>	TnfR	GAGCTTCTGCTGGCTGGCTGT	ChIP	(199)
<i>Il12b</i>	Il12bF	GGGGAGGGAGGAACCTTCTTA	ChIP	(199)

<i>Il12b</i>	Il12bR	CTTTCTGATGGAAACCCAAAG	ChIP	(199)
<i>Hbbs</i>	HbbsF	GCATGGAAGACAGGACAATC	ChIP	This study
<i>Hbbs</i>	HbbsR	GTGGGAGGAGTGTACAAGGA	ChIP	This study
<i>Ifnb</i>	IfnbF	AGATGTCCTCAACTGCTCTC	Transcript	(192)
<i>Ifnb</i>	IfnbR	AGATTCACTACCAGTCCCAG	Transcript	(192)
<i>Il1b</i>	Il1bF	CCTCTGATGGGCAACCACTT	Transcript	(200)
<i>Il1b</i>	Il1bR	TTCATCCCCCACACGTTGAC	Transcript	(200)
<i>Il12b</i>	Il12bF	TTGAAAGGCTGGGTATCGGT	Transcript	(186)
<i>Il12b</i>	Il12bR	GAATTTCTGTGTGGCACTGG	Transcript	(186)
<i>Il6</i>	Il6F	ACAGAAGGAGTGGCTAAGGA	Transcript	(186)
<i>Il6</i>	Il6R	CGCACTAGGTTTGCCGAGTA	Transcript	(186)
<i>SeV NP</i>	SeV NPF	TGCCCTGGAAGATGAGTTAG	Transcript	(192)
<i>SeV NP</i>	SeV NPR	GCCTGTTGGTTTGTGGTAAG	Transcript	(192)
<i>Cxcl2</i>	Cxcl2F	GATACTGAACAAAGGCAAGGC	Transcript	This study
<i>Cxcl2</i>	Cxcl2R	ATCAGGTACGATCCAGGCT	Transcript	This study
<i>Ccl22</i>	Ccl22F	GGCCATACAAAGTGATACCT	Transcript	This study
<i>Ccl22</i>	Ccl22R	GGAAGCAAGAATGGGTTCTA	Transcript	This study

### Chromatin Immunoprecipitation

Bone marrow-derived macrophages (BMDMs) were stimulated with LPS (50ng/mL, Sigma) for 2 hrs. Cells were cross-linked with disuccinimidyl glutarate (2mM, Thermo Fisher) for 30 min, then formaldehyde (1%, Sigma) for 10 min and quenched with glycine (0.125M) for 5 min. Nuclear lysis was performed with the truChIP Chromatin Shearing Reagent KIT (Covaris) and nuclei were sonicated using the Covaris S220 sonicator. Chromatin was immunoprecipitated using anti-p65 antibody sc-372X (Santa Cruz) and protein G agarose beads (Millipore). All samples were column purified with the QIAquick PCR purification Kit (Qiagen). qPCR was performed using SYBER Green PCR Master Mix (Thermo Fisher). Primer pairs were designed to amplify 80-250 bp fragments of the promoter region of each gene (Table S3) and melt curve analysis was used to confirm the amplification of unique products. All samples were normalized to a 5% input control and fold enrichment calculated using percent enrichment of treated over percent enrichment for untreated samples.

## **RNA-seq**

BMDMs were prepared as described above and  $1 \times 10^6$  BMDMs/well were plated in 6-well tissue culture-treated dishes and placed in a 5% CO<sub>2</sub> 37 °C incubator for 16 hours. BMDMs were stimulated with LPS (100 ng/mL) for 6 hrs. RNA was isolated using the RNeasy Mini Kit (Qiagen) and processed as per manufacturer's instructions. mRNA-seq libraries were prepared using the TruSeq Stranded Total RNA LT Kit with Ribo-Zero Gold, according to the manufacturer's instructions. Samples were run on Illumina NextSeq 500 to generate between 151 base-pair, paired-end reads with a Q30 score of ~80%, resulting in 25-50 million fragments/sample. All data processing and analyses were carried out using the R programming language (Version 3.2.2) and the RStudio interface (Version 0.99.489), as described previously (201) and can be reproduced using the supplementary code file. Briefly, raw fastq files were aligned to version 79 of mouse reference genome GRCm38 using the Subread aligner (202) in the RSubread package. BAM files were summarized to genes using the featureCounts algorithm (203). Raw data is available on the Short Read Archive (SRA) and Gene Expression Omnibus (GEO) (accession # pending). Differentially expressed genes were identified by linear modeling and Bayesian statistics using the VOOM function (204) in the Limma package (205). Gene Ontology (GO) was performed using the Database for Annotation, Visualization and Integration of Data (DAVID) (206, 207). Gene Set Enrichment Analysis (GSEA) (208) was performed against the Molecular Signatures Database (MSigDB) (209) using the C2 canonical pathways collection.

## **Statistics**

All statistical analyses were performed using the two-tailed unpaired Student's *t*-test, two-way ANOVA with Bonferonni correction or Mann-Whitney U test, where indicated.

### III. CASPASE-8 MEDIATES CASPASE-1 PROCESSING AND INNATE IMMUNE DEFENSE IN RESPONSE TO BACTERIAL BLOCKADE OF NF- $\kappa$ B AND MAPK SIGNALING<sup>2</sup>

#### Background

The innate immune response forms the first line of defense against pathogens. Microbial infection triggers the activation of pattern recognition receptors (PRRs), such as Toll-like receptors (TLRs) on the cell surface or cytosolic Nucleotide binding domain Leucine Rich Repeat family proteins (NLRs) (210). TLRs induce NF- $\kappa$ B and mitogen-activating protein kinase (MAPK) signaling to direct immune gene expression, whereas certain NLRs direct the assembly of multi-protein complexes known as inflammasomes that provide platforms for caspase-1, or -11 activation (211). Active caspase-1 and -11 mediate cleavage and secretion of the IL-1 family of proteins and a pro-inflammatory cell death termed pyroptosis. However, microbial pathogens can interfere with various aspects of innate immune signaling, and the mechanisms that mediate effective immune responses against such pathogens remain poorly understood. Pathogenic *Yersiniae* cause diseases from gastroenteritis to plague, and inject a virulence factor known as YopJ, which inhibits NF- $\kappa$ B and MAPK signaling pathways in target cells (107, 212, 213). YopJ activity inhibits proinflammatory cytokine production (213) and induces target cell death (87). YopJ activity induces processing of multiple caspases, including caspases-8, -3, -7, and -1 (93, 111, 121). Nevertheless, *Yersinia*-infected cells exhibit properties of both apoptosis and necrosis (96, 112), and no specific cellular factors have been identified as being absolutely required for YopJ-induced caspase activation and cell death. We previously found that the inflammasome

---

<sup>2</sup> This chapter is reprinted from Philip NH, *et al.* (2014) Caspase-8 mediates caspase-1 processing and innate immune defense in response to bacterial blockade of NF-kappaB and MAPK signaling. *Proc Natl Acad Sci U S A* 111(20):7385-7390.

proteins NLRC4, NLRP3, and ASC are dispensable for YopJ-induced caspase-1 processing and cell death (115). Thus, additional pathways likely mediate YopJ-induced caspase-1 activation and cell death.

Death receptors, such as TNF receptor and Fas, mediate caspase-8-dependent apoptosis via a death-inducing signaling complex (DISC) containing receptor-interacting serine/threonine kinase 1 (RIPK1), caspase-8, and Fas-associated death domain (FADD) (214, 215). Whether these proteins are required for *Yersinia*-induced cell death, and whether this death contributes to anti-bacterial immune responses is not known. The Ripoptosome complex, which contains RIPK1, FADD, caspase-8, as well as RIPK3 and cFLIP, regulates apoptosis, programmed necrosis, and survival in response to various stimuli including signaling by the TLR adaptor TRIF (22, 216). As YopJ-induced cell death is inhibited in the absence of either TLR4 or TRIF (16), we sought to determine whether YopJ-dependent cell death and caspase-1 activation is regulated by caspase-8 or RIPK3, and to define the role of YopJ-dependent cell death in host defense. Here, we describe a previously unappreciated requirement for RIPK1, FADD, and caspase-8, but not RIPK3, in YopJ-induced caspase-1 activation and cell death. Critically, loss of caspase-8 in the hematopoietic compartment resulted in a failure of innate immune cells to produce pro-inflammatory cytokines in response to *Yersinia* infection, and severely compromised resistance against *Yersinia* infection. Our data suggest that caspase-8-mediated cell death in response to blockade of NF- $\kappa$ B/MAPKs by YopJ allows for activation of host defense against *Yersinia* infection. This cell death may thus enable the immune system to override inhibition of immune signaling by microbial pathogens.

## **Results**

### **RIPK1 is required for *Yersinia*-induced cell death and caspase-1 activation**

Activation of multiple caspases, including caspase-1, -3, -7, and -8, is triggered due to YopJ activity in *Yersinia*-infected cells (93, 110, 111, 115). *Casp1<sup>-/-</sup>Casp11<sup>-/-</sup>* bone marrow-derived macrophages (BMDMs) exhibit a significant delay in cell death in response to *Yersinia pseudotuberculosis* (Yp), whereas both Yp-induced cell death and caspase-1 activation are indistinguishable between B6 and *Casp11<sup>-/-</sup>* or 129SvImJ BMDMs (Figure 5A-C). These data suggest that caspase-1 plays a functional role in YopJ-induced cell death. Surprisingly, NLRC4, NLRP3, ASC, and type I IFN receptor alpha are dispensable for *Yersinia*-induced caspase-1 processing and cell death, suggesting that these events occur via a distinct pathway (Figure 5D-H and (115)).

RIPK1, RIPK3, caspase-8 and FADD regulate cell survival and death fate decisions downstream of TRIF as a result of RIP Homotypic Interaction Motif (RHIM)-driven interactions between TRIF and RIPK1 (216, 217). This interaction can promote apoptosis through a RIPK1/FADD/caspase-8 complex (17), or programmed necrosis via RIPK1 and RIPK3 (23). We therefore investigated the potential involvement of RIPK1 in *Yersinia*-induced cell death. Necrostatin-1 (Nec-1) inhibits RIPK1 kinase activity and prevents TLR-induced necrosis (23, 218), but was previously reported to not inhibit *Y. pestis*-induced cell death (96). Surprisingly, we observed that both RIPK1-deficient BMDMs and B6 BMDMs treated with Nec-1, exhibited reduced levels of Yp-induced caspase-1 and -8 processing (Figure 6A-D), and cell death (Figure. 6E and F). *Tlr4<sup>-/-</sup>* BMDMs are partially protected from *Yersinia*-induced death (16), and TLR4 signaling induces programmed necrosis in cells treated with the pan-caspase inhibitor zVAD-fmk via a TRIF- and RIPK3-dependent pathway (23). Interestingly, zVAD-fmk still sensitized *Trif<sup>-/-</sup>* BMDMs to cell death in response to wild-type Yp, but not YopJ-deficient Yp ( $\Delta$ YopJ) infection, whereas B6 BMDMs were sensitized to both (Figure 6E and F, and Figure 7A). In contrast, *Ripk1<sup>-/-</sup>* cells were not sensitized to death in the presence of

zVAD-fmk in response to either  $\Delta$ YopJ or Yp (Figure 6E and F and Figure 7B). These data indicate that YopJ induces cell death through RIPK1 via both TRIF-dependent and -independent pathways. Notably, although Nec-1 treatment protects Yp-infected cells from death, expression of NF- $\kappa$ B-dependent cytokines were not restored (Figure 7D-E). These data demonstrate that YopJ-mediated blockade of cytokine production is independent of YopJ-induced cell death, and implies that this cell death may serve an alternative function. Nec-1 did inhibit YopJ-induced secretion of IL-18, consistent with its effect on caspase-1 activation (Figure 6G). Altogether, these data demonstrate a key role for RIPK1 in *Yersinia*-induced death and caspase-1 activation, and suggest that this cell death functions as a host defense against pathogen blockade of inflammatory signaling pathways.

### **Caspase-8 activity is required for YopJ-induced cell death and caspase-1 processing**

TLR signaling can trigger RIPK1-mediated cell death either via caspase-8 or RIPK3 (22, 23). The observation that zVAD-fmk-treatment did not protect B6 BMDMs from Yp-induced death suggests either caspases are not required for Yp-induced cell death, or blocking caspase activity in Yp-infected cells triggers cell death via RIPK3-mediated necrosis. Caspase-8 catalytic activity prevents a lethal RIPK3-dependent programmed necrosis that occurs in early embryonic development (26). Notably, we found that *Ripk3*<sup>-/-</sup> BMDMs had no defect in Yp-induced caspase-1 processing or cell death, whereas *Ripk3*<sup>-/-</sup>*Casp8*<sup>-/-</sup> BMDMs failed to process caspase-1 or undergo cell death in response to Yp infection, in contrast to STm or LPS+ATP treatment (Figure 8A-C). This failure was not the result of insufficient back-crossing of these mice, as there were no single nucleotide variants (SNVs) between B6 and three different lines of 129 mice in caspase-8, cFLIP, FasL or RIPK3, and the polymorphic genes immediately

flanking caspase-8 are not linked to these cell death pathways (Figure 9). Importantly, in *Ripk3*<sup>-/-</sup> BMDMs, zVAD-fmk abrogated Yp-induced death (Figure 8C). These data demonstrate that caspase inhibition induces RIPK3-dependent programmed necrosis in Yp-infected cells, and that RIPK3 is not required for YopJ-induced caspase-1 processing or cell death in the presence of caspase-8. RIPK3 can activate caspase-1 in the absence of caspase-8 in response to LPS (219) or cIAP inhibitors (220). Therefore, caspase-8 and RIPK3 might play redundant roles in caspase-1 activation or cell death during Yp infection. Intriguingly, conditional deletion of caspase-8 by inducible (ERT2-Cre), or developmental (LysM-Cre) approaches significantly reduced YopJ-mediated processing of caspase-1 in RIPK3-sufficient cells, indicating that caspase-8 and RIPK3 play a non-redundant role in YopJ-induced caspase-1 processing (Figure 8D and Figure 10A). This caspase-8-dependent processing of caspase-1 was functionally important, as IL-18 secretion was significantly reduced in *Ripk3*<sup>-/-</sup>*Casp8*<sup>-/-</sup>, but not *Ripk3*<sup>-/-</sup> BMDMs (Figure 8E). However, conditional deletion of caspase-8 was not sufficient to protect BMDMs from Yp-induced cell death (Figure 10B and C), in keeping with the finding that zVAD-fmk leads to programmed necrosis in RIPK3-sufficient cells. Importantly, caspase-1 activation in response to STm was completely unaffected in caspase-8 conditional BMDMs, indicating that these cells retained the ability to undergo inflammasome activation (Figure 10D). We also observed an apparent synergy between zVAD-fmk and Nec-1 in protection from LPS+ATP-treated cell death in B6 cells (Figure 8C). However, this is most likely because zVAD-fmk-pretreated cells that are then exposed to LPS+ATP undergo programmed necrosis, as *Ripk3*<sup>-/-</sup> cells treated with zVAD-fmk followed by LPS+ATP are protected from cell death (Figure 8C).

To dissect how caspase-8 mediates activation of caspase-1, we reconstituted immortalized *Ripk3*<sup>-/-</sup>*Casp8*<sup>-/-</sup> (*iR3*<sup>-/-</sup>*C8*<sup>-/-</sup>) macrophages with either wild-type caspase-8



(WT C8), or mutant caspase-8 lacking the three critical aspartate residues required for autoprocessing (D3A C8). Critically, expression of WT C8 but not D3A C8 restored both Yp-induced cell death and processing of caspase-1 in *iR3<sup>-/-</sup>C8<sup>-/-</sup>* cells (Figure 8F). Both forms of caspase-8 were expressed at similar levels in the reconstituted cells, but the D3A mutant lacked catalytic activity, consistent with observations that non-cleavable forms of caspase-8 do not exhibit catalytic activity in the absence of forced dimerization (142) (Figure 11A and B). Noncleavable caspase-8 nonetheless retains some function, as it interacts with cFLIP to inhibit programmed necrosis and mediate protection from embryonic lethality (26, 28). Consistently, zVAD-fmk-treatment abolished both caspase-8 and caspase-1 processing in response to *Yersinia* infection, but not in STM-infected cells (Figure 11C-E). These data indicate that zVAD-fmk does not block the autoprocessing of caspase-1 that occurs in canonical inflammasomes, but inhibits caspase-8-mediated caspase-1 processing. Altogether, these data indicate that the cleaved active caspase-8 homodimer mediates YopJ-induced processing of caspase-1.

Inhibition of NF- $\kappa$ B and MAPK signaling by YopJ is necessary for Yp-induced cell death (109), but whether this is responsible for RIPK1- and caspase-8-mediated caspase-1 activation is not known. Intriguingly, inhibition of both IKK $\beta$  and p38 MAPK induced RIPK1-dependent processing of caspase-8 and -1, and RIPK1-dependent death of  $\Delta$ YopJ-infected cells (Figure 12). Similarly to the outcome of WT Yp infection, this cell death was largely unaffected in *Ripk3<sup>-/-</sup>* cells, but was abrogated in the absence of both RIPK3 and caspase-8. Together, these data demonstrate that YopJ-dependent inhibition of NF- $\kappa$ B and MAPK signaling triggers RIPK1/caspase-8-mediated caspase-1 activation.

### **FADD is required for Yp-induced caspase-1 processing and cell death**

These findings, together with previous observations that YopP induces formation of a caspase-8, RIPK1, FADD complex (110), and that FADD plays a role in apoptosis

downstream of TRIF (22) suggested that FADD might play a role in YopJ-induced caspase-1 activation and cell death. *Fadd*<sup>-/-</sup> mice exhibit embryonic lethality that is reverted with loss of RIPK3 (160). As anticipated, YopJ-induced caspase-1 processing was indeed abrogated in *Ripk3*<sup>-/-</sup>*Fadd*<sup>-/-</sup> cells but not in *Ripk3*<sup>-/-</sup> cells (Figure 13A), whereas STm-infected cells exhibited robust caspase-1 processing in the absence of RIPK3 and FADD (Figure 13A and B). Consistent with the recent study by Gurung *et al.* (179), *Ripk3*<sup>-/-</sup>*Fadd*<sup>-/-</sup> BMDMs also showed a noticeable reduction in LPS+ATP-induced caspase-1 processing and cell death (Figure 13B and C). Moreover, pro-inflammatory cytokine production in response to LPS was reduced in BMDMs lacking RIPK3 and caspase-8 or FADD (Figure 14), consistent with recent findings that pro-IL1 $\beta$  expression is reduced in these cells (179, 180, 221). Whereas Gurung *et al.* observed that caspase-8 contributes to LPS+ATP-induced canonical inflammasome activation (179), unlike with FADD deficiency, we did not observe a consistent reduction in caspase-1 processing in *Ripk3*<sup>-/-</sup>*Casp8*<sup>-/-</sup> macrophages treated with LPS+ATP, and we were unable to detect caspase-8 processing in LPS+ATP-treated cells. The contribution of FADD and caspase-8 to LPS+ATP-induced caspase-1 activation may relate to differential effects on NLRP3 inflammasome priming.

### **YopJ-induced caspase-8 activation promotes *anti-Yersinia* immune defense *in vivo***

YopJ promotes dissemination of *Yersinia* to systemic tissues (97). However, increasing YopJ-mediated cytotoxicity paradoxically enhances immune clearance and reduces virulence (89). How this cytotoxicity contributes to host defense *in vivo* is not known. We therefore infected bone marrow chimeric mice lacking both RIPK3 and caspase-8 in the hematopoietic compartment, as these cells cannot undergo YopJ-induced cell death. Critically, in contrast to littermate control, B6, or *Ripk3*<sup>-/-</sup> BM chimeras,

mice with a caspase-8-deficient hematopoietic compartment rapidly succumbed to infection with a Yp strain that is non-lethal to WT mice (222), (Figure 15A and Figure 16A). Surprisingly, *Ripk3<sup>-/-</sup>Casp8<sup>-/-</sup>* chimeric mice were deficient in production of serum IFN $\gamma$ , IL-6 and IL-1 $\beta$  despite a several-log increase in bacterial CFU in infected tissues on day 6 post-infection, (Figure 15B, C and Figure 16B). Both innate and adaptive *Ripk3<sup>-/-</sup>Casp8<sup>-/-</sup>* cells failed to produce cytokines, as inflammatory monocytes in the mLNs, and splenic NK and T cells were all defective in production of TNF $\alpha$ , and IFN $\gamma$  at day 6 post-infection (Figure 15D-H and Figure 16C). In contrast, the chemokine MCP-1 was not affected in *Ripk3<sup>-/-</sup>Casp8<sup>-/-</sup>* chimeric mice (Figure 15B). On day 3 post-infection., *Ripk3<sup>-/-</sup>Casp8<sup>-/-</sup>* chimeras had a higher proportion of TNF-producing inflammatory monocytes in the spleen (Figure 17B) suggesting that caspase-8 deficiency *in vivo* does not lead to a failure of cell-intrinsic cytokine production per se. However, in contrast to caspase-8-sufficient animals, *Ripk3<sup>-/-</sup>Casp8<sup>-/-</sup>* chimeras failed to maintain or upregulate cytokine production in the spleen over the course of infection, while cytokine production in the mLNs, where bacterial burdens were similar across genotypes, was defective on both days 3 and 5 (Figure 17A-C).

These findings demonstrate that combined deficiency of RIPK3 and caspase-8 results in severe susceptibility to WT Yp infection, but whether this is due to a failure to respond to the activity of YopJ, or due to a more global failure to induce immune responses was not clear. Importantly, *Ripk3<sup>-/-</sup>Casp8<sup>-/-</sup>* bone marrow chimeric animals were capable of surviving infection with  $\Delta$ YopJ Yp, had significantly lower bacterial burdens of  $\Delta$ YopJ in their spleen and liver, and partially recovered production of intracellular TNF (Figure 18A-C). Despite elevated bacterial burdens, in the *Ripk3<sup>-/-</sup>Casp8<sup>-/-</sup>* chimeras, these mice had smaller splenic lesions that lacked close association of neutrophils with bacteria, as compared with control caspase-8-sufficient chimeras,

which had extensive lesions containing bacterial colonies surrounded by visible cell debris and neutrophilic infiltrates (Figure 18D and Figure 17D and E). These data are consistent with reduced levels of *in vivo* death of *Ripk3<sup>-/-</sup>Casp8<sup>-/-</sup>* cells. Intriguingly,  $\Delta$ YopJ-infected *Ripk3<sup>-/-</sup>Casp8<sup>-/-</sup>* chimeras showed significantly elevated numbers and extent of liver lesions as compared with Yp-infected animals, suggesting that in the absence of NF- $\kappa$ B blockade, *Ripk3<sup>-/-</sup>Casp8<sup>-/-</sup>* cells can generate protective inflammatory responses that correlate with increased cell death *in vivo* (Figure 18E-G). Together these findings demonstrate that YopJ-dependent triggering of caspase-8 plays a critical role in mediating anti-*Yersinia* immune defense *in vivo*, and that loss of RIPK3 and caspase-8 results in dysregulated inflammatory responses and failure to control *Yersinia*.

## Discussion

Caspase-1 and caspase-8 activation are generally induced by distinct stimuli. In contrast to caspase-1, which causes pyroptosis independently of other caspases, caspase-8 induces apoptosis through caspases-3 and -7. Caspase-8 can also mediate cleavage and secretion of IL-1 $\beta$  and IL-18 downstream of Fas/FasL signaling or ER stress (182, 223), and was recently reported to regulate expression of pro-IL1 $\beta$  (180, 221). We now demonstrate that caspase-8, RIPK1 and FADD mediate caspase-1 activation in response to the *Yersinia* virulence factor YopJ, thus revealing an unanticipated integration of caspase-1 and caspase-8 death pathways in response to *Yersinia* infection.

We cannot currently exclude the possibility that RIPK3 and caspase-8 function redundantly to mediate cell death, or that RIPK3-mediated necrosis contributes to host defense against *Yersinia*. Nevertheless, in caspase-8-sufficient cells, RIPK3 is dispensable for YopJ-induced cell death or caspase-1 activation, and in caspase-8

conditional knockout cells, RIPK3 does not contribute to YopJ-induced caspase-1 processing. Under certain conditions, RIPK3 can mediate caspase-1 activation and cell death in response to LPS (219) or cIAP inhibitors (220). Thus, while TLR stimulation alone triggers RIPK3-dependent necrosis in caspase-8-deficient cells, our data demonstrates that YopJ triggers cell death and caspase-1 processing through caspase-8. Engagement of caspase-1 by both of these pathways may enable the release of caspase-1-dependent inflammatory signals by dying cells, even when this caspase-1 activation does not occur in a canonical inflammasome platform. Our data suggest a model (Figure 19) whereby RIPK1, caspase-8, and FADD engage a cell death and caspase-1-activation pathway that promotes anti-microbial immune defense in response to pathogen-mediated interference with innate immune signaling pathways.

In addition to controlling cell-extrinsic death, caspase-8 also plays a role in NF- $\kappa$ B signaling and gene expression (170, 172, 180, 221), potentially via cleavage of cFLIP (120, 169). However, YopJ-induced caspase-1 activation and cell death via caspase-8 and FADD are independent of LPS-induced priming, because they are triggered by NF- $\kappa$ B inhibition, and are independent of ASC, NLRP3, and IFNAR. Indeed, LPS priming prevents YopJ-driven cell death (93, 115), either due to upregulation of NF- $\kappa$ B-dependent survival genes, or inhibition of caspase-1 by YopM in LPS-primed cells (120).

A related study by Weng *et al.* observes a role for ASC in caspase-1 activation in *Y. pestis*-infected cells, in contrast to our studies here (124). YopJ isoforms from different *Yersinia* isolates exhibit different degrees of NF- $\kappa$ B inhibitory activity, and this also correlates with their degree of ASC/NLRP3 inflammasome activation (92). An alternative possibility is that Weng *et al.*, examine cleaved caspase-1 in supernatants (124), whereas we measure caspase-1 processing in cell lysates. Future studies will dissect the underlying basis for this apparent difference.

Finally, whether cell death or dysregulated cytokine production or both are directly responsible for the inability of caspase-8-deficient animals to clear *Yersinia* infection remains to be determined. The drop in cytokine production over the course of Yp infection in *Ripk3<sup>-/-</sup>Casp8<sup>-/-</sup>* chimeric mice may be due to increased blockade of signaling pathways as a consequence of progressively greater bacterial burden over time. Caspase-8-mediated cell death and caspase-1 activation in response to blockade of innate signaling may thus mobilize bystander cells for rapid cytokine production and/or phagocytosis of pathogen-associated cell debris.

**Figure 5**

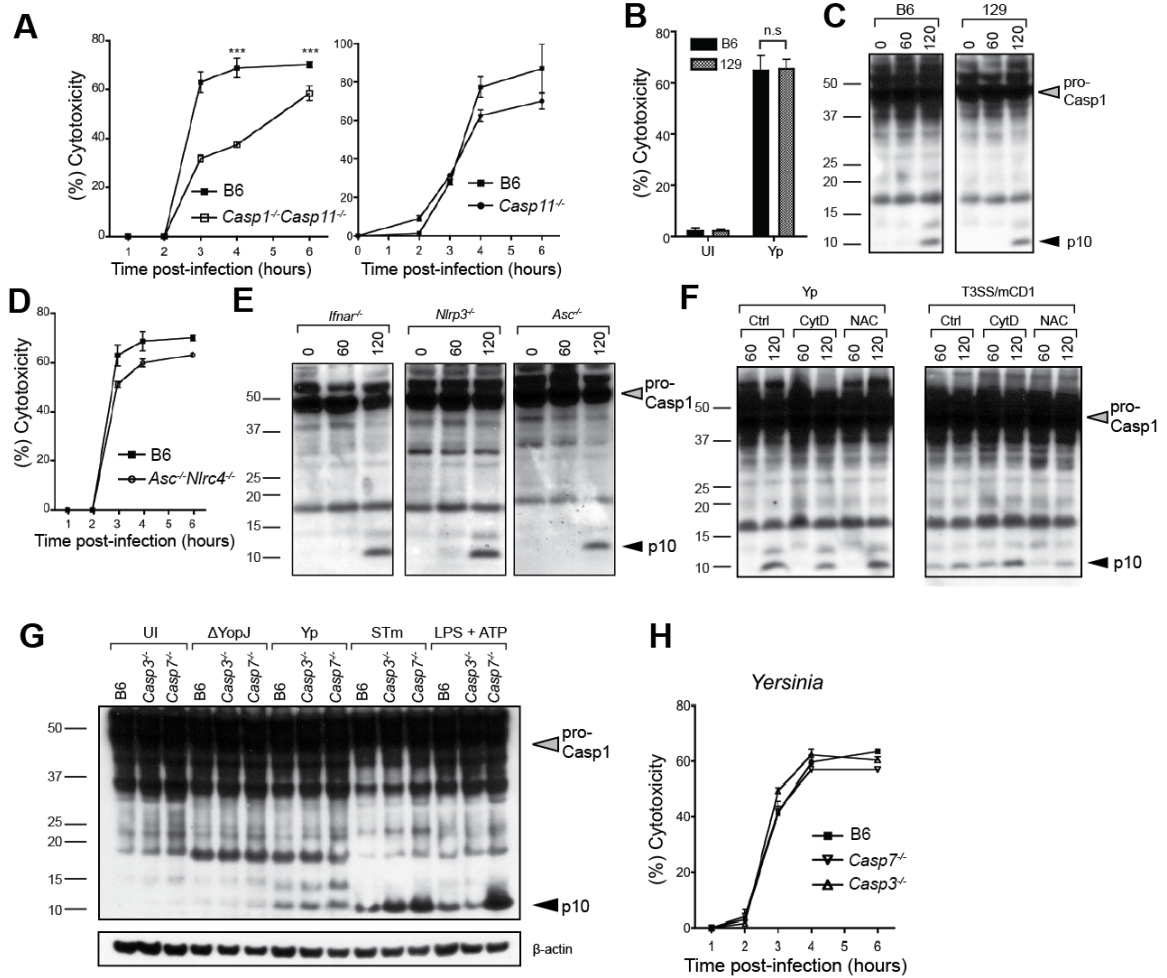


**Figure 5. Caspase-1 contributes to *Yersinia*-induced cell death and neither ASC, NLR4, NLRP3, nor IFNAR are required for *Yersinia*-induced death.**

(A) B6, *Casp1<sup>-/-</sup>Casp11<sup>-/-</sup>* or *Casp11<sup>-/-</sup>* BMDMs were infected with Yp and LDH release was measured at indicated time points. (B) % Cytotoxicity (LDH release) from B6 and 129/SvImJ BMDMs infected with Yp for 4 hrs. (C) Cell lysates from B6 and 129/SvImJ BMDMs were probed for caspase-1 processing by western analysis at 0, 60 and 90 minutes post-infection with Yp. (D) % Cytotoxicity (LDH release) from B6 and *Asc<sup>-/-</sup>Nlr4<sup>-/-</sup>* BMDMs at indicated time points. (E) Cell lysates from *Ifnar<sup>-/-</sup>*, *Nlrp3<sup>-/-</sup>* and *Asc<sup>-/-</sup>* BMDMs were probed for caspase-1 processing at 0, 60 and 120 minutes post-infection with *Yersinia*. (F) B6 BMDMs were pretreated with 0.5  $\mu$ g/mL cytochalasin D (CytD) or 25 mM N-acetylcysteine (NAC) prior to infection with *Yersinia* (Yp) or *Yersinia* expressing the type three secretion system on a plasmid (T3SS/mCD1). Cell lysates were probed for caspase-1 processing at 60 and 120 minutes post-infection. (G) B6, *Casp3<sup>-/-</sup>* and *Casp7<sup>-/-</sup>* BMDMs were infected with wild type *Yersinia* (Yp), YopJ-deficient Yp ( $\Delta$ YopJ) for 2 hrs or *Salmonella* (STm) for 1 hr, or were primed with LPS (50 ng/mL) for 3 hrs followed by ATP (2.5 mM) for 1 hr, or left uninfected (UI). Cell lysates were assayed for caspase-1 processing by western analysis. (H) B6, *Casp3<sup>-/-</sup>* and *Casp7<sup>-/-</sup>* BMDMs were infected with Yp and LDH release was measured at indicated time points. Error bars indicate mean  $\pm$  s.e.m of triplicates. \*\*\*  $p < 0.0001$

**Figure 6**

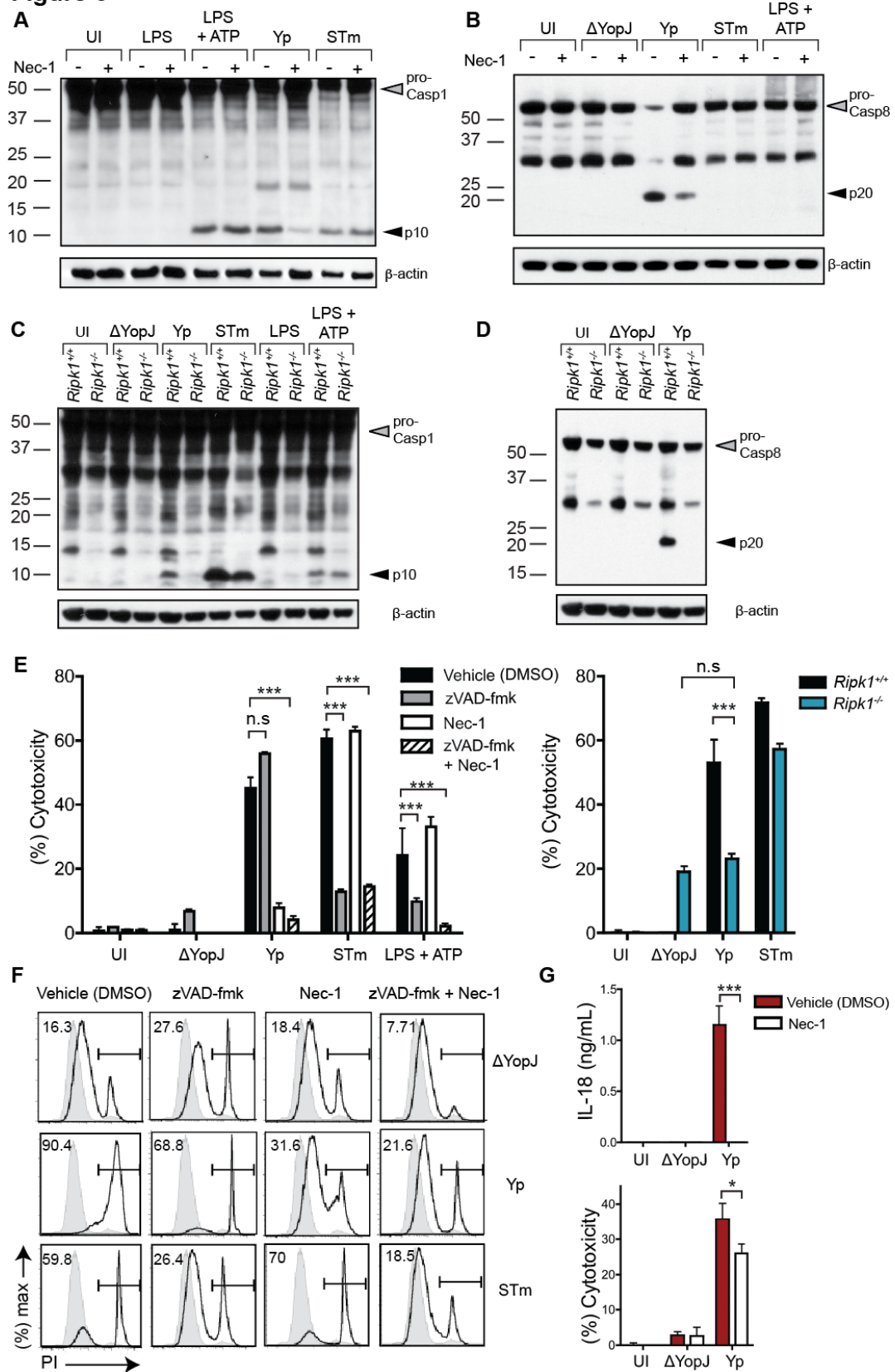




**Figure 6. RIPK1 is required for *Yersinia*-induced caspase-1 processing and cell death.**

(A, B) B6 BMDMs were either left uninfected (UI), LPS-primed (50 ng/mL) for 3 hrs followed by ATP (2.5 mM) for 1 hr (LPS+ATP), infected with wild type *Yersinia* (Yp) or YopJ-deficient Yp ( $\Delta$ YopJ) for 2 hrs or *Salmonella* (STm) for 1 hr. Cell lysates were probed for caspase-1 or -8 processing by western analysis. (C, D) *Ripk1*<sup>+/+</sup> and *Ripk1*<sup>-/-</sup> FLDMs were infected as in (A, B). (E) % Cytotoxicity was measured by lactate dehydrogenase (LDH) release from B6 BMDMs (left) and *Ripk1*<sup>+/+</sup> or *Ripk1*<sup>-/-</sup> FLDMs (right) that were uninfected or infected with  $\Delta$ YopJ, Yp or LPS + ATP for 4 hrs, or STm for 1 hr. (F) Flow cytometry for propidium iodide uptake (% PI<sup>+</sup> cells) by cells as treated in (E). (G) IL-18 assayed by ELISA, and LDH release on cells treated as in (E). 30  $\mu$ M necrostatin-1 (Nec-1) and 100  $\mu$ M zVAD-fmk were used 3 hrs prior to infection where indicated. Error bars indicate mean  $\pm$  s.e.m of triplicates and are representative of three or more independent experiments. \*\*\*  $p < 0.0001$ , \*\*  $p < 0.001$ , \*  $p < 0.01$ .

**Figure 7**

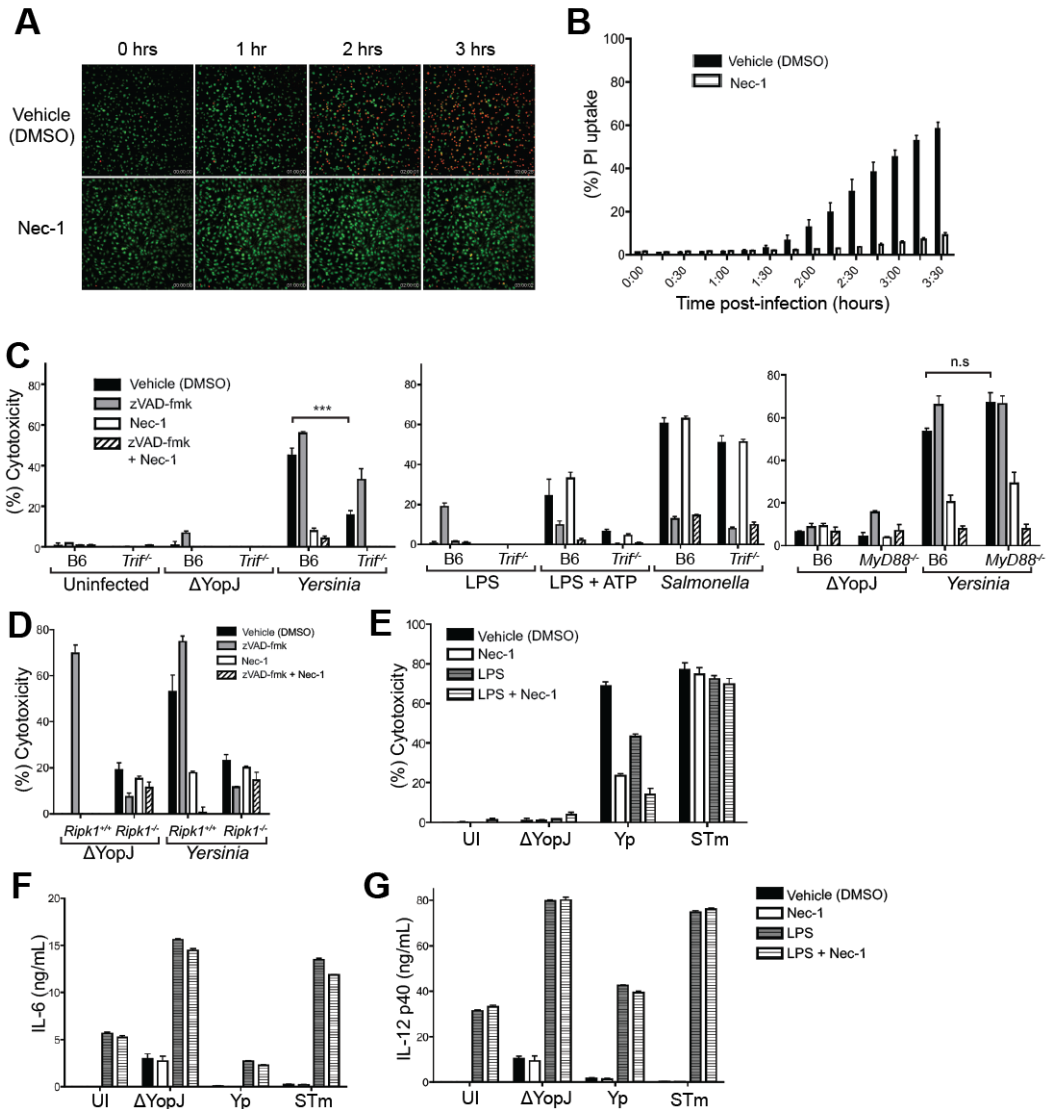


**Figure 7. YopJ induces caspase-1 activation and cell death during *Yersinia* infection is TRIF-dependent and reduced cytokine production during *Yersinia* infection is not due to cell death.**

(A-D) % Cytotoxicity (LDH release) from BMDMs uninfected or infected with the following strains of *Yersinia*  $\Delta$ YopJ, IP2666, YopJC172A and 32777 for 4 hrs, *Salmonella* (STm) for 1 hr or were primed with LPS (50 ng/mL) for 3 hrs followed by ATP (2.5 mM) for 1 hr, (see Table S1). (A) B6 BMDMs. (B) B6 and *Trif*<sup>-/-</sup> BMDMs. (C) *Ripk1*<sup>+/+</sup> and *Ripk1*<sup>-/-</sup> FLDMs. (D) B6 and *MyD88*<sup>-/-</sup> BMDMs. (E, F). B6 BMDMs were loaded with Cell-Tracker Green, washed and treated with Nec-1 (30  $\mu$ M) 3 hrs prior to infection with *Yersinia* as described in Figure 1. PI uptake was measured by time-lapse confocal microscopy. (E) Representative images at indicated times, 10x magnification, (F) average percentage PI+ cells from 5 fields/time point, approx. 500 cells/field. (G) % Cytotoxicity (LDH release) from BMDMs infected with wild type *Yersinia* (Yp), YopJ-deficient Yp ( $\Delta$ YopJ), or left uninfected (UI) for 4 hrs or infected with *Salmonella* (STm) for 1 hr. (H) IL-6, IL-12p40/70 assayed by ELISA on cells treated as in (G). Cells were treated with LPS (50 ng/mL), Nec-1 (30  $\mu$ M) or zVAD-fmk (100  $\mu$ M) 3 hrs prior to infection where indicated. Error bars indicate mean  $\pm$  s.e.m of triplicates. \*\*\*  $p < 0.0001$ .

**Figure 8**

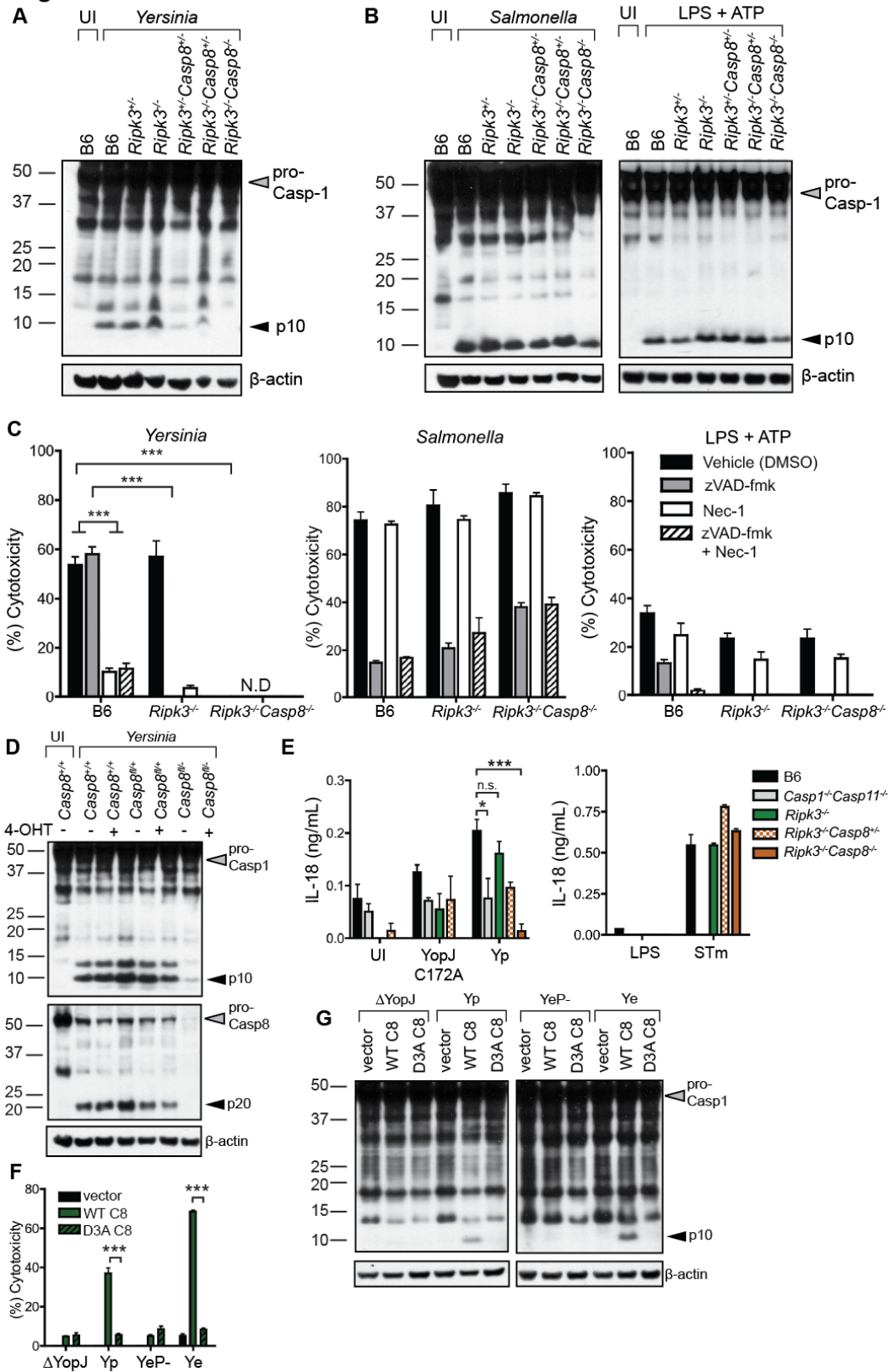


**Figure 8. Caspase-1 activation and IL-18 secretion in response to *Yersinia* infection require caspase-8.**

(A, B) Lysates from BMDMs left uninfected (UI), infected with Yp for 2 hrs, STm for 1 hr or LPS-primed for 3 hrs and ATP for 1 hr (LPS+ATP) were probed for caspase-1 processing by western analysis. (C) % Cytotoxicity (LDH release) of BMDMs infected with Yp for 4 hrs, STm for 1 hr or treated with LPS+ATP as in (A). (D) 4-OHT-treated (50 nM) BMDMs infected as in (A). (E) IL-18 assayed by ELISA from BMDMs left uninfected (UI), infected with isogenic Yp 32777, YopJ C172A or STm or LPS-primed for 4 hrs. (F, G) *iR3<sup>-/-</sup>C8<sup>-/-</sup>* BMDMs were reconstituted with empty vector, wild type caspase-8 (WT C8) or non-cleavable mutant caspase-8 (D3A C8). (F) LDH release 4 hrs post-infection. (G) caspase-1 processing by western analysis, MOI of 50:1. 30  $\mu$ M necrostatin-1 (Nec-1) and 100  $\mu$ M zVAD-fmk were used 3 hrs prior to infection where indicated. N.D., not detected. Error bars indicate mean  $\pm$  s.e.m of triplicates and are representative of three or more independent experiments. \*\*\*  $p < 0.0001$ .

**Figure 9**

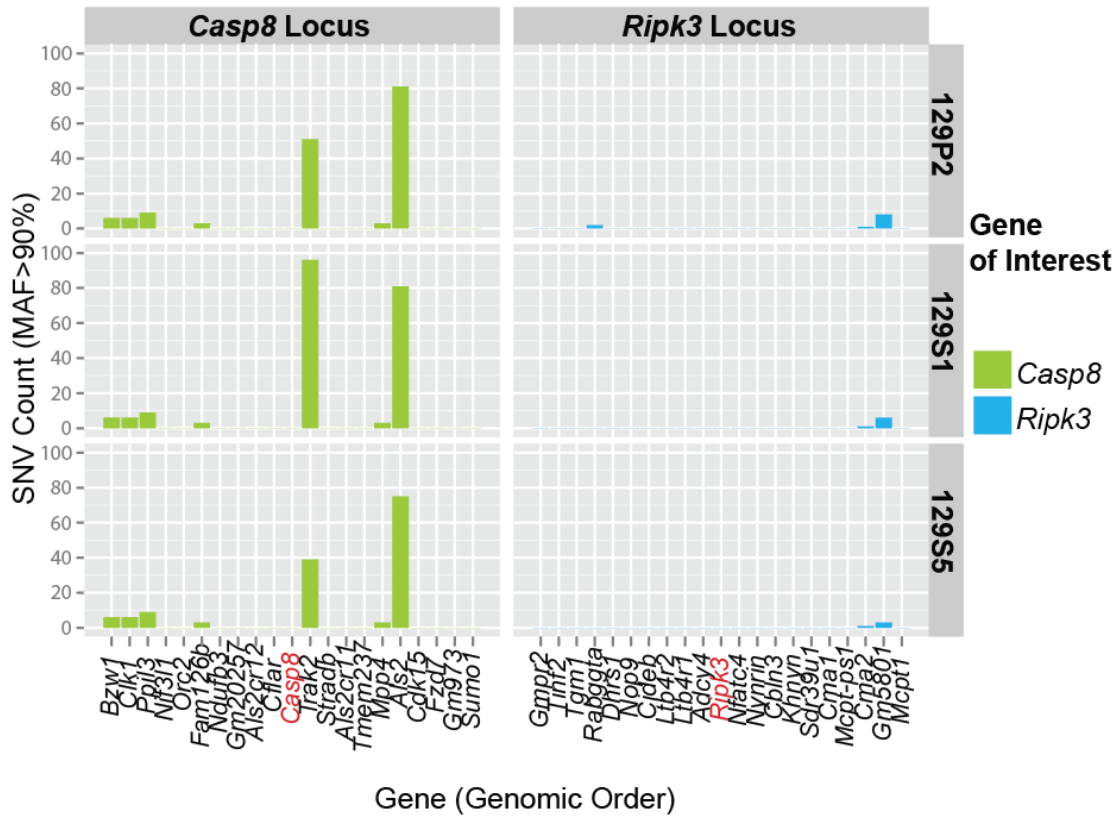


**Figure 9. Caspase-8, cFLIP and RIPK3 loci are identical in B6 and 129 mice.**

Whole genome sequencing data were downloaded from the Sanger Center (UK) for inbred mouse strains B6, 129P2, 129S1, 129S5. A modified version of Bambino variant detector was run, using C57BL/6 as the reference sample for comparison, to call single nucleotide variations (SNVs). Only SNVs with a variant allele frequency (VAF) > 90% based on NGS read counts were used in this analysis. All SNVs (including synonymous and non-synonymous) +/- 10 genes on either side of *Casp8* or *Ripk3* are reported here.

**Figure 10**

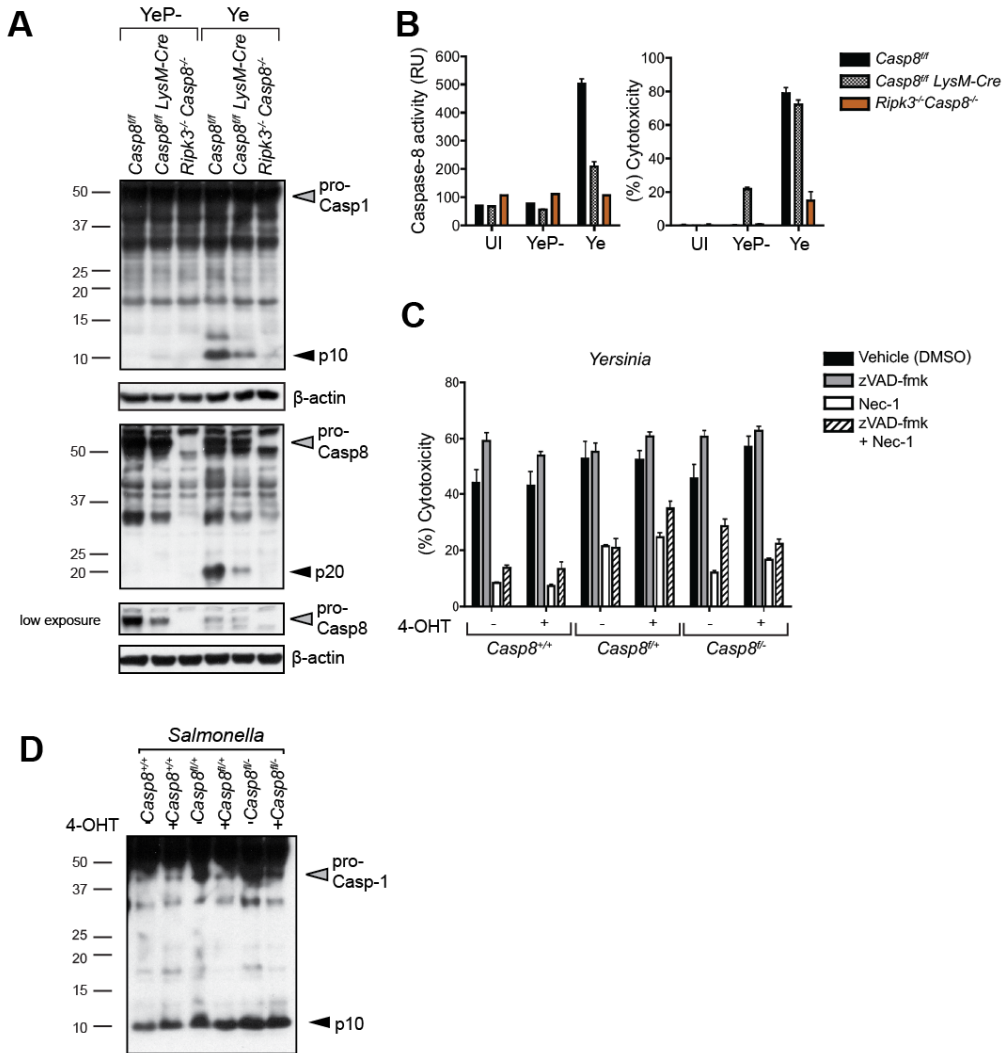


**Figure 10. YopJ-dependent caspase-1 processing requires caspase-8.**

(A) Caspase-1 and -8 processing in cell lysates of BMDMs and (B) caspase-8 activity measured 2 hrs post-infection with YeP- and Ye (see Table S2). (C) % Cytotoxicity (LDH release) in cells treated as in Fig 2D. (D) 4-OHT-treated (50 nM) BMDMs of indicated genotypes were infected with *Salmonella* (1 hr) and cell lysates were probed for caspase-1 processing by western analysis. *Casp8<sup>fl/fl</sup> LysM-Cre* = *Casp8<sup>fl/fl</sup> x LysM-Cre*. 30  $\mu$ M necrostatin-1 (Nec-1) and 100  $\mu$ M zVAD-fmk were used 3 hrs prior to infection where indicated. Error bars indicate mean  $\pm$  s.e.m of triplicates.

**Figure 11**

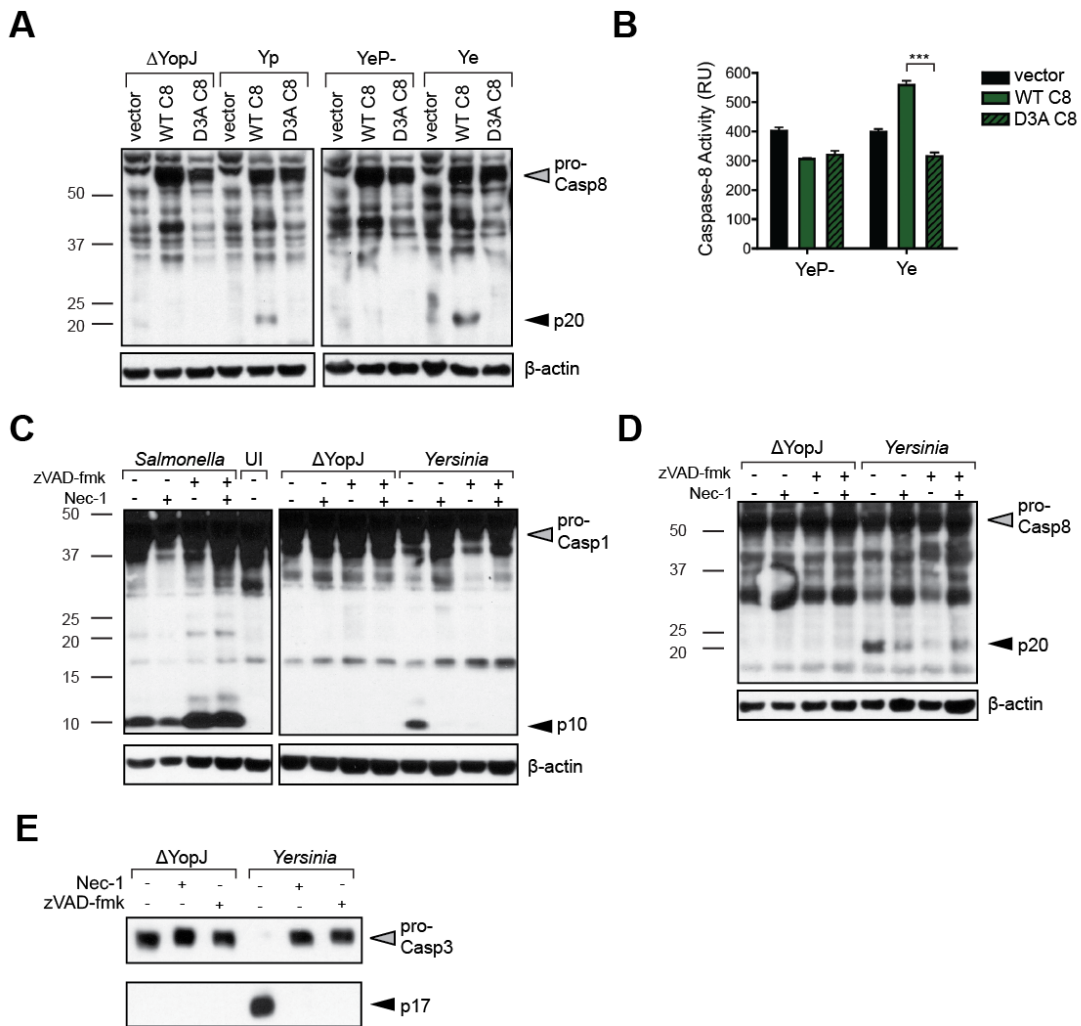


**Figure 11. Active caspase-8 is required for *Yersinia*-induced caspase-1 processing.**

(A) Caspase-8 processing by western blotting and (B) caspase-8 activity from immortalized *Ripk3*<sup>-/-</sup>*Casp8*<sup>-/-</sup> BMDMs reconstituted with empty vector, wild type caspase-8 (WT C8) or non-cleavable caspase-8 (D3A C8) and infected with the indicated *Yersinia* strains as in Fig 2f and e, MOI of 50:1. (C-E) B6 BMDM cell lysates were probed for caspase-1, -8 and -3 processing 2 hrs post-infection with indicated *Yersinia* strains and 1 hr post-infection with *Salmonella*. 30  $\mu$ M necrostatin-1 (Nec-1) and 100  $\mu$ M zVAD-fmk were used 3 hrs prior to infection where indicated. Error bars indicate mean  $\pm$  s.e.m of triplicates.

**Figure 12**

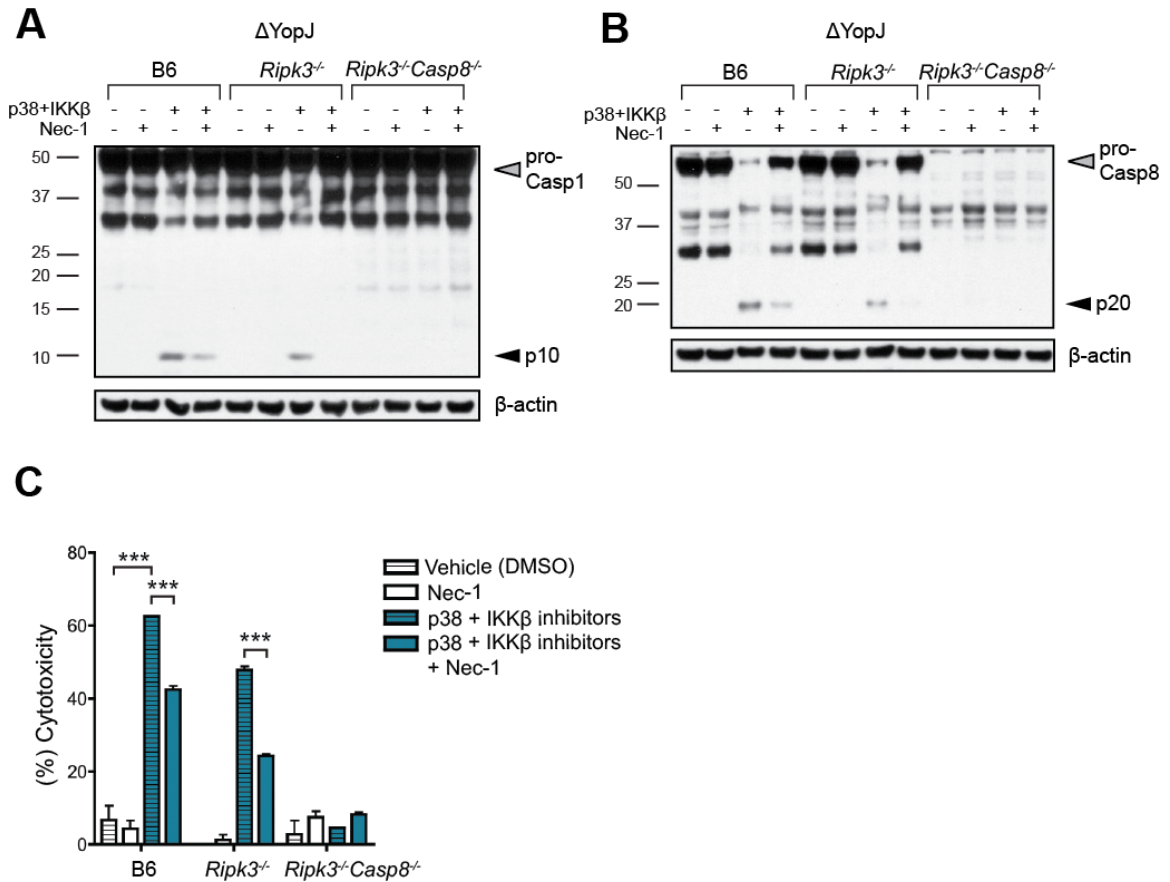


**Figure 12. YopJ-deficient *Yersinia* induces caspase-8-dependent caspase-1 processing in the presence of NF- $\kappa$ B and MAPK inhibitors.**

B6, *Ripk3<sup>-/-</sup>* (*R3<sup>-/-</sup>*), or *Ripk3<sup>-/-</sup>Casp8<sup>-/-</sup>* (*R3<sup>-/-</sup>C8<sup>-/-</sup>*) BMDMs were infected with  $\Delta YopJ$ . 60  $\mu$ M necrosta-tin-1 (Nec-1) and IKK $\beta$  and p38 inhibitors (5  $\mu$ M) were used 2 hrs and 1 hr prior to infection, respec-tively. Cell lysates were assayed for (A) caspase-1 and (B) caspase-8 processing by western analy-sis 4 hrs post-infection. (C) % Cytotoxicity was measured by LDH release 8 hrs post-infection. Error bars indicate mean  $\pm$  s.e.m of triplicates. \*\*\*  $p < 0.0001$ .



**Figure 13**

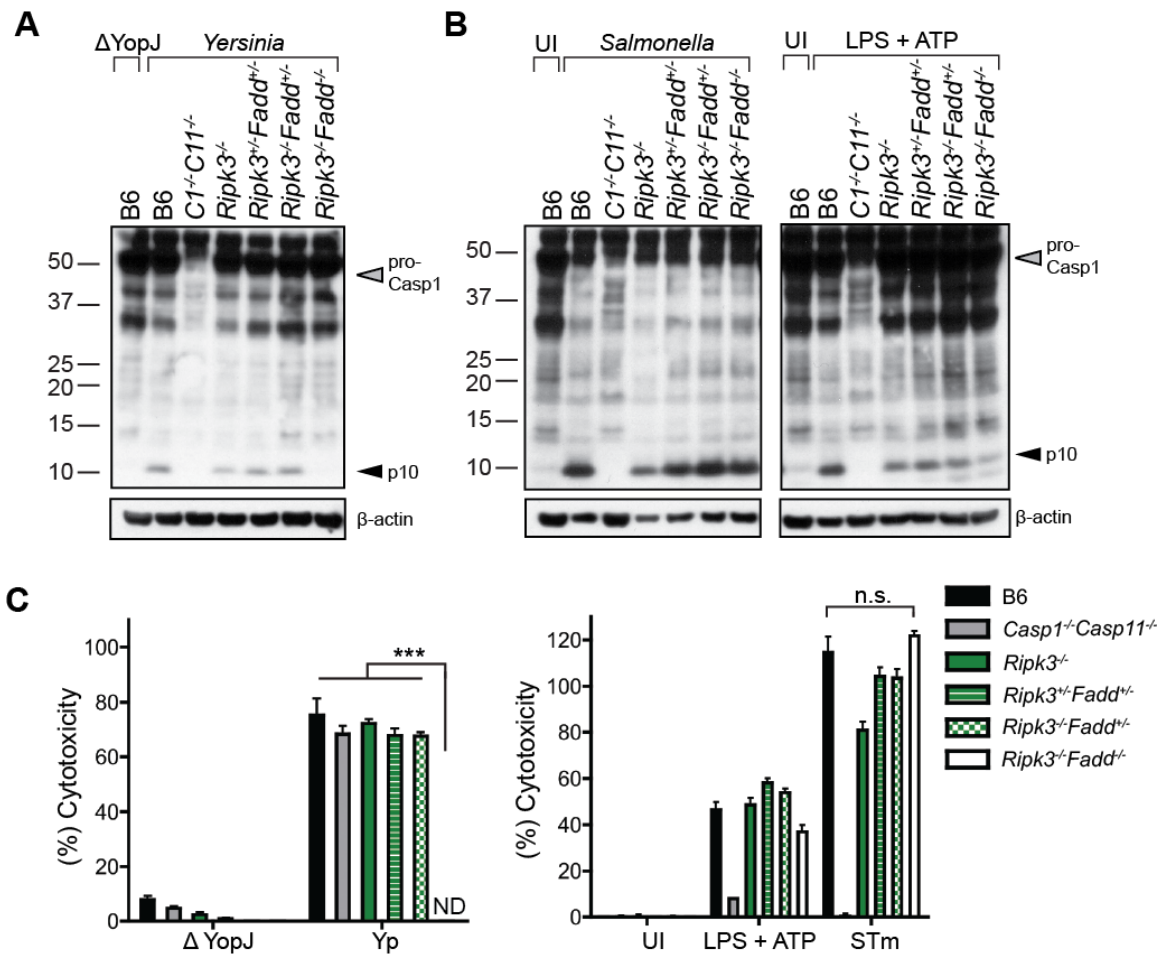


**Figure 13. FADD is required for *Yersinia*-induced caspase-1 processing and cell death in the absence of RIPK3.**

(A, B) BMDM cell lysates were probed for caspase-1 by western after infection with  $\Delta$ YopJ or Yp for 2 hrs, STm for 1 hr, treated with LPS for 3 hrs and ATP for 1 hr (LPS+ATP), or left uninfected (UI). (C) % Cytotoxicity (LDH release) of BMDMs left uninfected, infected with  $\Delta$ YopJ or Yp for 4 hrs, STm for 1 hr or LPS+ATP as in (A). N.D., not detected. Error bars indicate mean  $\pm$  s.e.m. of triplicates and are representative of three or more independent experiments. \*\*\*  $p < 0.0001$

**Figure 14**

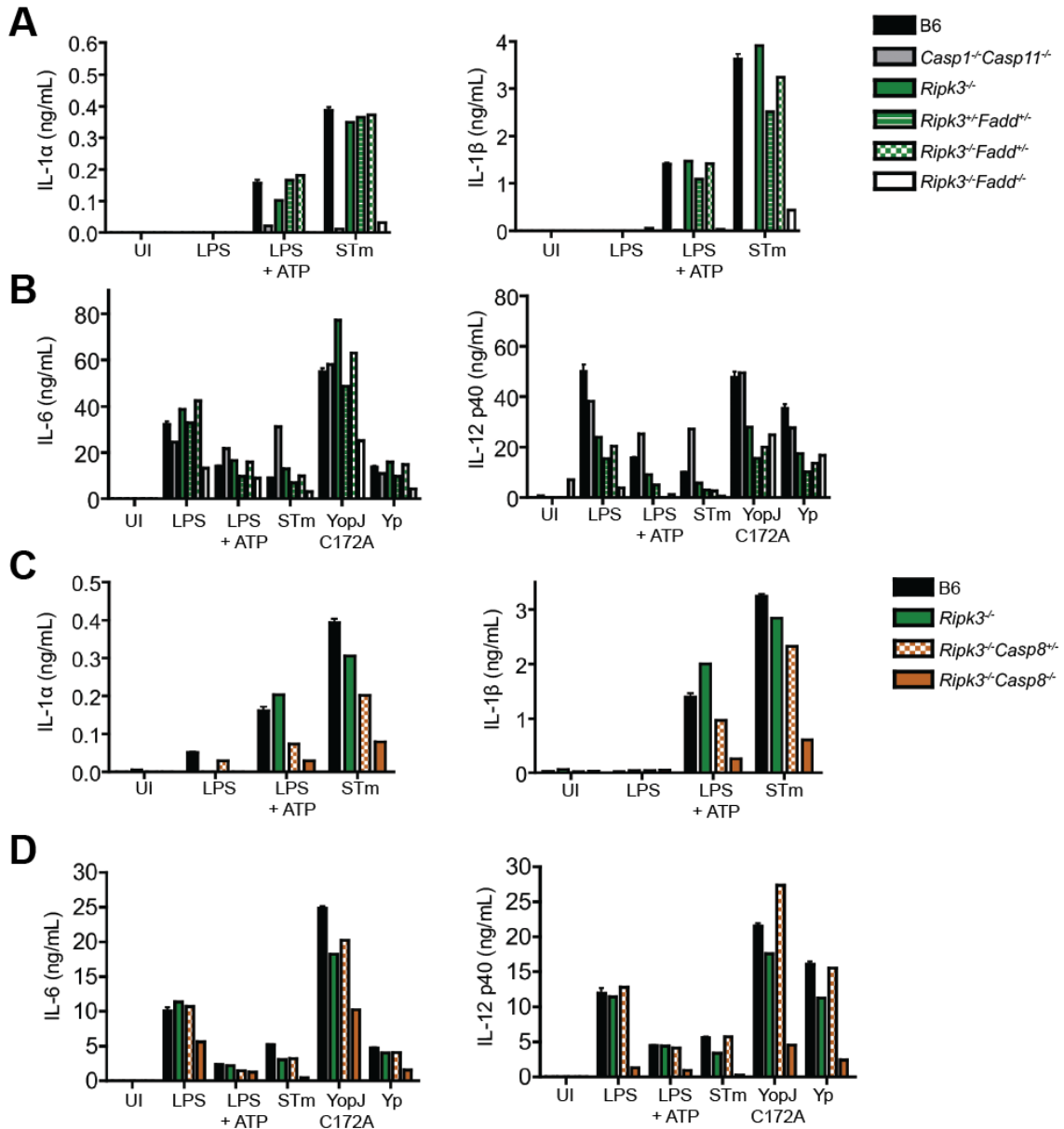


**Figure 14. *Ripk3<sup>-/-</sup>Casp8<sup>-/-</sup>* and *Ripk3<sup>-/-</sup>Fadd<sup>-/-</sup>* BMDMs have a defect in LPS priming.** BMDMs were primed with LPS (50 ng/mL) 3 hrs prior to infection with *Yersinia* (YopJ C172A or isogenic 32777, Yp) or *Salmonella*, or treated with ATP (2.5mM) for 4 hrs. Supernatants were assayed for caspase-1-dependent and -independent cytokine secretion by ELISA. (A, C) IL-1 $\alpha$ , - $\beta$  (B, D) IL-6, IL-12p40. Error bars indicate mean  $\pm$  s.e.m. of triplicates.

**Figure 15**

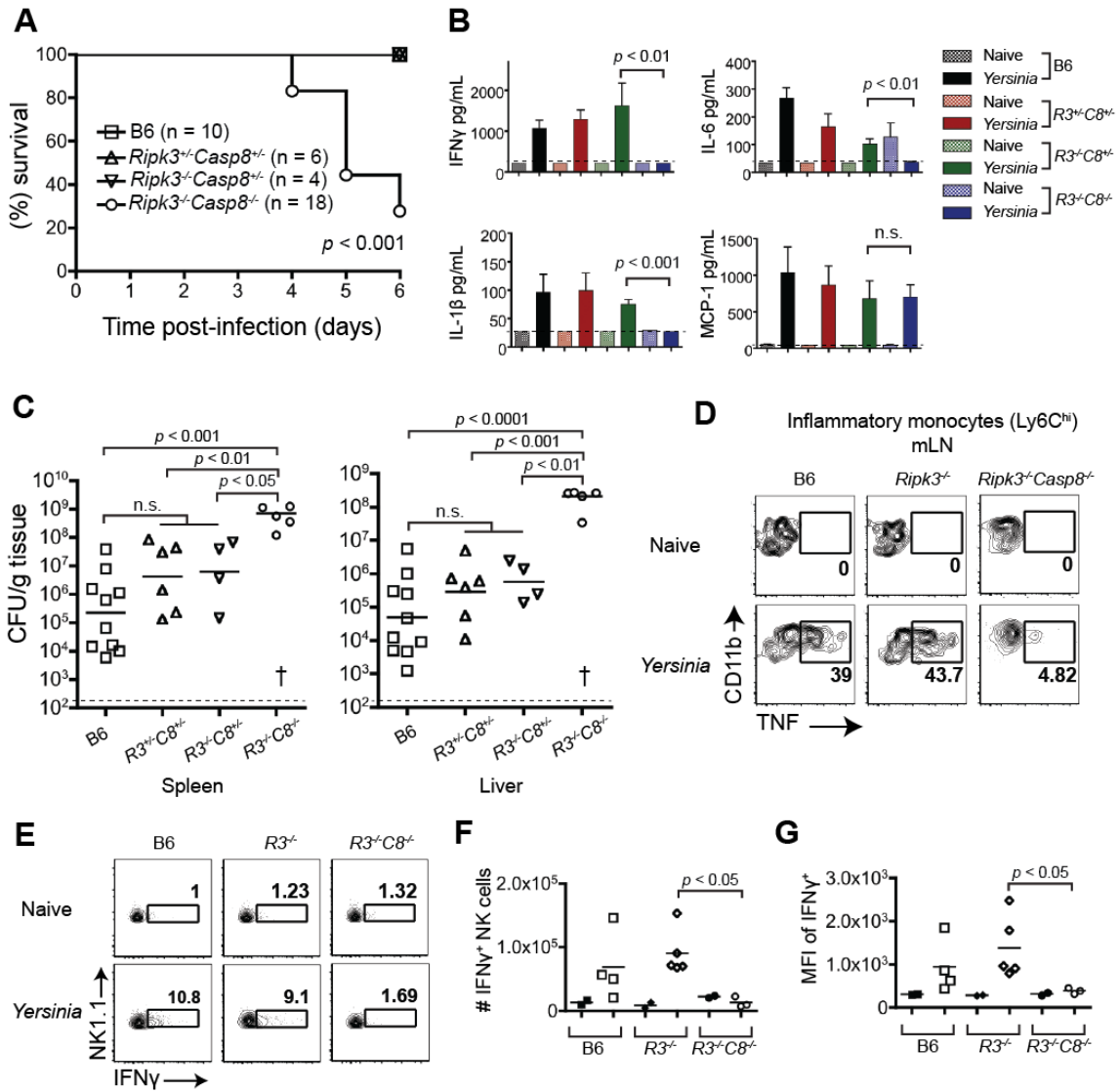


**Figure 15. RIPK3/caspase-8-deficient mice are highly susceptible to *Yersinia* infection and have dysregulated cytokine production.**

Lethally-irradiated B6.SJL mice were reconstituted with B6, *Ripk3<sup>-/-</sup>Casp8<sup>-/-</sup>*, *Ripk3<sup>-/-</sup>Casp8<sup>-/-</sup>*, *Ripk3<sup>-/-</sup>* or *Ripk3<sup>-/-</sup>Casp8<sup>-/-</sup>* BM and orally infected with 8-10 $\times$ 10<sup>7</sup> cfu *Yersinia* (Yp)/mouse. Mice were assayed for (A) survival, (B) serum IFN $\gamma$ , IL-6, IL-1 $\beta$  and MCP-1 by Luminex, (C) bacterial loads/gram tissue, (D) %TNF<sup>+</sup> inflammatory monocytes in mesenteric lymph nodes (mLN) by flow cytometry. (E-H) IFN $\gamma$  production from splenic NK cells (NK1.1<sup>+</sup>) was assessed by flow cytometry. (E) Representative plots (F) total numbers (G) MFI. (H) MFI of splenic CD4<sup>+</sup> and CD8<sup>+</sup> T cell-IFN $\gamma$  production. (B-H) day 6 post-infection. “†” denotes 13 dead or moribund mice not harvested for CFUs. Dotted lines represent limit of detection. Solid lines represent means (ELISA) or geometric means (CFU). Flow cytometry plots in D were gated on live CD45.2<sup>+</sup>, CD11c<sup>-</sup>, Ly6C<sup>hi</sup> cells and in (E-G) on live CD45.2<sup>+</sup> cells. *R3C8* = *Ripk3Casp8*. Statistical analysis in F-G was performed using the Mann-Whitney U Test. Data representative of two or more independent experiments.

**Figure 16**

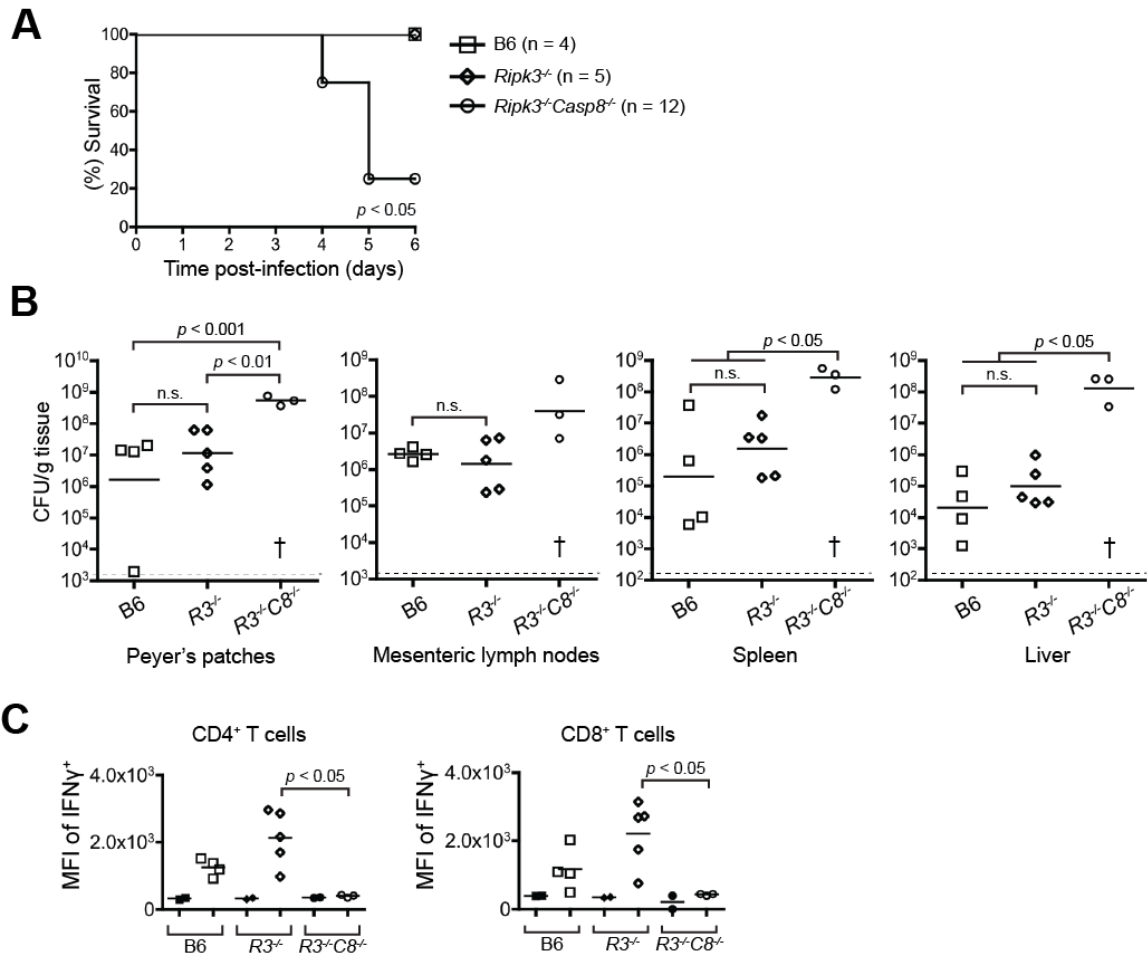


**Figure 16. RIPK3-deficient mice are not more susceptible to *Yersinia* infection and exhibit wild-type levels of IFN $\gamma$  production from adaptive cells.**

Lethally-irradiated B6.SJL mice were reconstituted with B6, *Ripk3*<sup>-/-</sup> or *Ripk3*<sup>-/-</sup>*Casp8*<sup>-/-</sup> BM and orally infected with  $8-10 \times 10^7$  cfu Yp/mouse as in Figure 4. Mice were monitored for (A) survival, (B) bacterial loads/gram tissue at day 6 post-infection. “†” denotes 9 dead mice not harvested for CFUs. Dotted lines represent limit of detection. Solid lines represent or geometric means (CFU). (C) Cells were gated on live CD45.2<sup>+</sup> CD4<sup>+</sup> or CD8<sup>+</sup> cells.

**Figure 17**

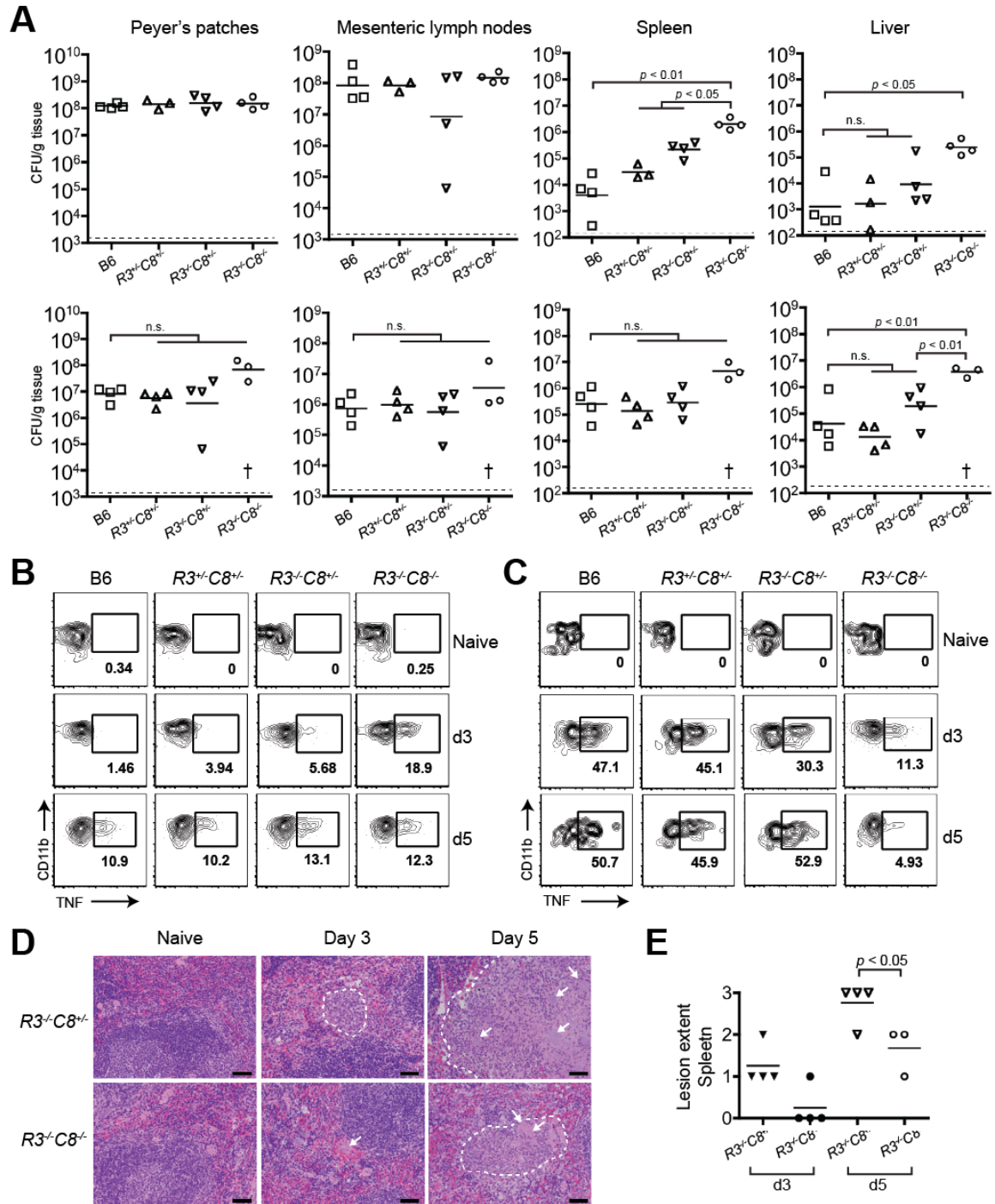


**Figure 17. RIPK3/caspase-8-deficient mice experience faster bacterial dissemination and dysregulated cytokine production even at early time points during *Yersinia* infection.**

Lethally-irradiated B6.SJL mice were reconstituted and infected as in Figure 4. (A) Bacterial loads/gram tissue on days 3 (top) and 5 (bottom) post-infection. (B, C) %TNF<sup>+</sup> inflammatory monocytes in (B) spleens and (C) mesenteric lymph nodes were analyzed by flow cytometry. (D) Representative images of spleen in naïve and *Yersinia*-infected *Ripk3*<sup>-/-</sup>*Casp8*<sup>+/-</sup> and *Ripk3*<sup>-/-</sup>*Casp8*<sup>-/-</sup> chimeric mice at days 3 and 5, showing lesions of necrosuppurative splenitis (dashed white lines) and extracellular bacterial colonies (arrows) in infected mice. Hematoxylin and eosin staining. scale bars = 50 μm. (E) Quantification of lesion severity in spleens. “†” denotes 3 dead mice not harvested for CFUs. Dotted lines represent limit of detection. Solid lines represent geometric means. Flow cytometry plots were gated on live CD45.2<sup>+</sup>, CD11c<sup>-</sup>, CD11b<sup>hi</sup>, Ly6C<sup>hi</sup>. R3C8 = *Ripk3Casp8*.

**Figure 18**

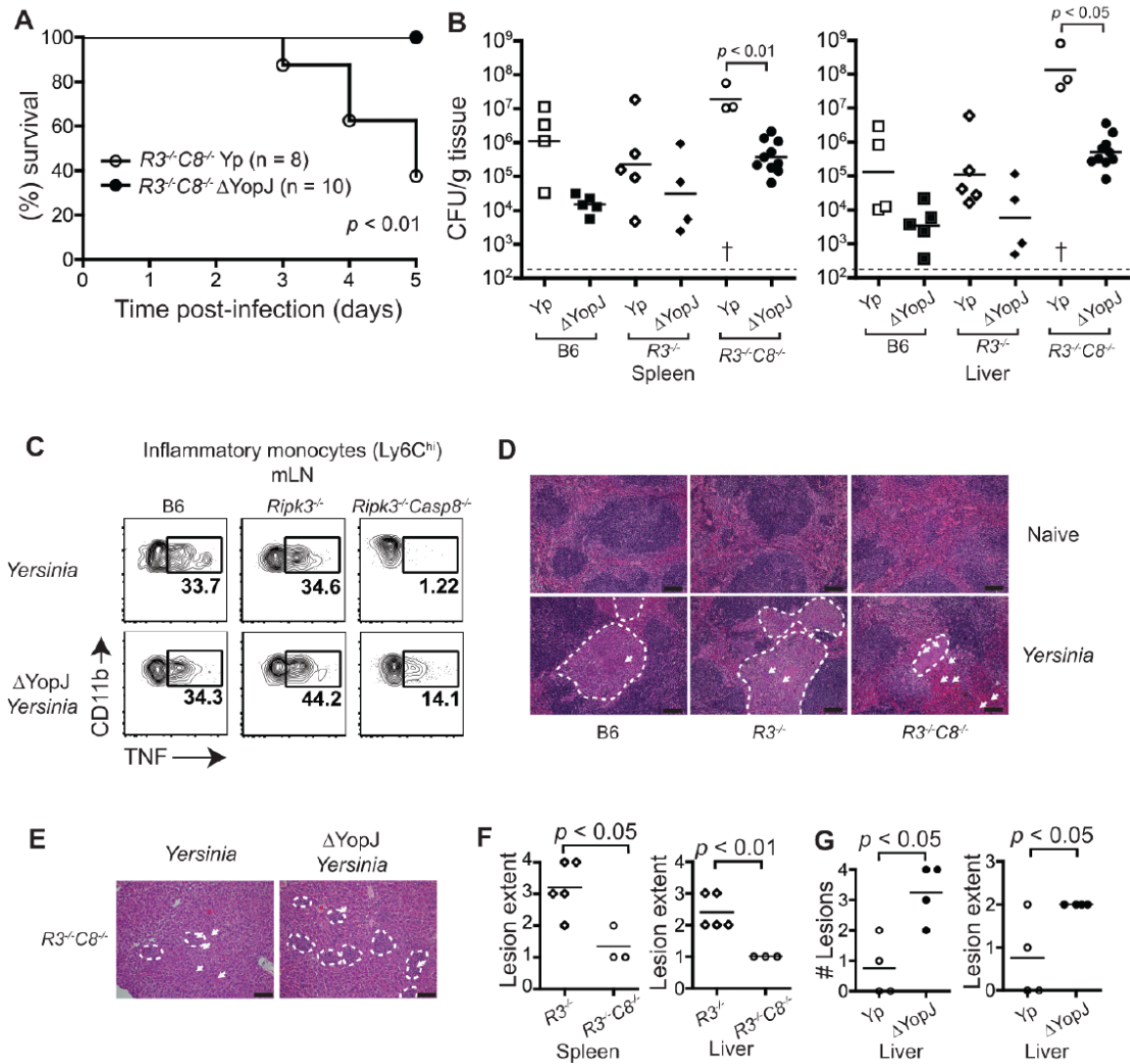


**Figure 18. RIPK3/caspase-8-deficient mice survive  $\Delta$ YopJ infection and partially recover intracellular cytokine production.**

Lethally-irradiated B6.SJL mice were reconstituted with B6,  $Ripk3^{-/-}$  or  $Ripk3^{-/-}Casp8^{-/-}$  BM and orally infected with  $8-10 \times 10^7$  cfu *Yersinia* (Yp) or  $\Delta$ YopJ *Yersinia* ( $\Delta$ YopJ)/mouse. Mice were assayed for (A) survival, (B) bacterial loads/gram tissue and (C) %TNF<sup>+</sup> inflammatory monocytes in mesenteric lymph nodes (mLN) by flow cytometry. (D, E) Representative images of H&E stained (D) spleen and (E) liver sections in naïve and infected chimeric mice, showing lesions of necrosuppurative inflammation (dashed white lines) and extracellular bacterial colonies (arrows) in infected mice. Scale = 50  $\mu$ m. (F, G) Quantification of number and extent of lesions. (B) Day 5. (C) Representative plots from pooled data on days 5 and 6 (%  $\pm$  s.e.m). (D-G) Day 6. “†” denotes 5 dead or moribund mice not harvested for CFUs. Dotted lines represent limit of detection. Solid lines represent means (histology) or geometric means (CFU). Flow cytometry plots were gated on live CD45.2<sup>+</sup>, CD11c<sup>+</sup>, CD11b<sup>hi</sup>, Ly6C<sup>hi</sup> cells. \*\* $p < 0.01$ , WT vs.  $\Delta$ YopJ infected  $Ripk3^{-/-}Casp8^{-/-}$  monocytes.  $R3C8 = Ripk3Casp8$ . Data representative of two or more independent experiments.

**Figure 19**

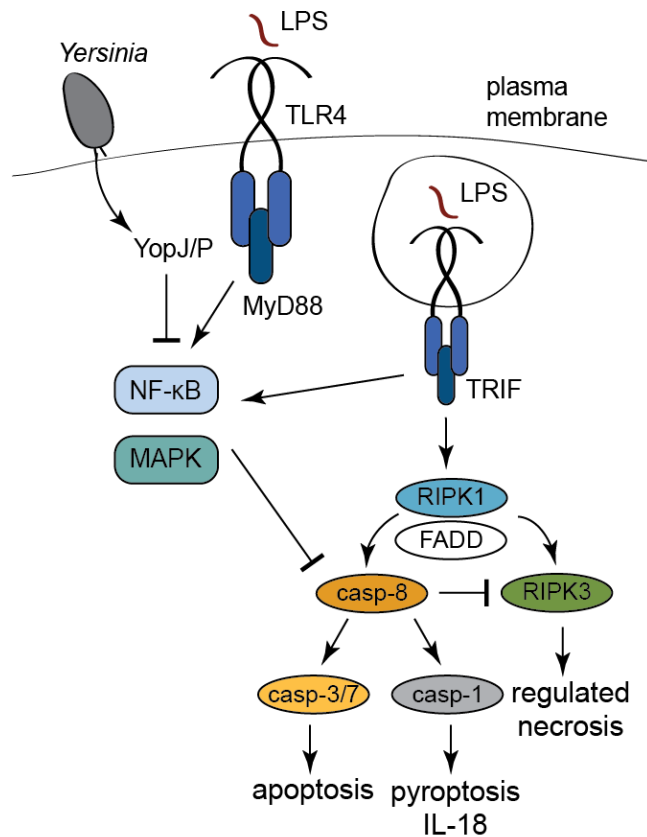


**Figure 19. *Yersinia* YopJ induces caspase-8/RIPK1/FADD dependent caspase-1 processing and cell death via inhibition of NF-κB and MAPK.**

*Yersinia* secretes YopJ into the host cytosol, which inhibits NF-κB and MAPK signaling. TRIF-dependent signals activate FADD/RIPK1, which can trigger caspase-8-dependent caspase-1 activation and cell death (pyroptosis). In the absence of caspase-8, *Yersinia* induces RIPK3-dependent necrosis. This pathway of Yp-induced cell death may enable the host to override inhibition of cytokine production by YopJ and promote anti-bacterial immune responses.



## **IV. CELL-INTRINSIC ACTIVITY OF UNCLEAVED CASPASE-8 CONTROLS EXPRESSION OF TLR-INDUCED INFLAMMATORY RESPONSES**

### **Background**

Pattern recognition receptors such as Toll-like receptors (TLRs) sense conserved microbial structures including lipopolysaccharide (LPS) or peptidoglycans (2). TLR ligation triggers MyD88- and TRIF-dependent MAPK and NF- $\kappa$ B signaling, which induces the expression of cell survival and inflammatory programs that are critical for host defense (224). TLR3 and TLR4 can also engage extrinsic death pathways, as TLR3/4 activation in the presence of pharmacological or microbial inhibitors of NF- $\kappa$ B results in cell death that is mediated by the cysteine protease caspase-8 (14-16). Upon receptor ligation, caspase-8 is recruited to a TRIF/RIPK1/FADD-containing complex via specific homotypic protein-protein interaction motifs (17). RIPK1 interacts with TRIF by means of RIP homology interaction motifs (RHIM) and can bind FADD through shared death domains (DD), which in turn engages caspase-8 via death effector domains (DED) (18, 19). Upon recruitment to this complex, caspase-8 undergoes dimerization and autoprocessing, which stabilizes the active enzyme, and initiates the proteolytic cascade that ultimately results in apoptotic disassembly of the cell (20).

Interestingly, spontaneous mutations in human caspase-8 that render it catalytically inactive are linked with primary immunodeficiency and recurrent sinopulmonary and mucocutaneous infections (225, 226). Similarly, individuals with mutations in the adaptor FADD suffer from recurrent infections and liver pathology, suggesting a role for caspase-8 and FADD in antimicrobial responses (227). Whereas initial studies observed that T, B and NK cells from patients with caspase-8 deficiency displayed defects in activation (172, 225), subsequent work revealed that caspase-8 is critical for lymphocyte survival and that rescuing this survival defect restored the ability

of T cells to respond to viral infection (25, 228). These studies suggested the possibility that the effect of caspase-8 on activation, at least in lymphocytes, may relate to its control of cell death.

The prosurvival function of caspase-8 serves to limit receptor-interacting serine/threonine protein kinase-3 (RIPK3)-dependent necroptosis, which occurs in the context of developmental and inflammatory cues (25, 26, 29-32). During homeostasis, RIPK3 is repressed by heterodimers of caspase-8 and its catalytically inactive homologue, cFLIP. However, inhibition of caspase-8 activity or deletion of caspase-8 releases the brake on RIPK3-dependent necroptosis (25, 26). TLR signaling normally prevents caspase-8-, FADD- and RIPK3-dependent cell death pathways both through transcriptional upregulation of pro-survival genes and through post-translational modification of key signaling proteins such as RIPK1 (229). Induction of cell death and inflammatory gene expression are therefore thought to be mutually exclusive programs. However, a number of recent studies including our own have demonstrated that caspase-8 nonetheless regulates anti-microbial innate responses (123, 124, 173, 179-182).

Specifically, combined deficiency of RIPK3 and caspase-8 or RIPK3 and FADD result in significant reduction in the secretion of a number of pro-inflammatory mediators as well as loss of inflammasome priming and activation in response to some stimuli (123, 124, 173, 179). Interestingly, while many of these inflammatory mediators are regulated by the NF- $\kappa$ B signaling pathway, whether caspase-8 regulates proximal NF- $\kappa$ B signaling, and even whether caspase-8 acts as a negative or positive regulator of inflammatory gene expression remains unresolved, due to the coupling of caspase-8 deficiency with induction of programmed necrosis. Thus, these studies take place either under conditions where RIPK3 is ablated (123, 124, 173, 179), or under conditions

where programmed necrosis may be occurring due to conditional deletion of caspase-8 (170, 172, 174, 230). Thus, how caspase-8 might function to regulate both cell death and inflammatory gene expression, and whether enzymatic activity plays a role in the latter response is currently unknown.

We now demonstrate that caspase-8 is necessary for cell-intrinsic control of key inflammatory cytokine gene expression in response to gram-negative bacterial pathogens as well as multiple TLR agonists. Notably, caspase-8 controls expression of a specific subset of genes critical for controlling inflammation and host defense. Moreover, regulation of gene expression by caspase-8 was independent of cell death and the known apoptotic caspases that are targets of caspase-8 cleavage. Surprisingly, the catalytic activity of caspase-8 was crucial for its control of optimal cytokine responses. As caspase-8 enzymatic activity is essential for both the apoptotic function of cleaved caspase-8 homodimers and the cell survival function of caspase-8/cFLIP heterodimers, we generated CRISPR-based caspase-8 knock-in mice in which the self-cleavage of caspase-8 was abrogated due to a mutation in aspartate 387 to alanine (*Casp8<sup>DA</sup>*). Intriguingly, *Casp8<sup>DA</sup>* macrophages were unable to undergo caspase-8-dependent apoptosis, but displayed no loss of caspase-8-dependent control of gene expression. These findings implicate a novel function for the caspase-8/cFLIP heterodimer in induction of innate inflammatory gene expression and provide mechanistic insight into how caspase-8 controls antimicrobial host defense.

## Results

### **Caspase-8 plays a cell-intrinsic role in inflammatory cytokine production during bacterial infection *in vivo***

*Ripk3<sup>-/-</sup>Casp8<sup>-/-</sup>* mice exhibit severely diminished cytokine responses following a number of bacterial infections, in contrast to *Ripk3<sup>-/-</sup>* mice, which have no discernible

defect (123, 124, 179). This could be due to a role for caspase-8-dependent apoptosis in the release of intracellular alarmins that promote inflammatory cytokine production by bystander cells, or a cell-intrinsic contribution of caspase-8 to inflammatory gene expression. To distinguish between these possibilities, we generated mixed bone marrow chimeras using transfer of congenically marked WT, *Ripk3*<sup>-/-</sup>, and *Ripk3*<sup>-/-</sup>*Casp8*<sup>-/-</sup> donor bone marrow at 1:1 ratios into lethally-irradiated wild-type (B6.SJL) recipients (Figure 20A and Figure 21A). Eight weeks post-reconstitution, these mixed chimeric animals were infected with *Yersinia pseudotuberculosis* (Yp), a gram-negative bacterial pathogen that causes a rapid and lethal bacteremia in animals with hematopoietic caspase-8 deficiency (123, 124). Strikingly, five days post-infection, *Ripk3*<sup>-/-</sup>*Casp8*<sup>-/-</sup> inflammatory monocytes isolated from the mesenteric lymph nodes (mLN) of mixed BM chimeras had a significant defect in intracellular TNF and IL-6 production compared with either wild-type or *Ripk3*<sup>-/-</sup> cells from the same animal (Figure 20B, C and Figure 21B, C). Moreover, this defect was equivalent to monocytes from recipients that received only *Ripk3*<sup>-/-</sup>*Casp8*<sup>-/-</sup> BM, indicating that the presence of caspase-8-sufficient cells did not restore cytokine production in cells lacking it (Figure 21B, C). Interestingly, not only did *Ripk3*<sup>-/-</sup>*Casp8*<sup>-/-</sup> cells have a lower frequency of cytokine-producing cells, the mean fluorescence intensity of *Ripk3*<sup>-/-</sup>*Casp8*<sup>-/-</sup> cytokine positive cells was significantly lower than *Ripk3*<sup>-/-</sup> or B6 cells from the same mouse, indicating a reduced level of cytokine production per cell (Figure 20D). We also observed that a significantly lower frequency of *Ripk3*<sup>-/-</sup>*Casp8*<sup>-/-</sup> neutrophils produced TNF compared to either *Ripk3*<sup>-/-</sup> or wild type control neutrophils, indicating a broader cytokine defect that extended to other innate cell types (Figure 20E, F). Importantly, the percent chimerism of these cell types was similar across all the genotypes, indicating that there were no differences in the generation or maintenance of *Ripk3*<sup>-/-</sup>*Casp8*<sup>-/-</sup> monocytes or neutrophils in a competitive environment

at these timepoints (Figure 21D). *Ripk3<sup>-/-</sup>Casp8<sup>-/-</sup>* chimeras cannot control *Yersinia* and harbor much higher bacterial burdens in their lymph nodes and spleen (123, 124). Importantly, however, the presence of congenically marked WT or *Ripk3<sup>-/-</sup>* cells in the *Ripk3<sup>-/-</sup>Casp8<sup>-/-</sup>* mixed BM chimeras provided significant protection from *Yersinia* infection, as the *Ripk3<sup>-/-</sup>Casp8<sup>-/-</sup>* mixed BM chimeras had similar bacterial burdens compared to chimeric mice that contained only wild-type or a mixture of *Ripk3<sup>-/-</sup>* and wild-type bone marrow (Figure 20G and Figure 21D). Together, these data provide direct evidence for a key cell-intrinsic role for caspase-8 in cytokine gene expression in innate immune cells in response to bacterial infection.

### **Caspase-8 regulates inflammatory cytokine production downstream of multiple TLRs**

We next sought to determine the contribution of caspase-8 to cytokine production in response to bacterial infection and individual pathogen-associated molecular patterns (PAMPS) in an in vitro system as a means to further define this response. We observed that *Ripk3<sup>-/-</sup>Casp8<sup>-/-</sup>* BMDMs showed dramatically reduced IL-6 and IL-12p40 production compared with B6 or *Ripk3<sup>-/-</sup>* cells in response to either *Yersinia* or *Salmonella* infection (Figure 22A). Consistent with this, *Ripk3<sup>-/-</sup>Casp8<sup>-/-</sup>* BMDMs also produced lower levels of secreted IL-6, IL-12p40, and TNF, as well as intracellular pro-IL-1 $\beta$  in response to LPS treatment (Figure 22B, C). Interestingly, *Ripk3<sup>-/-</sup>Casp8<sup>-/-</sup>* BMDMs did not have a global defect in all responses to LPS stimulation, as *Ifnb* transcript levels were not decreased, suggesting a more selective effect of caspase-8 deficiency (Figure 22D). Importantly, peritoneal macrophages isolated from *Ripk3<sup>-/-</sup>Casp8<sup>-/-</sup>* mice and stimulated *ex vivo* with LPS also showed a significant defect in TNF production relative to B6 and *Ripk3<sup>-/-</sup>* peritoneal macrophages (Figure 22E), further supporting a role for caspase-8 in cytokine production by innate cells following TLR stimulation.

TLR4-mediated apoptosis requires both TRIF and caspase-8. Therefore, we hypothesized that caspase-8 could be coupled to TLR-mediated gene expression via TRIF, and that TLRs that signal through MyD88 would not require caspase-8 for cytokine expression. Surprisingly, RIPK3/caspase-8-deficient BMDMs exhibited reduced production of the cytokines IL-6, IL-12p40, and TNF in response to not only the TRIF-dependent TLR3 agonist Poly(I:C), but also the MyD88-dependent TLR2 ligand Pam3CSK4 and the TLR9 ligand CpG (Figure 22F). These data suggest that caspase-8 mediates gene expression downstream of both TRIF- and MyD88-dependent pathways.

These cytokines depend on NF- $\kappa$ B and AP-1 transcription factor family members, and previous studies have suggested that caspase-8 regulates the activation of NF- $\kappa$ B activation (124, 170, 172). At what step and how caspase-8 might regulate NF- $\kappa$ B is nevertheless unclear. TLR signaling induces assembly of MyD88 into a complex with proteins of the IRAK family called the myddosome (6, 7), which initiates the signaling events that lead to the activation of NF- $\kappa$ B transcription factors to mediate NF- $\kappa$ B-dependent cytokine and chemokine gene expression (6, 7). However, we did not detect caspase-8 in the myddosome, and caspase-8 did not affect IRAK2 localization to the myddosome in response to LPS-treatment (Figure 23A, B), suggesting that caspase-8 is not involved in TLR-proximal signaling events. Initial studies had observed a role for caspase-8 in regulating the NF- $\kappa$ B pathway in lymphocytes (170, 172). We therefore examined whether caspase-8 regulates NF- $\kappa$ B in macrophages. Consistent with a recent report (173), degradation and resynthesis of I $\kappa$ B $\alpha$  was similar among B6, *Ripk3*<sup>-/-</sup>, and *Ripk3*<sup>-/-</sup>*Casp8*<sup>-/-</sup> BMDMs in response to LPS stimulation (Figure 23C). We also did not observe a difference in phosphorylation of AKT, p38 or ERK in LPS-treated *Ripk3*<sup>-/-</sup> *Casp8*<sup>-/-</sup> BMDMs compared to B6 and *Ripk3*<sup>-/-</sup> BMDMs (Figure 23D, E and data not shown). Moreover, recruitment of the NF- $\kappa$ B p65 subunit to caspase-8-inducible gene

promoters was unaffected in *Ripk3<sup>-/-</sup>Casp8<sup>-/-</sup>* BMDMs (Figure 23F). Together, these data suggest that the role of caspase-8 in control of gene expression likely does not occur via receptor-proximal effects on classical NF-κB or MAPK signaling pathways.

To test whether caspase-8 regulates inflammatory cytokine production at the transcriptional level, we examined mRNA levels of representative cytokines. Indeed, LPS-stimulated *Ripk3<sup>-/-</sup>Casp8<sup>-/-</sup>* BMDMs produced significantly less *Il1b*, *Il12b* and *Il6* mRNA compared to either *Ripk3<sup>-/-</sup>* or wild type BMDMs (Figure 22G). Importantly, this reduction in cytokine mRNAs was likely due to decreased transcriptional induction rather than transcript instability, as *Ripk3<sup>-/-</sup>Casp8<sup>-/-</sup>* BMDMs did not exhibit a more rapid decline of mRNA levels following treatment with the transcription synthesis inhibitor actinomycin D (ActD) 2 hours after LPS stimulation (Figure 24A, B).

#### **Caspase-8-regulated genes are enriched for cytokine signaling pathways**

These findings support a role for caspase-8 in the expression of TLR-dependent inflammatory cytokines, but the extent to which caspase-8 impacts the TLR-dependent transcriptional program is unclear. To define the breadth of the caspase-8-dependent transcriptional response, we performed genome-wide transcriptional profiling of B6, *Ripk3<sup>-/-</sup>*, and *Ripk3<sup>-/-</sup>Casp8<sup>-/-</sup>* BMDMs following LPS treatment. Based on our observations that maximal differences between *Ripk3<sup>-/-</sup>Casp8<sup>-/-</sup>* and B6 or *Ripk3<sup>-/-</sup>* BMDMs occurred at 6 hours post-infection, we stimulated these three genotypes of macrophages with LPS for 6 hours and performed RNA-Seq analysis (Figure 25 A). This timepoint also allowed for detection of both primary and secondary response genes (231). To define the contribution of caspase-8 to the TLR4-induced transcriptional program, we analyzed the LPS-induced genes by Principle Component Analysis (PCA), Gene Set Enrichment Analysis (GSEA), and performed hierarchical clustering and Gene Ontology (GO) analysis (Figure 25B). The PCA analysis revealed that, as expected, LPS

treatment accounted for almost 96% of the variance among the samples (PC1), demonstrating that neither RIPK3 deficiency alone, nor combined deficiency of caspase-8 and RIPK3 resulted in a global impact on LPS-induced gene expression. Interestingly, RIPK3/caspase-8-deficiency contributed to the second highest variance (PC2), implying a role for caspase-8 in LPS-induced gene expression. To determine the precise contribution of caspase-8 to the LPS response, we identified LPS-regulated genes that were altered in either *Ripk3<sup>-/-</sup>Casp8<sup>-/-</sup>* or *Ripk3<sup>-/-</sup>* BMDMs. Interestingly, 527 of the 6379 (8.3%) genes were RIPK3/caspase-8-dependent, whereas only 62 of 6379 (less than 1%) were RIPK3-dependent (Appendix I). Importantly, 479 (or 91%) of the 527 genes affected in *Ripk3<sup>-/-</sup>Casp8<sup>-/-</sup>* BMDMs were unaffected by RIPK3 deficiency alone, implying a specific role for caspase-8 in induction of these genes. Hierarchical clustering of the caspase-8-dependent genes by Pearson correlation revealed two major clusters of coordinately regulated genes (Figure 25C). Genes in cluster 1 were more highly expressed in response to LPS in *Ripk3<sup>-/-</sup>Casp8<sup>-/-</sup>* BMDMs, whereas cluster 2 was composed of genes that were not as strongly induced by LPS stimulation in *Ripk3<sup>-/-</sup>Casp8<sup>-/-</sup>* BMDMs compared to B6 or *Ripk3<sup>-/-</sup>* BMDMs. Interestingly, and consistent with previous findings suggesting that caspase-8 regulates inflammatory cytokine production, functional enrichment of cluster 2 genes using Gene Ontology (GO) analysis revealed genes associated with immune defense and transcriptional regulation (Figure 25D). Genes belonging to the category of transcriptional regulation included *JunB*, *Rel* and *Stat5a* (Figure 25E), while the category of immune defense included *Il1a*, *Il1b*, *Ccl17*, *Il12b*, and *Tnf* (Figure 25E). Although this subset of genes was still upregulated by LPS stimulation in *Ripk3<sup>-/-</sup>Casp8<sup>-/-</sup>* BMDMs, the degree of induction was significantly reduced relative to control cells (Figure 26A). Intriguingly, *Il1a*, *Il1b*, *Ccl17* and *Il12b* were among the top 20 most differentially expressed genes. Furthermore, Gene Set Enrichment



Analysis (GSEA), which provides an unbiased way to identify coordinated changes in gene expression, demonstrated that genes involved in cytokine and chemokine signaling were significantly enriched in wild type BMDMs compared to caspase-8-deficient cells (Figure 25F). These findings demonstrate that caspase-8 deficiency is associated with altered transcriptional responses of a subset of LPS-induced genes that play a particularly important role in inflammatory responses to infection.

Caspase-8 has been reported to localize to the nucleus of B cells, raising the possibility that nuclear caspase-8 might play a role in gene expression (232). However, we did not observe caspase-8 in the nucleus of either untreated or LPS-treated macrophages, suggesting that caspase-8 does not play a direct role in transcriptional activation of these target genes (Figure 26B). Furthermore, both *Ripk3*<sup>-/-</sup> and *Ripk3*<sup>-/-</sup> *Casp8*<sup>-/-</sup> BMDMs phagocytosed and degraded *Salmonella* and *Yersinia* equivalently to wild-type cells, indicating that direct killing mechanisms of macrophages were still intact (Figure 26C). Together, these data indicate that the loss of caspase-8 is associated with altered expression of a significant number of TLR-induced genes involved in inflammation and transcription, potentially providing an explanation for the profound susceptibility of caspase-8-deficient animals to bacterial infections. Interestingly, despite the key role of caspase-8 in regulating cell death and survival decisions in the context of TNFR signaling (233), the role of caspase-8 in gene expression in macrophages is specific to TLRs, as caspase-8 deletion did not affect the expression of *Cxcl2* or *Ccl22* chemokine genes in response to TNF, despite the clear impact of caspase-8 on LPS-dependent induction of these genes (Figure 26D, E).

### **Sendai virus-induced cytokine production does not require caspase-8**

Our observations imply a specific contribution of caspase-8 to TLR signaling. To test the possibility of a more general role for caspase-8 in other innate immune signaling

pathways, we employed Sendai virus (SeV), which induces innate immune cytokine responses primarily via the RIG-I and MDA-5 pathways (234, 235). In contrast to bacterial infection and TLR stimulation, caspase-8 was dispensable for SeV-induced expression of IL-6 and IL-12p40 in BMDMs (Figure 27A). Moreover, consistent with a robust innate response to SeV *in vitro*, *Ripk3<sup>-/-</sup>Casp8<sup>-/-</sup>* mice also showed similar or reduced levels of weight loss in response to SeV, and controlled and cleared SeV infection similarly to WT and *Ripk3<sup>-/-</sup>* mice (Figure 27B and C). Importantly, *Ripk3<sup>-/-</sup>Casp8<sup>-/-</sup>* mice also expressed similar levels of *Ifnb*, *Il6* and *Il1b* in the lung during SeV infection relative to WT and *Ripk3<sup>-/-</sup>* mice (Figure 27D). Thus, while caspase-8 is important for maximal inflammatory gene expression in response to bacterial infection, it is dispensable for innate responses and clearance of SeV infection.

### **Caspase-8 is necessary for optimal inflammatory cytokine production independent of RIPK3**

Caspase-8 and RIPK3 are present in the same complex as FADD and RIPK1. While caspase-8 inhibits RIPK3-regulated necrosis via a caspase-8/cFLIP complex, mutation or inhibition of RIPK3 kinase activity can also promote caspase-8-dependent apoptosis (19, 236-238). Given this close link between caspase-8 and RIPK3, we considered the possibility that the observed effect of caspase-8 on gene regulation could be due to combined loss of both RIPK3 and caspase-8. However, due to the embryonic lethality of caspase-8-deficient animals because of unrestrained RIPK3-mediated necrosis, the effect of single deficiency in caspase-8 has been difficult to separate from its effect on programmed necrosis. Conditional deletion of caspase-8 *in vitro* also results in significant toxicity due to induction of RIPK3-mediated necrosis in response to tonic signaling (24). RIPK3 induces programmed necrosis through Mixed Lineage Kinase Like (MLKL) (33-35). Importantly, while caspase-8-deficient mice are embryonic lethal,

deletion of MLKL also rescues this embryonic lethality, analogous to deletion of RIPK3. Intriguingly, *Mkl1<sup>-/-</sup>Casp8<sup>-/-</sup>* BMDMs also produced significantly lower levels of IL-6, IL-12p40 and TNF in response to LPS, Pam3CSK4 and CpG, relative to *Mkl1<sup>-/-</sup>* BMDMs (Figure 28). These data demonstrate that caspase-8 controls cytokine expression independently of RIPK3.

### **Caspase-8 catalytic activity, but not auto-processing, is required for optimal TLR-induced cytokine production**

Caspase-8 homodimerization results in activation of apoptosis, whereas heterodimerization of caspase-8 with its catalytically inactive homolog cFLIP prevents both apoptosis and regulated necrosis (26, 154). Conditions that trigger extrinsic apoptosis induce assembly of caspase-8 homodimers or oligomers, wherein caspase-8 undergoes autoprocessing (141, 239). While homodimerization is sufficient to activate the enzyme, subsequent autoprocessing stabilizes the cleaved dimer, and is required for caspase-8 to cleave its downstream apoptotic substrates such as Bid, caspase-3 and -7 (20). In contrast, the caspase-8/cFLIP heterodimer does not require caspase-8 processing, but does require catalytic activity to prevent necrosis (26). Thus, blocking caspase activity in the context of TNF or TLR stimulation leads to programmed necrosis that depends on RIPK3 (240). In order to test whether caspase-8 catalytic activity is responsible for the effect of caspase-8 on TLR-induced gene expression, we treated RIPK3-deficient cells with the pan-caspase inhibitor zVAD-fmk. Notably, zVAD-fmk significantly reduced production of IL-12p40, IL-6 and IL-1 $\beta$  in LPS-treated *Ripk3<sup>-/-</sup>* BMDMs (Figure 29A-C). As expected, *Ripk3<sup>-/-</sup>Casp8<sup>-/-</sup>* BMDMs exhibited significantly blunted responses to LPS, which were not substantially altered by inhibitor treatment. QVD-oph is another widely used pan-caspase inhibitor that does not display the same cytotoxicity as zVAD-fmk (241). Critically, QVD-oph also significantly reduced IL-12p40

and IL-6 production following LPS treatment in both B6 and *Ripk3*<sup>-/-</sup> BMDMs (Figure 29D). Notably, QVD-oph did not induce cytotoxicity in either B6 or *Ripk3*<sup>-/-</sup> BMDMs, and, *Ripk3*<sup>-/-</sup> cells did not undergo cell death in response to zVAD-fmk, demonstrating that caspase activity contributes to LPS-induced gene expression independently of cell death (Figure 29E). Importantly, cells deficient in both caspase-3 and -7 were fully competent to induce expression of cytokines following LPS treatment, demonstrating that caspase-8 activity regulates TLR-induced gene expression independently of these apoptotic caspases (Figure 30).

To further define how caspase-8 regulates TLR-induced gene expression, we generated a caspase-8 mutant knock-in mouse, termed *Casp8*<sup>DA/DA</sup>, in which aspartate 387 is replaced with an alanine, thereby rendering it non-cleavable (Figure 31A). Although caspase-8 deficiency is embryonically lethal, mice expressing non-cleavable caspase-8 are viable, due to the enzymatic activity of caspase-8 in the context of a caspase-8/cFLIP heterodimer (26, 160, 242). Self-cleavage at D387 releases the catalytically active p20 subunit, and under most cellular conditions, this self-processing is necessary for caspase-8-dependent apoptosis (20). However, catalytic activity of the caspase-8/cFLIP heterodimer prevents RIPK3-mediated necrosis (26), but can also mediate the processing of substrates (148, 162). Therefore, the *Casp8*<sup>DA/DA</sup> mouse provides a means to distinguish the roles of the caspase-8 homodimer and caspase-8/cFLIP heterodimer in gene expression. Notably, *Casp8*<sup>DA/DA</sup> BMDMs were unable to process caspase-8 in response to *Yersinia*, which induces caspase-8 cleavage and cell death in wild type or *Casp8*<sup>DA/+</sup> macrophages that depend on the *Yersinia* effector protein YopJ (110) (Figure 31B-D). Importantly, *Yersinia*-induced caspase-3 cleavage, which is caspase-8-dependent (123) is specifically abrogated in *Casp8*<sup>DA/DA</sup> BMDMs (Figure 31C). Surprisingly, despite the absence of caspase-3 cleavage, *Casp8*<sup>DA/DA</sup>

macrophages exhibited equivalent levels of cell death in response to *Yersinia* infection (Figure 31D). We therefore considered the possibility that *Yersinia* infection of these macrophages might induce RIPK3-dependent necrosis. Indeed, while *Casp8*<sup>+/+</sup>, *Casp8*<sup>DA/+</sup> and *Casp8*<sup>DA/DA</sup> BMDMs exhibited similar levels of *Yersinia*-induced cell death, only *Casp8*<sup>DA/DA</sup> BMDMs were protected from this cell death upon treatment with the RIPK3 inhibitor, GSK' 872 (Figure 31D). Together, these data demonstrate that caspase-8 cleavage is necessary for apoptosis in macrophages, and in the absence of this cleavage, *Yersinia*-infected *Casp8*<sup>DA/DA</sup> BMDMs undergo RIPK3-dependent necrosis. These data imply that caspase-8 D387A does not activate apoptosis, but likely forms a heterodimer with cFLIP in macrophages.

Critically, *Casp8*<sup>DA/DA</sup> and *Casp8*<sup>DA/+</sup> BMDMs responded equally well to stimulation with LPS, Pam3CSK4 or CpG as compared to littermate control WT BMDMs, as we observed similar frequencies of IL-12p40<sup>+</sup>, IL-1β<sup>+</sup> and IL-6<sup>+</sup> cells among *Casp8*<sup>+/+</sup>, *Casp8*<sup>DA/+</sup> and *Casp8*<sup>DA/DA</sup> BMDMs (Figure 31E-G). Consistently, *Casp8*<sup>DA/DA</sup> BMDMs produced WT levels of TNF in response to LPS, Pam3 or CpG (Figure 31H). Altogether, our findings indicate that caspase-8 enzymatic but not its auto-processing activity plays an important role in optimal production of TLR-dependent inflammatory cytokines, and implicate the activity of the caspase-8/cFLIP heterodimer in this response.

## Discussion

Caspase-8 and caspase-8-containing protein complexes have emerged as central regulators of cell fate decisions in the context of infection and inflammatory stimuli. Caspase-8 interacts with a number of key adaptors and signaling proteins, including cFLIP, RIPK1, RIPK3 and FADD. The precise nature of the interactions between caspase-8 and these components in the context of specific extracellular cues

determine whether the cell initiates inflammatory gene expression, or undergoes apoptosis or RIPK3-dependent programmed necrosis. While the molecular and biochemical mechanisms of caspase-8-induced apoptosis and caspase-8-dependent control of RIPK3 necrosis have been extensively characterized, how caspase-8 might control cell-intrinsic gene expression is not clear.

Germline mutations in human caspase-8 or FADD cause a primary immunodeficiency associated with severe recurrent bacterial and viral infections, encephalopathy and hepatopathy (225, 227). While initial studies proposed that caspase-8 regulates NF- $\kappa$ B signaling in lymphocytes following antigen receptor activation (170, 172), *Ripk3<sup>-/-</sup>Casp8<sup>-/-</sup>* T cells did not exhibit defects in NF- $\kappa$ B activation or, antigen-specific IFN $\gamma$  production (25, 173, 175, 228). This suggested that caspase-8 regulates T cell responses by limiting RIPK3-dependent necrosis rather than controlling T cell activation itself. Nevertheless, several recent studies examining macrophages and dendritic cells from *Ripk3<sup>-/-</sup>Casp8<sup>-/-</sup>* animals have linked caspase-8 to the production of innate cytokines as well as to inflammasome activation (124, 170, 172, 173, 175, 182, 221, 223, 243-245). The role of caspase-8 in NF- $\kappa$ B signaling in innate cells is not precisely defined, as recent studies have come to opposite conclusions about the contribution of caspase-8 to activation of the IKK complex and I $\kappa$ B degradation (124, 173). Moreover, while caspase-8 mediates apoptosis and prevents RIPK3-necrosis downstream of the TLR4- or TLR3-TRIF axes (14-16, 23, 24), the extent to which caspase-8 regulates TLR-induced gene expression has not been defined.

Here, we report a pleiotropic role for caspase-8 in the control of gene expression downstream of multiple TLRs, including those that signal through TRIF (TLR3, 4) and those that signal through MyD88 (TLR2, 4, 9). We have now defined the contribution of caspase-8 to LPS-induced gene expression, and find that caspase-8 regulates a small

but critical subset of genes that play an important role in inflammation and anti-microbial immune defense. Caspase-8 acts as an important modifier of gene expression, as it is necessary for the maximal induction of particular genes, rather than absolutely required for their expression. Notably, IL-12, IL-6, pro-IL-1 $\alpha$ , pro-IL-1 $\beta$ , as well as multiple chemokine genes were among the 527 LPS-induced genes that required caspase-8 for optimal induction, which collectively constitutes 8.3% of total LPS-induced genes in WT cells. Mechanistically, our data also demonstrate that caspase-8 enzymatic activity, but not auto-processing, plays a key role in the induction of gene expression independently of apoptotic caspases or any other effects on cell death signaling (Figure 32). These data provide new insight into the susceptibility phenotypes associated with caspase-8 deficiency.

Our findings imply that caspase-8 has an apoptosis-independent function in the context of TLR engagement because TLR stimulation alone does not induce cell death under the conditions employed here. The precise targets of this activity remains to be defined, but do not involve the known apoptotic substrates caspase-3 and -7. Moreover, our findings that the gene expression defect of caspase-8-deficient cells is cell-intrinsic exclude a model in which the diminished cytokine production by caspase-8-deficient cells results from the lack of release of intracellular alarmins in the absence of RIPK3 and caspase-8.

It is possible that some of the effects we observe are the result of the dual deletion of RIPK3 and caspase-8. RIPK3 has been implicated in inflammatory responses independent of cell death, as RIPK3 itself can promote IL-1 $\beta$  expression in dendritic cells via induction of mitochondrial ROS (245). Similarly, conditional deletion of caspase-8 in dendritic cells resulted in elevated production of IL-1 $\beta$  due to RIPK3-dependent activation of the NLRP3 inflammasome (219), and led to systemic autoimmunity (246).

Caspase-8 and RIPK3 may play cell type-specific roles in regulating inflammatory gene expression. However, the increased inflammatory responses observed in the setting of conditional deletion of caspase-8 or FADD *in vivo* are likely due to de-repression of RIPK3-dependent necrosis (30, 32, 247). We did not observe a contribution of RIPK3 to the caspase-8-dependent gene expression program, in that loss of RIPK3 alone did not substantially affect expression of pro-IL-1 $\beta$  or other inflammatory cytokines, either *in vitro* in BMDMs, or *in vivo* in monocytes or neutrophils in response to bacterial infection. Furthermore, several lines of evidence support a role for caspase-8 in regulating gene expression independent of RIPK3: first, *Mik1<sup>-/-</sup>Casp8<sup>-/-</sup>* but not *Mik1<sup>-/-</sup>* BMDMs have a significant defect in production of pro-inflammatory cytokines in response to multiple TLR agonists, despite having functional RIPK3. Second, treatment of RIPK3-sufficient B6 BMDMs with the caspase inhibitor QVD-oph prior to TLR stimulation did not induce any detectable cytotoxicity, but still significantly reduced cytokine production in response to TLR stimulation. Cumulatively, these data imply a key role for caspase-8 activity independent of RIPK3 in TLR-induced inflammatory responses.

The role of caspase-8 as a key modulator of gene expression makes it functionally analogous to RIPK1, which is also a central regulator of apoptosis, necrosis and gene expression (19). It is possible that like RIPK1, distinct post-translational modifications or recruitment to distinct complexes mediate the switch between caspase-8-dependent apoptosis and gene expression. Caspase-8 may regulate gene expression through a RIPK1-containing complex distinct from complex II. However, since RIPK1 plays a central scaffolding role in receptor-proximal activation of the IKK complex, the effect of RIPK1 deficiency on TLR-induced gene expression is likely more profound than that of caspase-8.

Like TLR signaling, TNFR activation can trigger survival and cytokine production,



apoptosis, or necrosis (18, 19). Caspase-8 controls cell death in response to both TLR and TNFR signaling pathways. Nevertheless, the common chemokine genes *Cxcl2* and *Ccl22* that are induced by both LPS and TNF in BMDMs, required caspase-8 for maximal induction in response to LPS but not TNF. Whether caspase-8 contributes to TNFR-dependent gene expression in other cell types remains to be determined. Furthermore, although caspase-8-deficient BMDMs had a defect in their ability to respond to infection by several gram-negative bacteria as well as multiple TLR agonists, *Ripk3<sup>-/-</sup>Casp8<sup>-/-</sup>* BMDMs produced equivalent levels of cytokines in response to Sendai virus infection, which engages the cytosolic PRRs RIG-I and MDA5. Caspase-8 was previously shown to negatively regulate type I IFN in response to SeV in human fibroblasts, in part through cleaving RIPK1 and shutting off RIPK1 signaling (181). Nonetheless, our findings suggest that macrophages do not require caspase-8 for induction of inflammatory cytokines by cytosolic nucleic acid sensors. Thus, while caspase-8 regulates apoptosis and programmed necrosis downstream of multiple receptors, in macrophages, caspase-8 specifically controls gene expression in response to TLR signaling.

The defect in production of IL-6, TNF, IL-12p40 and proIL-1 $\beta$  by *Ripk3<sup>-/-</sup>Casp8<sup>-/-</sup>* cells in response to MyD88-dependent TLR agonists such as CpG and Pam3CSK could be due to the recently reported role of TRIF participating in signaling downstream of classical MyD88-dependent TLRs, as was suggested in the case of TLR2 (248). However, TRIF did not contribute to TLR2-dependent induction of IL-6 or TNF (248), which we observed was affected by caspase-8 deficiency. Therefore, caspase-8 may participate at a distal step of TLR signaling in a manner that affects both MyD88- and TRIF-dependent gene expression. This may occur through control of a shared accessory factor that is important for expression of these genes. Notably, caspase-8 does not

regulate the early receptor-proximal events, such as myddosome formation, I $\kappa$ B $\alpha$  degradation, or MAPK activation. Recruitment of p65 to the promoters of a number of caspase-8-dependent genes was also unaltered. These observations, along with the finding that I $\kappa$ B $\alpha$  resynthesis, which depends on NF- $\kappa$ B itself, was unaffected by caspase-8 deficiency, are consistent with our transcriptional profiling studies indicating that over 90% of LPS-induced gene expression remains unaffected in caspase-8-deficient cells. However, the approximately 8% of genes that are affected include critical inflammatory mediators and chemokines.

Caspase-8 is a cysteine protease that forms homodimers to activate apoptosis and heterodimers with its homolog cFLIP to inhibit apoptosis and necroptosis (20, 148). Both functions of caspase-8 require catalytic activity, however the caspase-8/cFLIP heterodimer does not need to undergo self-cleavage to inhibit cell death (26). Using a newly-generated non-cleavable caspase-8 knock-in mouse, we demonstrate that the catalytic, but not self-cleavage activity of caspase-8 is required for maximal cytokine production, suggesting that an adaptor or scaffolding function is insufficient and that the caspase-8/cFLIP heterodimer regulates gene expression. The precise target or targets of caspase-8/cFLIP activity that mediate this gene regulatory function remain to be identified. Nevertheless, our findings provide the first definitive demonstration that the enzymatic activity of caspase-8 in TLR-induced gene expression plays a key cell-intrinsic role in TLR-dependent gene expression. Together, these data provide new mechanistic insight into the non-apoptotic function of caspase-8 in host immune defense, which may account for the severe susceptibility of mice and humans lacking caspase-8 to poly-microbial infections.

**Figure 20**

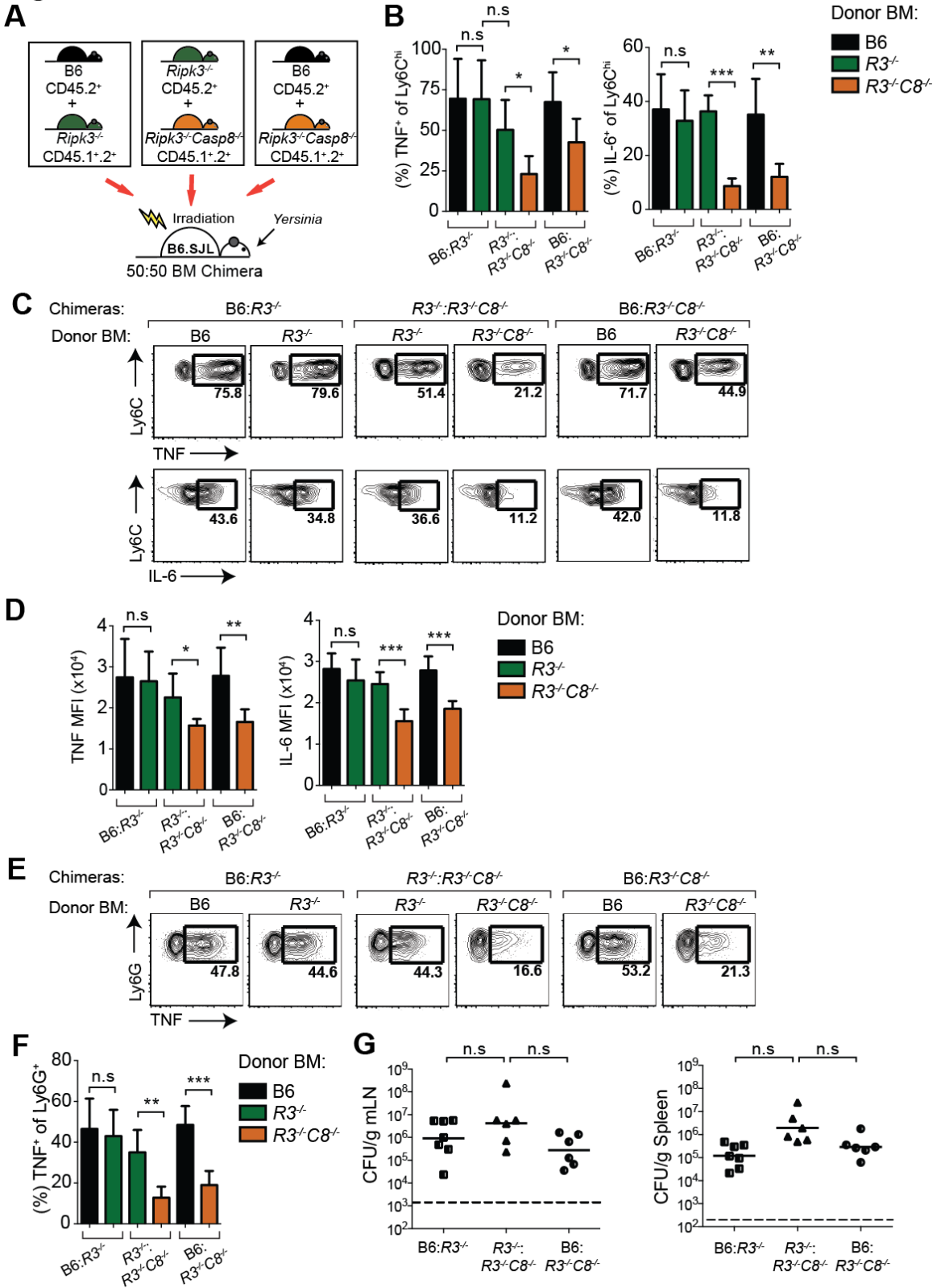


**Figure 20. *Ripk3*<sup>-/-</sup>*Casp8*<sup>-/-</sup> inflammatory monocytes and neutrophils have a cell-intrinsic defect in IL-6 and TNF production.**

(A) Schematic of mixed bone marrow chimera experimental set-up. Congenically marked B6 (black), *Ripk3*<sup>-/-</sup> (green) or *Ripk3*<sup>-/-</sup>*Casp8*<sup>-/-</sup> (orange) bone marrow (BM) were injected at a 1:1 ratio into lethally-irradiated recipient B6.SJL mice. 8 weeks after reconstitution, chimeras were orally infected with *Yersinia* (1x10<sup>8</sup>/mouse) and immune responses were assayed at day 5 post-infection. (B) Quantification of percentage of Ly6C<sup>hi</sup> inflammatory monocytes that express TNF or IL-6 for each genotype of cells in the B6:*Ripk3*<sup>-/-</sup> (B6:*R3*<sup>-/-</sup>), *Ripk3*<sup>-/-</sup>:*Ripk3*<sup>-/-</sup>*Casp8*<sup>-/-</sup> (*R3*<sup>-/-</sup>:*R3*<sup>-/-</sup>*C8*<sup>-/-</sup>) and B6:*Ripk3*<sup>-/-</sup>*Casp8*<sup>-/-</sup> (B6:*R3*<sup>-/-</sup>*C8*<sup>-/-</sup>) mixed chimeras, as indicated. Color scheme of bars is as in (A) with black bars representing B6, green bars representing *Ripk3*<sup>-/-</sup>, and orange bars representing *Ripk3*<sup>-/-</sup>*Casp8*<sup>-/-</sup> cells. (C) Representative flow plots of TNF (top row of plots) and IL-6 (bottom row of plots) production in inflammatory monocytes from mixed chimeras in (B). Flow plots within each set of brackets represent cells analyzed from the same mixed bone marrow recipient mouse; genotypes of the cells analyzed are indicated above each plot *R3*<sup>-/-</sup> – *Ripk3*<sup>-/-</sup>, *R3*<sup>-/-</sup>*C8*<sup>-/-</sup> – *Ripk3*<sup>-/-</sup>*Casp8*<sup>-/-</sup>. (D) Quantification of mean fluorescence intensity (MFI) of TNF<sup>+</sup> and IL-6<sup>+</sup> inflammatory monocytes from B6:*R3*<sup>-/-</sup>, *R3*<sup>-/-</sup>:*R3*<sup>-/-</sup>*C8*<sup>-/-</sup> and B6:*R3*<sup>-/-</sup>*C8*<sup>-/-</sup> mixed chimeras in (B) and (C). (E) Representative flow plots of TNF production in Ly6G<sup>+</sup> neutrophils from B6:*R3*<sup>-/-</sup>, *R3*<sup>-/-</sup>:*R3*<sup>-/-</sup>*C8*<sup>-/-</sup> and B6:*R3*<sup>-/-</sup>*C8*<sup>-/-</sup> mixed chimeras analyzed as described in (C). (F) Quantification of percentage of TNF<sup>+</sup> neutrophils from (E). (G) Quantification of bacterial burden per gram tissue (CFU/g). Solid bars indicate geometric mean of samples. Dotted lines indicate the limit of detection. Gating strategy is described in detail in Experimental Procedures. Data are representative of 2-4 independent experiments. \*  $p < 0.05$ , \*\*  $p < 0.01$ , \*\*\*  $p < 0.001$  by Student's unpaired *t*-test.

**Figure 21**

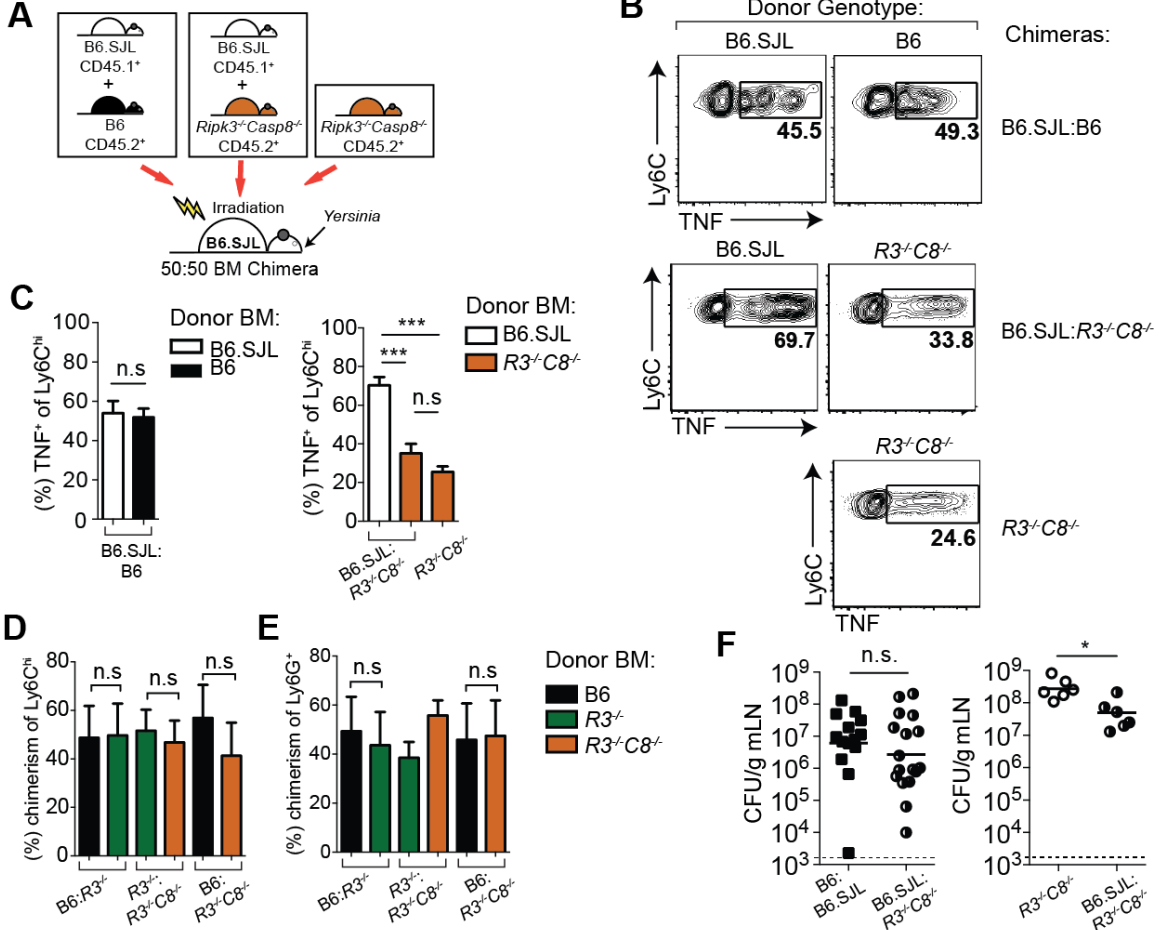


**Figure 21. Caspase-8 plays a cell-intrinsic role in inflammatory cytokine production during bacterial infection *in vivo*.**

(A) Schematic of mixed bone marrow chimera experimental set-up. Congenically marked B6 (white or black) or *Ripk3*<sup>-/-</sup>*Casp8*<sup>-/-</sup> (orange) bone marrow (BM) were injected at a 1:1 ratio into lethally-irradiated recipient B6.SJL mice. 8 weeks after reconstitution, chimeras were orally infected with *Yersinia* ( $4 \times 10^9$ /mouse) and immune responses were assayed at day 3 post-infection. (B) Representative flow plots of percentage of TNF-expressing Ly6Chi inflammatory monocytes from B6.SJL:*R3*<sup>-/-</sup>*C8*<sup>-/-</sup>, *R3*<sup>-/-</sup>*C8*<sup>-/-</sup> and B6:B6.SJL chimeras. Labels above plots indicate genotype of donor cells and labels to the right of the plots indicate genotype of chimeras. (C) Quantification of percentage of TNF<sup>+</sup> monocytes from (B). Bars are color-coded to represent genotype of donor bone marrow (B6 = black, B6.SJL = white, *Ripk3*<sup>-/-</sup>*Casp8*<sup>-/-</sup> = orange). Brackets on the x-axis indicate genotype of mixed chimeras. (D) Degree of chimerism of inflammatory monocytes from infected mice analyzed in Figure 1B-D. (E) Degree of chimerism of neutrophils from infected mice analyzed in Figure 1E. (F) Bacterial loads/g tissue (CFU/g). Dotted lines represent limit of detection. Solid lines represent geometric means.

*R3C8* = *Ripk3Casp8*. Representative of 2 independent experiments. \*  $p < 0.05$ , \*\*  $p < 0.01$ , \*\*\*  $p < 0.001$  by t-test.

**Figure 22**

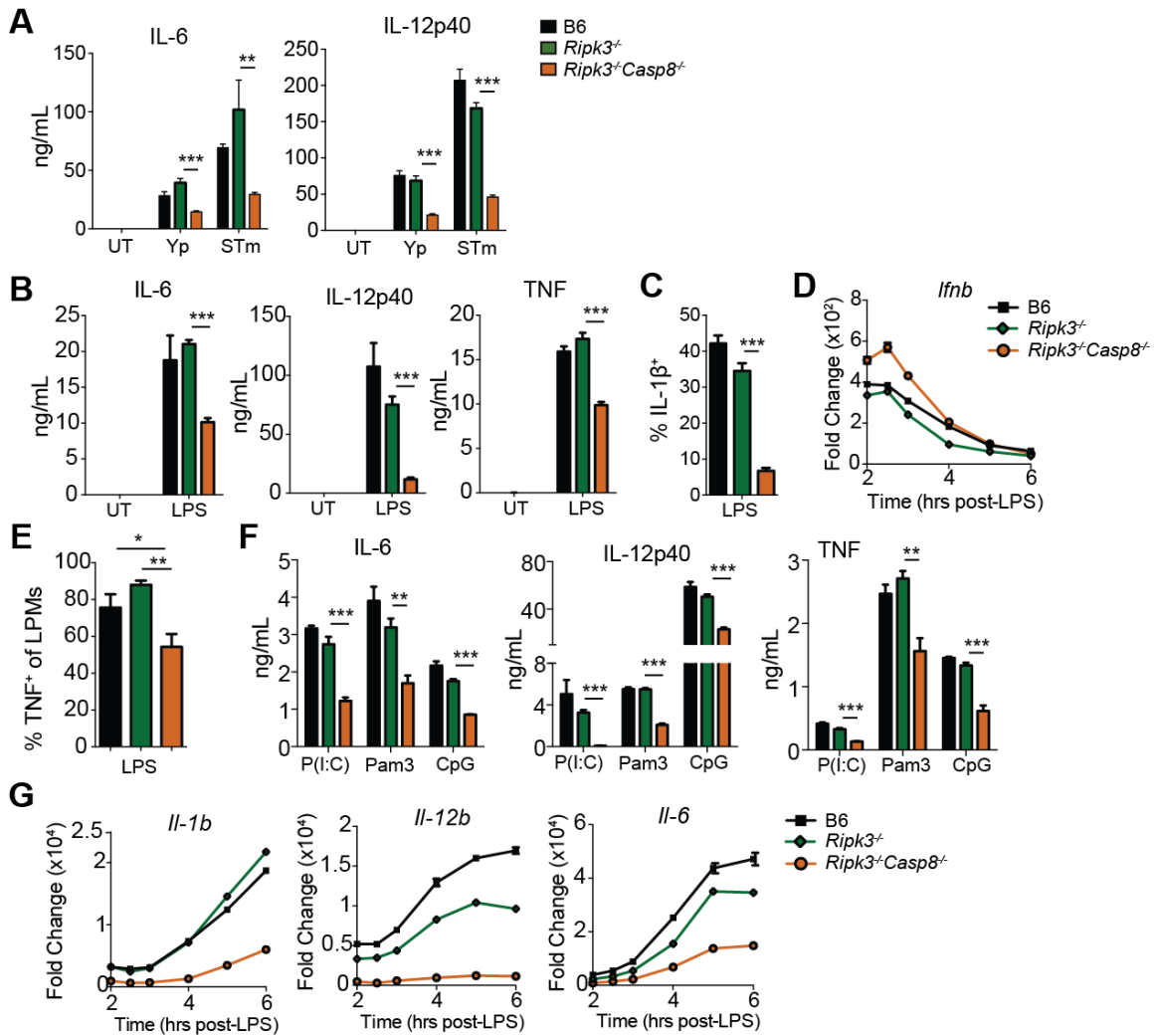


**Figure 22. *Ripk3*<sup>-/-</sup> *Casp8*<sup>-/-</sup> bone marrow-derived macrophages are defective in both MyD88 and TRIF-dependent cytokine production**

(A) Bone marrow-derived macrophages (BMDMs) from B6, *Ripk3*<sup>-/-</sup> and *Ripk3*<sup>-/-</sup> *Casp8*<sup>-/-</sup> were infected with *Yersinia* or *Salmonella* for 24hrs, and IL-6 and IL-12p40 cytokine levels present in supernatants were quantified by ELISA. (B) IL-6, IL-12p40 and TNF production was measured by ELISA from the indicated BMDMs treated with LPS (100 ng/mL) for 6hrs. (C) IL-1 $\beta$  expression was measured by flow cytometry from the indicated BMDMs treated with LPS (100 ng/mL) for 5hrs. (D) BMDMs were treated with LPS (100 ng/mL) and *lfnb* mRNA was assayed by RT-qPCR at the indicated time points. (E) Resident peritoneal macrophages from indicated mouse genotypes were isolated and stimulated ex vivo with LPS (10 ng/mL) for 4 hrs. TNF production by large peritoneal macrophages (LPMs) was measured by flow cytometry. (F) IL-6, IL-12p40 and TNF production was measured by ELISA from BMDMs treated with Poly(I:C) (50  $\mu$ g/mL) for 24 hrs, CpG (1  $\mu$ g/mL) or Pam3CSK4 (1  $\mu$ g/mL) for 6hrs. (G) BMDMs were treated with LPS (100 ng/mL) and *Il1b*, *Il12b* and *Il6* mRNA was assayed by RT-qPCR at the indicated time points.

\*  $p < 0.05$ , \*\*  $p < 0.01$ , \*\*\*  $p < 0.001$  by t-test. Representative of three or more independent experiments.

**Figure 23**

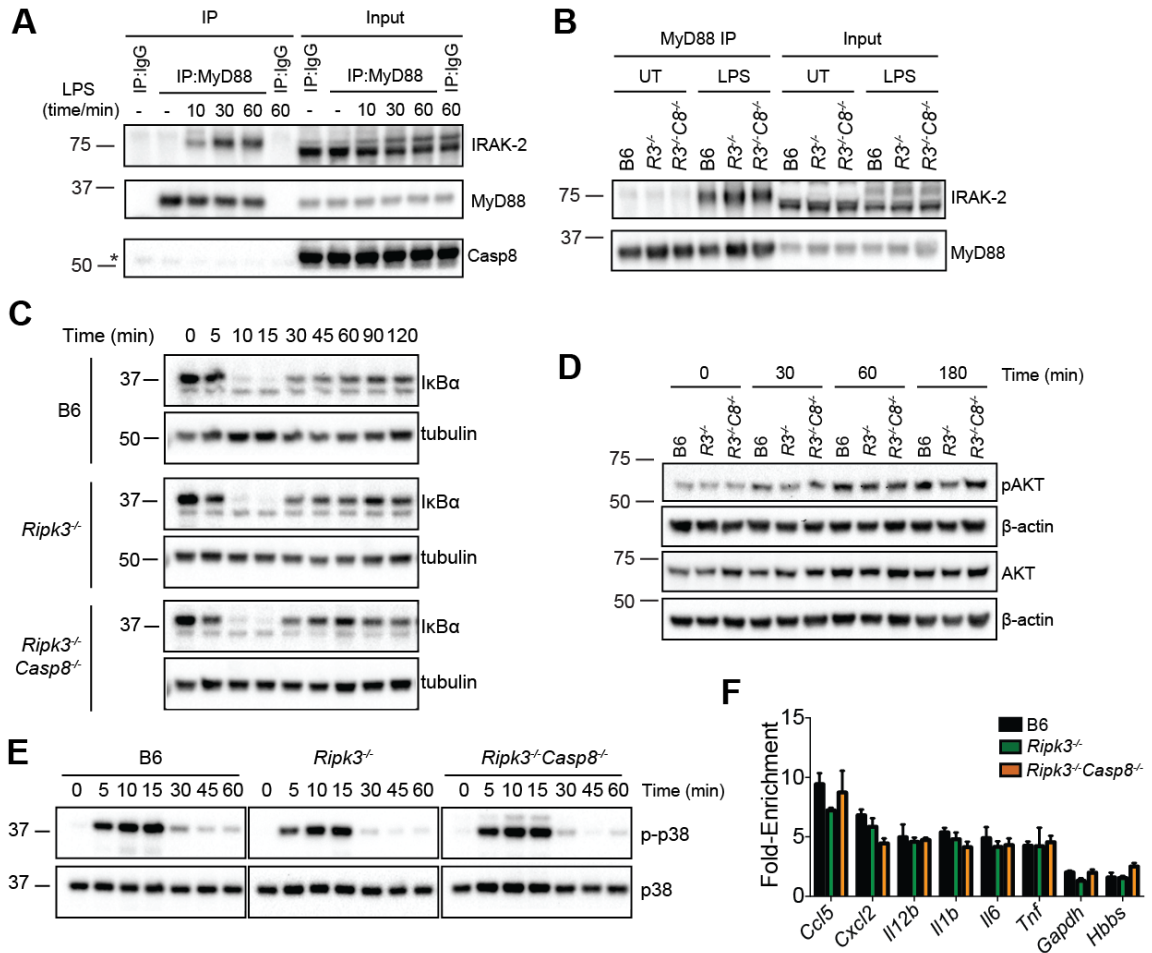


**Figure 23. Caspase-8 is not required for induction of NF- $\kappa$ B and MAPK signaling or p65 recruitment to inflammatory gene promoters.**  
 (A) B6 BMDMs were treated with LPS for indicated time points and lysates were immunoprecipitated with antibodies against MyD88 or control IgG and probed for MyD88, IRAK2 and caspase-8 (Casp8) by western analysis. Star represents background band. (B) B6, *Ripk3<sup>-/-</sup>* and *Ripk3<sup>-/-</sup>Casp8<sup>-/-</sup>* BMDMs were treated with LPS for 2hrs and lysates were immunoprecipitated with antibodies against MyD88 or control IgG and probed for MyD88 and IRAK2. (C) Kinetics of I $\kappa$ B $\alpha$  degradation and resynthesis post-LPS treatment was detected by western analysis. (D, E) Phosphorylation of AKT and p38 was probed by western post LPS-stimulation. Representative of two or more independent experiments. (F) Fold enrichment (% input in LPS-treated/% input untreated, see Methods) for p65 recruitment to promoters of *Ccl5*, *Cxcl2*, *Il12b*, *Il6*, *Tnf*, *Hbb-bs* and *Gapdh* in LPS-treated B6, *Ripk3<sup>-/-</sup>* and *Ripk3<sup>-/-</sup>Casp8<sup>-/-</sup>* BMDMs. *Hbb-bs* is not expressed in BMDMs (negative control) and *Gapdh* is a housekeeping gene. Samples were normalized to 5% input, error bars indicate indicate +/- SD.

**Figure 24**

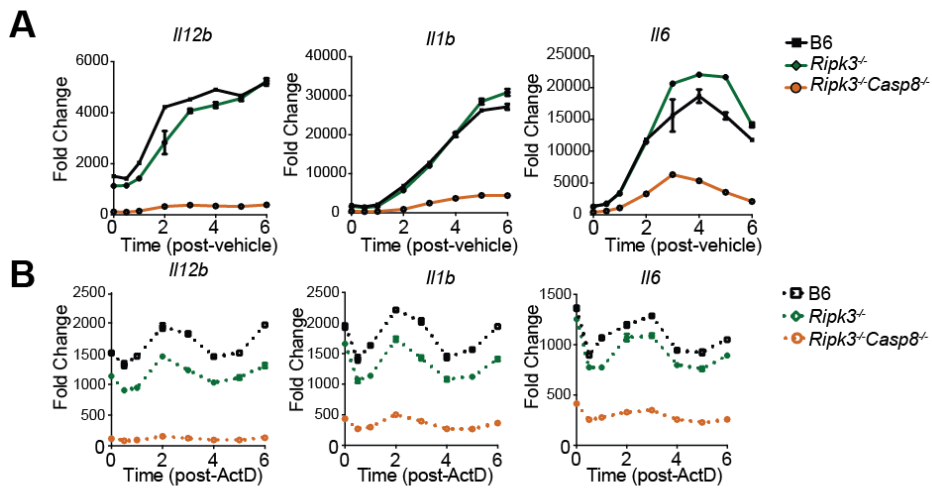


**Figure 24. Caspase-8 deficiency does not impact the stability of caspase-8-dependent mRNAs.**

(A, B) B6, *Ripk3*<sup>-/-</sup> and *Ripk3*<sup>-/-</sup>*Casp8*<sup>-/-</sup> BMDMs were treated with LPS (100 ng/mL) for 2 hrs before addition of vehicle (DMSO) (A) or 5  $\mu$ m actinomycin D (B). *Il-12b*, *Il-1b* and *Il-6* mRNA was assayed by RT-qPCR at the indicated time points. Representative of two independent experiments.



**Figure 25**

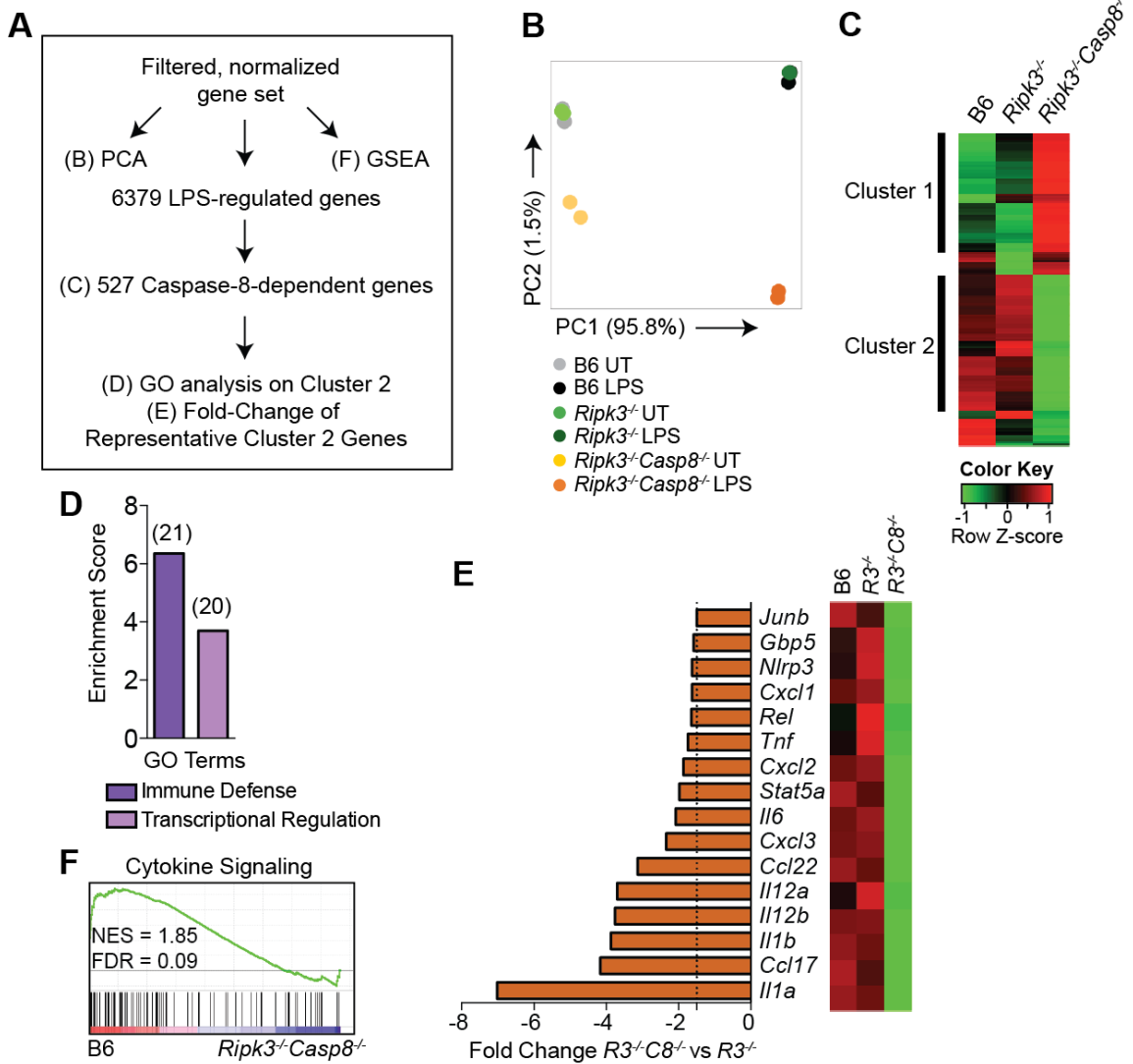


**Figure 25. Caspase-8 regulates a functionally important subset of LPS-induced genes.**

RNA was extracted from B6, *Ripk3*<sup>-/-</sup> and *Ripk3*<sup>-/-</sup>*Casp8*<sup>-/-</sup> BMDMs following 6 hours of LPS treatment (100 ng/mL) and RNA-seq was performed. (A) Schematic of analysis of the data obtained from RNA-Seq indicating figure panel where the results of each type of analysis is shown. (B) Principal Component Analysis (PCA) of filtered, normalized gene set displaying PC1 (95.8% of variance) against PC2 (1.5% of variance). (C) Hierarchical clustering by Pearson correlation of differentially expressed LPS-responsive caspase-8-dependent genes. Columns represent genotype and rows represent individual genes. Colored to indicate expression levels based on Z-scores. (D) GO enrichment performed in DAVID showing Biological Process terms enriched in cluster 2 from (C). Number of genes in each group are denoted above bars. Genes in cluster 1 did not show significant enriched for any Biological Process terms. (E) Differential expression of select genes from cluster 2 and fold change (LPS-treated *Ripk3*<sup>-/-</sup>*Casp8*<sup>-/-</sup> vs LPS-treated *Ripk3*<sup>-/-</sup> BMDMs).

(F) GSEA showing enrichment in cytokine signaling from the KEGG MSigDb canonical pathways collection 2 comparing B6 and *Ripk3*<sup>-/-</sup>*Casp8*<sup>-/-</sup> LPS-treated BMDMs.

GO, gene ontology; DAVID, database for annotation visualization and integrated discovery; GSEA, gene set enrichment analysis; KEGG, Kyoto Encyclopedia of Genes and Genome. *R3C8* = *Ripk3Casp8*

**Figure 26**

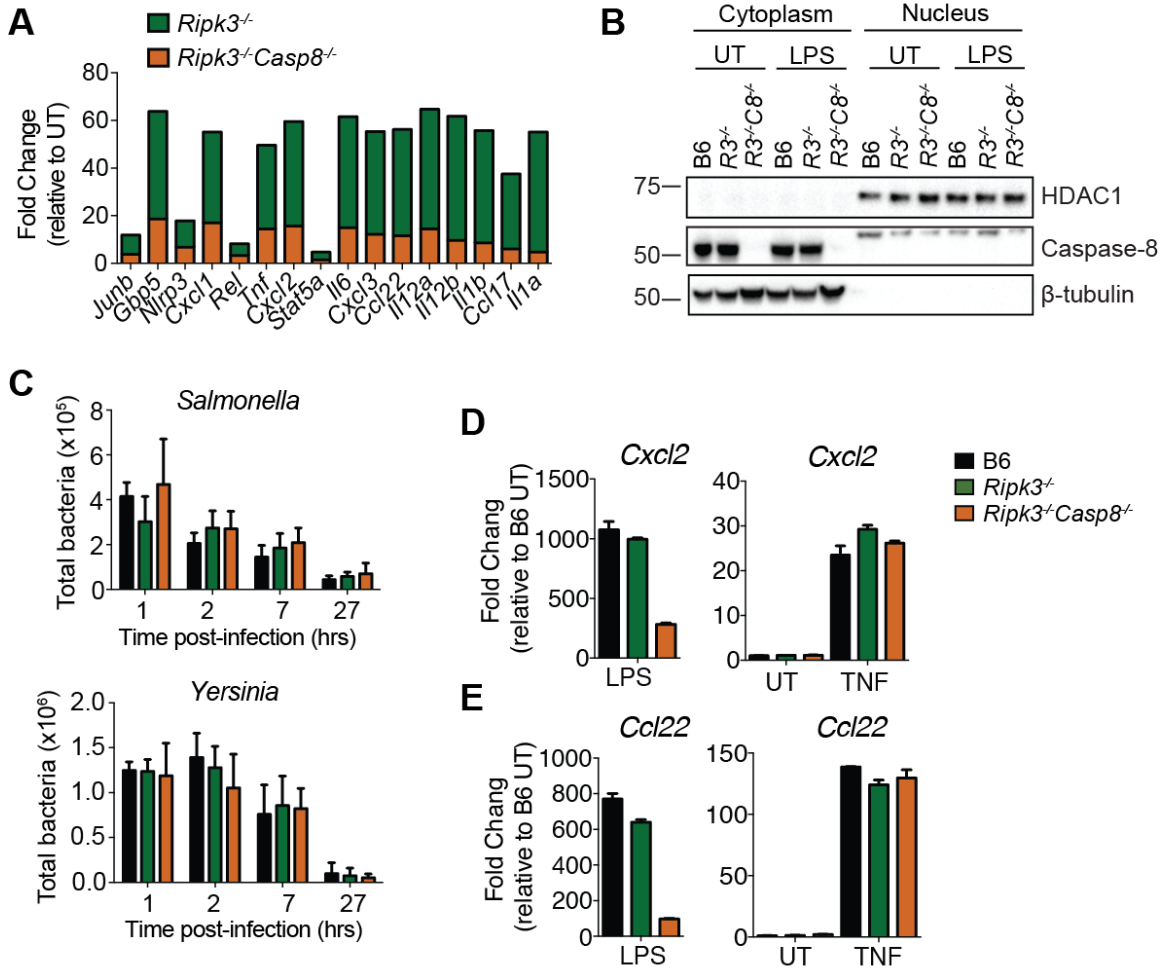


**Figure 26. Caspase-8-deficient cells exhibit wild-type levels of intracellular bacterial killing and responsiveness to TNF.**

(A) Cells were treated as in Figure 13 and fold change of select genes from cluster 2 (refer to Figure 13E) (LPS vs UT). (B) BMDMs were treated with LPS (100 ng/mL) for 3 hrs, lysates were fractionated into cytoplasmic and nuclear extracts and probed for caspase-8, HDAC1 and  $\beta$ -tubulin by western blotting. (C) BMDMs were infected with *Salmonella* or *Yersinia* for 1hr, gentamycin was added, cells were lysed and CFUs were enumerated at the indicated time points. (D, E) RT-qPCR of *Cxcl2* (D) and *Ccl22* (E) from BMDMs treated with LPS (100 ng/mL) or TNF (10 ng/mL) for 6hrs.

**Figure 27**

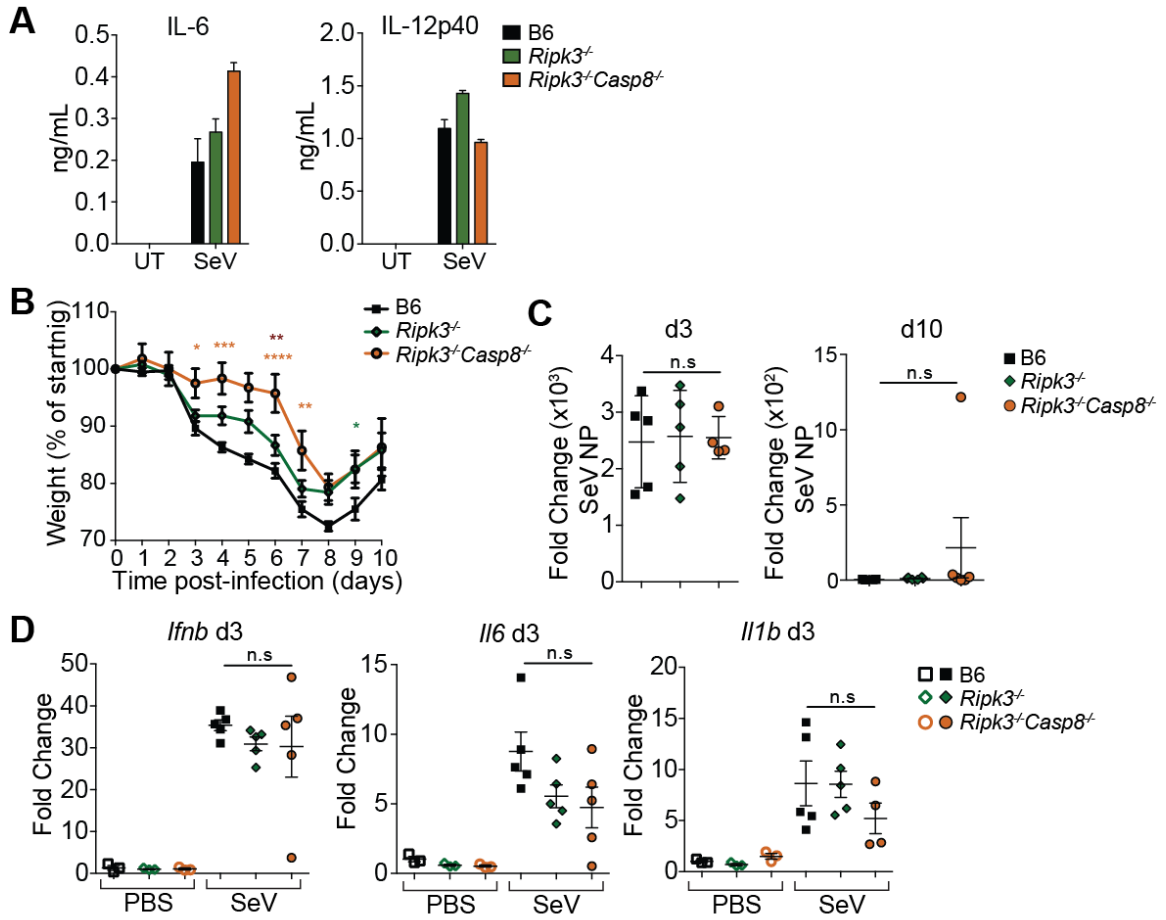


**Figure 27. Caspase-8 is not required for cytokine production in response to Sendai virus infection.** (A) B6, *Ripk3*<sup>-/-</sup> and *Ripk3*<sup>-/-</sup>*Casp8*<sup>-/-</sup> BMDMs were infected with Sendai virus (SeV) at an MOI of 10 for 6hrs. IL-6 and IL-12p40 release were measured by ELISA. (B) Weight loss in B6, *Ripk3*<sup>-/-</sup> and *Ripk3*<sup>-/-</sup>*Casp8*<sup>-/-</sup> mice that were infected intranasally with Sendai virus 52 (SeV). (C) Sendai virus nucleoprotein (SeV NP) levels in the lung were measured by RT-qPCR on day 3 (left) and day 10 (right) post-infection. (D) Transcript levels of *Ifnb*, *Il6* and *Il1b* from lungs of mock-infected (PBS) and SeV-infected (SeV) mice were assayed by RT-qPCR on day 3 post-infection. \*  $p < 0.05$ , \*\*  $p < 0.01$ , \*\*\*  $p < 0.001$  \* = B6 vs *Ripk3*<sup>-/-</sup>*Casp8*<sup>-/-</sup>, \* = B6 vs *Ripk3*<sup>-/-</sup>, \* = *Ripk3*<sup>-/-</sup> vs *Ripk3*<sup>-/-</sup>*Casp8*<sup>-/-</sup>. (B) two-way ANOVA with Bonferonni correction. (C, D) t-test. Representative of two independent experiments.

**Figure 28**

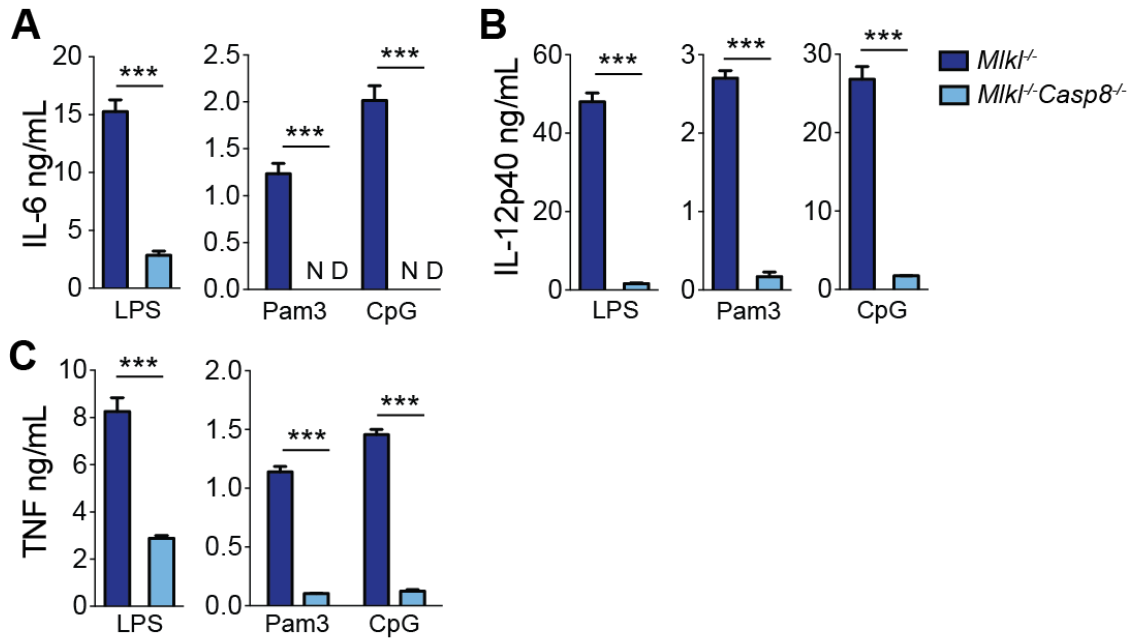


**Figure 28. Caspase-8 is required for optimal cytokine production in RIPK3-sufficient cells.** *Mik1<sup>-/-</sup>* and *Mik1<sup>-/-</sup>Casp8<sup>-/-</sup>* BMDMs were treated with LPS (100 ng/mL), Pam3CSK4 (1  $\mu$ g/mL) or CpG (1  $\mu$ g/mL) for 6hrs. (A) IL-6, (B) IL-12p40 and (C) TNF release was assayed by ELISA. \*\*\*  $p < 0.001$  by t-test. Representative of two independent experiments.

**Figure 29**

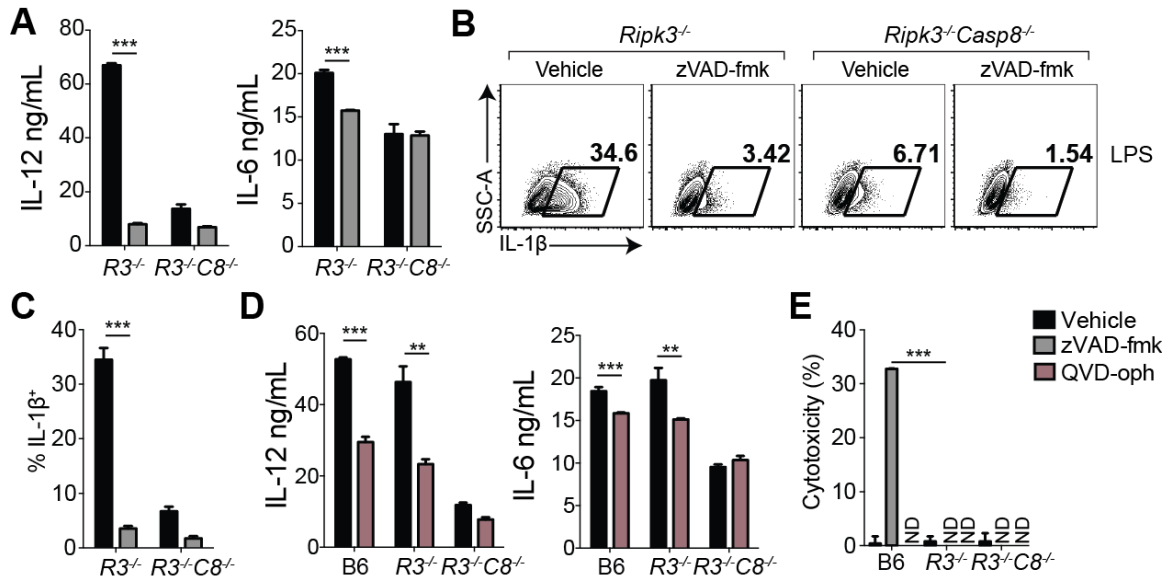


**Figure 29. Caspase-8 catalytic activity is required for maximal TLR-induced cytokine production.**

(A-E) Indicated BMDMs were pretreated with the pan-caspase inhibitor zVAD-fmk (A-C, E) or QVD-oph (D, E) for 1hr prior to 6 hr stimulation with LPS (100 ng/mL). (A, D) IL12p40 and IL-6 were measured by ELISA, (B, C) IL-1 $\beta$  was measured by flow cytometry. (E) Cytotoxicity was measured by lactate dehydrogenase release (LDH).

\*\*  $p < 0.01$ , \*\*\*  $p < 0.001$ , Student's unpaired t-test. Representative of 4 or more independent experiments.

**Figure 30**

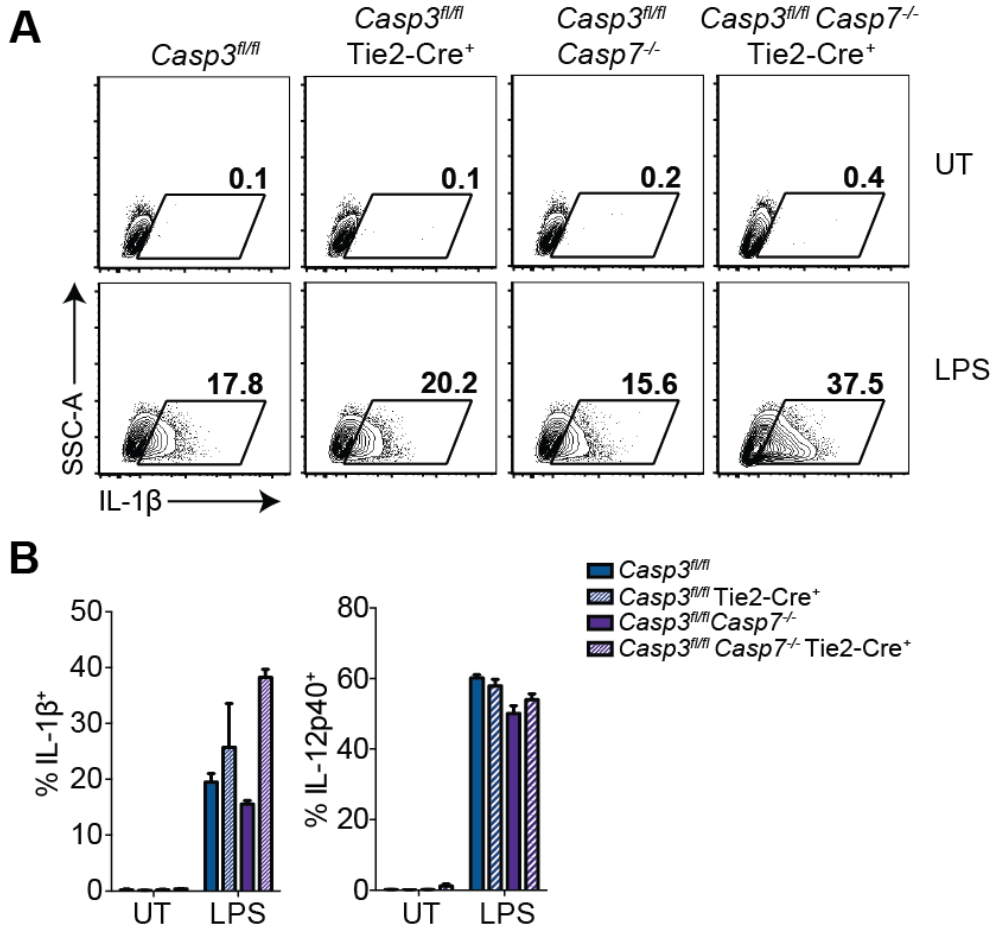


**Figure 30. The control of TLR-induced gene expression by caspase-8 is independent of caspases-3 and -7.**

Indicated BMDMs treated with LPS (100 ng/mL) or left unstimulated for 5 hrs. (A) Representative flow plots of IL-1 $\beta$  production as measured by flow cytometry. (B) Summary data of (A) and IL-12p40 release measured in BMDMs 5 hrs after LPS treatment.

**Figure 31**

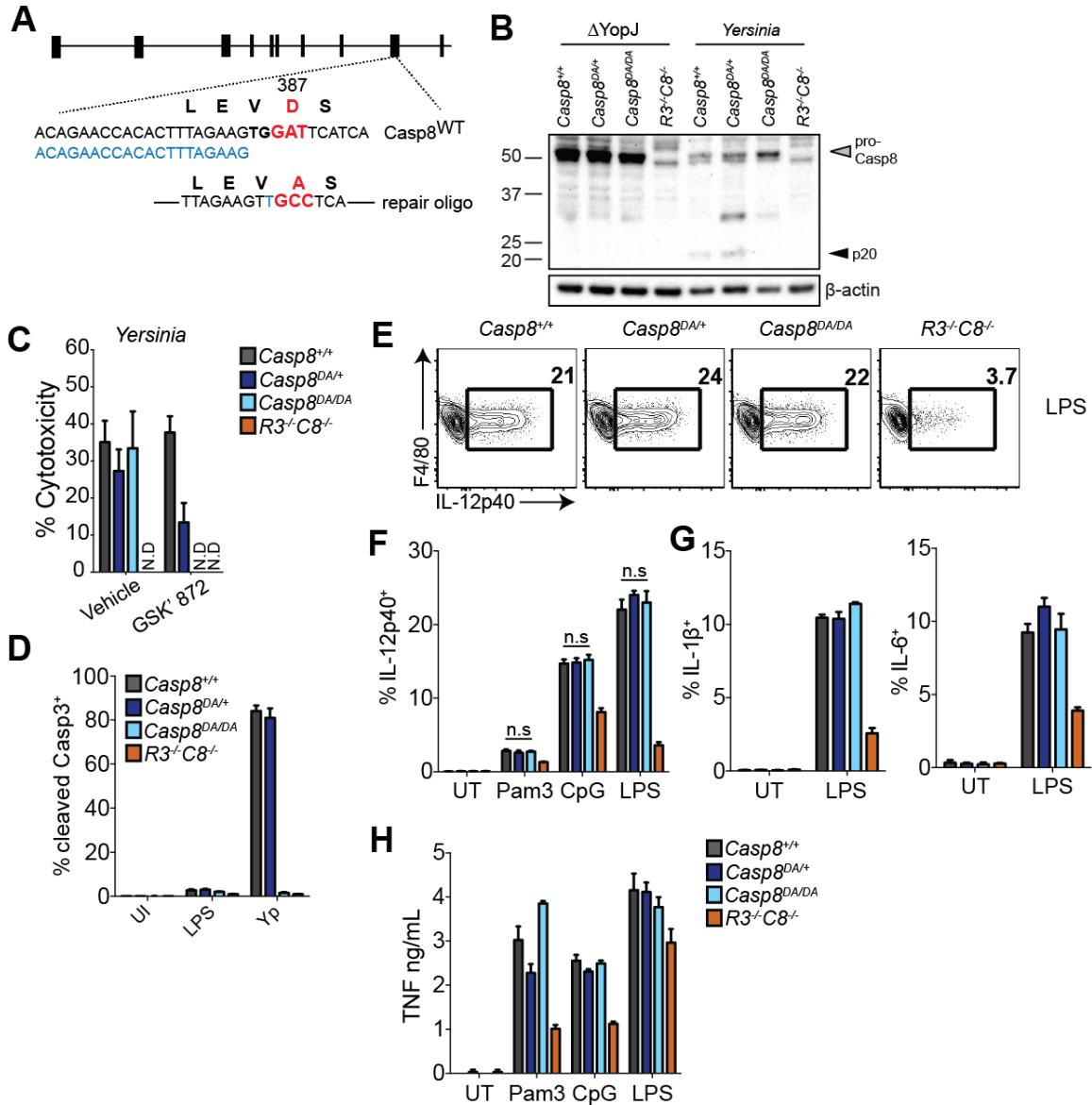


**Figure 31. Caspase-8 self-cleavage is necessary for apoptosis but not cytokine responses.**

(A) Schematic of strategy used to generate Casp8DA/DA mice using CRISPR/Cas9. GuideRNA is in blue. (B) Casp8<sup>+/+</sup>, Casp8<sup>DA/DA</sup>, Casp8<sup>DA/DA/DA</sup> and Ripk3<sup>-/-</sup>Casp8<sup>-/-</sup> BMDMs were infected with YopJ-deficient ( $\Delta$ YopJ) and wild type *Yersinia* and caspase-8 processing was measured by western analysis. (C) BMDMs were pretreated with GSK' 872 or vehicle control 1 hr prior to infection with *Yersinia*. Cytotoxicity was measured by LDH release 4 hrs post-infection. (D) Cleaved caspase-3 was measured by flow cytometry in BMDMs 2 hrs post-indicated treatments. (E-G) Casp8<sup>+/+</sup>, Casp8<sup>DA/DA</sup>, Casp8<sup>DA/DA/DA</sup> and Ripk3<sup>-/-</sup>Casp8<sup>-/-</sup> BMDMs were treated with PAMPs and cytokine production was measured after 6 hrs by flow cytometry. Representative flow plots of IL-12p40 production in response to LPS (100 ng/mL) (E), quantification of percentage of IL-12p40<sup>+</sup> in response to LPS (100 ng/mL), Pam3CSK4 (1  $\mu$ g/mL) or CpG (1  $\mu$ g/mL) (F), IL-1 $\beta$ <sup>+</sup> and IL-6<sup>+</sup> in response to LPS (100 ng/mL) (G), (H) BMDMs were treated with LPS (100 ng/mL), Pam3CSK4 (1  $\mu$ g/mL) or CpG (1  $\mu$ g/mL) for 6 hrs and TNF production was measured by ELISA.

Student's unpaired t-test. Representative of 2 independent experiments.

**Figure 32**

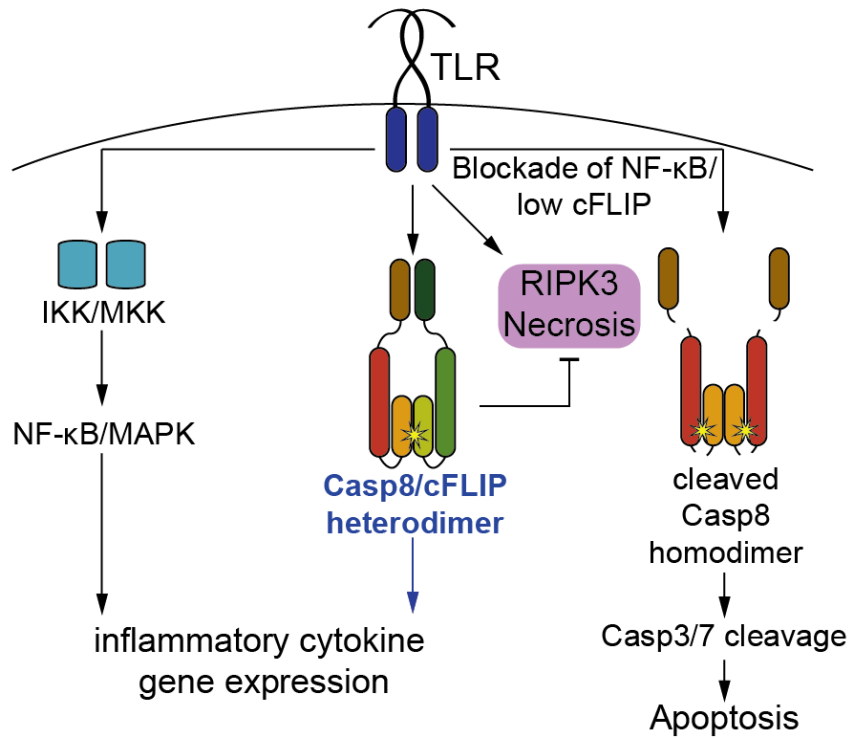


**Figure 32. Cell-intrinsic uncleaved caspase-8 enzymatic activity controls inflammatory cytokine production.** TLR ligation activates NF- $\kappa$ B and MAPK signaling, which induces expression of inflammatory cytokines, among other genes. Under certain conditions, TLR3/4 triggers extrinsic apoptosis via caspase-8. In this case, caspase-8 undergoes homodimerization and self-cleavage. Cleaved caspase-8 homodimers subsequently process the executioner caspases caspase-3 and -7 resulting in apoptotic cell death. Paradoxically, caspase-8 regulates cell survival via blocking RIPK3 necrosis and apoptosis. This function of caspase-8 is mediated by a complex containing caspase-8 and its catalytically inactive homolog, cFLIP. Here, we ascribe a novel function to the catalytically active, uncleaved caspase-8/cFLIP heterodimer in inflammatory cytokine expression.



## V. CONCLUDING REMARKS

Microbes are recognized by a variety of PRRs that trigger a cascade of signaling events, resulting in the expression of pro-survival proteins and inflammatory cytokines. Pathogens such as the gram-negative bacteria *Yersinia*, express virulence factors that can inhibit and manipulate anti-microbial responses. Therefore, the immune system must succeed in eliciting an effective immune response in the presence of microbial inhibition. The *Yersinia* effector protein YopJ impairs NF- $\kappa$ B and MAPK signaling, resulting in host cell death. The precise mechanism of *Yersinia*-induced cell death and its effect on disease outcomes remain to be determined. Death receptor ligation can induce two distinct forms of caspase-8-dependent apoptosis that are differentially dependent on the kinase activity of RIPK1 (229, 249). Additionally, ablation of caspase-8 elicits RIPK3-dependent necrosis (25, 26). We demonstrated that *Yersinia* activated RIPK1 kinase-dependent cell death. Remarkably, absence of both RIPK3 and caspase-8 or FADD abrogated cell death in response to *Yersinia*. *Yersinia*-induced cell death is associated with the activation of multiple caspases. Notably, both caspase-1 and -3 activation required caspase-8, RIPK1 and FADD, but not RIPK3, implying that the activity of *Yersinia* YopJ elicits both pyroptosis and apoptosis. Mice deficient in both RIPK3 and caspase-8 were highly susceptible to *Yersinia* infection and harbored more bacteria in their lymphoid tissues compared to RIPK3-deficient and B6 mice. Interestingly, this defect was partially restored in mice infected with *Yersinia* lacking YopJ, suggesting that cell death has a host protective role in *Yersinia* infection.

Caspase-1 is a critical mediator of pyroptosis, while caspase-3 orchestrates apoptotic cell death. Whether both pyroptosis and apoptosis are activated in the same cell is completely unknown, as these assays were performed at the population level. Furthermore, the impact of activating two distinct forms of cell death in the same cell on

inflammation, is unclear. Since we showed that caspase-1 and -3 do not affect one another's activation in our experimental system, these caspases are likely activated in parallel pathways. It is plausible that the activation of caspase-1 actively represses caspase-3-dependent apoptosis and vice versa. Single cell analysis by microscopy would reveal whether *Yersinia* induces active caspase-1 and active caspase-3 in distinct cells. Another possibility is that caspase-1 and -3 are activated in the same cell in response to *Yersinia* infection. Through cleavage of IL-1 and other substrates, active caspase-1 may provide inflammatory signals to an otherwise silent apoptotic cell death. Further work will need to identify DAMPs that are released during *Yersinia*-induced cell death and assess whether caspase-1 contributes to the release of these DAMPs. If this is the case, caspase-1 activity could be a new biomarker for immunogenic cell death and modulating caspase-1 activity could potentially benefit treatment strategies against infections or cancer.

*Yersinia*-induced cell death requires inhibition of MAPK and NF- $\kappa$ B signaling and is concurrent with a YopJ-dependent block in cFLIP expression (109). We demonstrated that *Ripk3<sup>-/-</sup>Casp8<sup>-/-</sup>* BMDMs are resistant to *Yersinia*-induced cell death. Together, these data provoke a model whereby YopJ-dependent inhibition of cFLIP expression and consequently activity of the caspase-8/cFLIP heterodimer affects two cell death check points (Figure 33). First, depletion of cFLIP releases the break on caspase-8/FADD/RIPK1 complex IIb formation and caspase-8 homodimerization. Cleaved caspase-8 homodimers would then process caspase-3 and caspase-1, resulting in cell death. Second, reduced caspase-8/cFLIP activity, derepresses RIPK3-mediated necrosis, even in the absence of stimulation. Therefore, deletion of both caspase-8 and RIPK3 is required to protect macrophages from *Yersinia*-induced cell death.

How caspase-8 is activated during *Yersinia* infection is not known. A recent study demonstrated a novel function of the IKK complex in regulating RIPK1-mediated cell death, implying that RIPK1 may be the link between *Yersinia* YopJ and caspase-8 (229). *Yersinia* YopJ inhibits TAK1, which prevents IKK $\beta$  phosphorylation, NF- $\kappa$ B signaling and the block in expression of pro-survival proteins, resulting in cell death (16, 108, 109). Dondelinger and colleagues discovered that IKK $\beta$  phosphorylates RIPK1, which maintains RIPK1 in an inactive conformation and blocks RIPK1-dependent cell death. Since *Yersinia*-induced cell death requires RIPK1, it is possible that *Yersinia* YopJ potentiates RIPK1-dependent cell death by inhibiting IKK $\beta$  phosphorylation and consequently increasing the cellular pool of dephosphorylated RIPK1. Dephosphorylated RIPK1 would activate caspase-8/FADD/RIPK1 complex formation and cell death, independent of NF- $\kappa$ B signaling. RIPK1-dependent cell death is fast, as are the kinetics of *Yersinia*-induced cell death, suggesting that YopJ induces a cell death pathway that is at least partially independent of its effect on pro-survival protein expression (Figure 33).

Since *Yersinia* can activate different cell death cascades, what are the factors that determine whether caspase-dependent apoptosis or RIPK3-dependent necrosis is triggered? Active caspase-8 can cleave RIPK3 and repress RIPK3 necroptosis (250). It is plausible that apoptosis is the dominant pathway that is activated by *Yersinia*, because *Yersinia* infection induces RIPK3 cleavage (Lance Peterson, unpublished). However, this doesn't preclude a role for RIPK3 or RIPK3 cleavage products in the control of apoptosis, as recent studies have shown that mutations in RIPK3 can trigger caspase-8-dependent apoptosis (236, 237). Nevertheless, *Casp8*<sup>DA/DA</sup> BMDMs that cannot undergo apoptosis, due to a mutation in D387, had a significant delay in *Yersinia*-induced cell death compared to B6 BMDMs. This cell death was completely blocked by the RIPK3 kinase inhibitor GSK-872, suggesting that in the absence of caspase-8-

dependent apoptosis, YopJ potentiates RIPK3 necrosis. *Casp1<sup>-/-</sup>Casp11<sup>-/-</sup>Casp3<sup>-/-</sup>* and *Casp1<sup>-/-</sup>Casp11<sup>-/-</sup>Ripk3<sup>-/-</sup>* BMDMs, are not protected from *Yersinia*-induced death (Naomi Philip and Baofeng Hu, unpublished observations), suggesting that other apoptotic caspases, such as caspase-7, may play a complementary role in cell death. Since caspase-3 and -7 share some substrates and are activated by similar stimuli, I would expect that caspase-7 would also be cleaved during *Yersinia* infection. Similarly, deficiency in all executioner caspases and RIPK3, *Casp1<sup>-/-</sup>Casp11<sup>-/-</sup>Casp3<sup>-/-</sup>Casp7<sup>-/-</sup>Ripk3<sup>-/-</sup>* BMDMs will probably be protected from cell death in response to *Yersinia*.

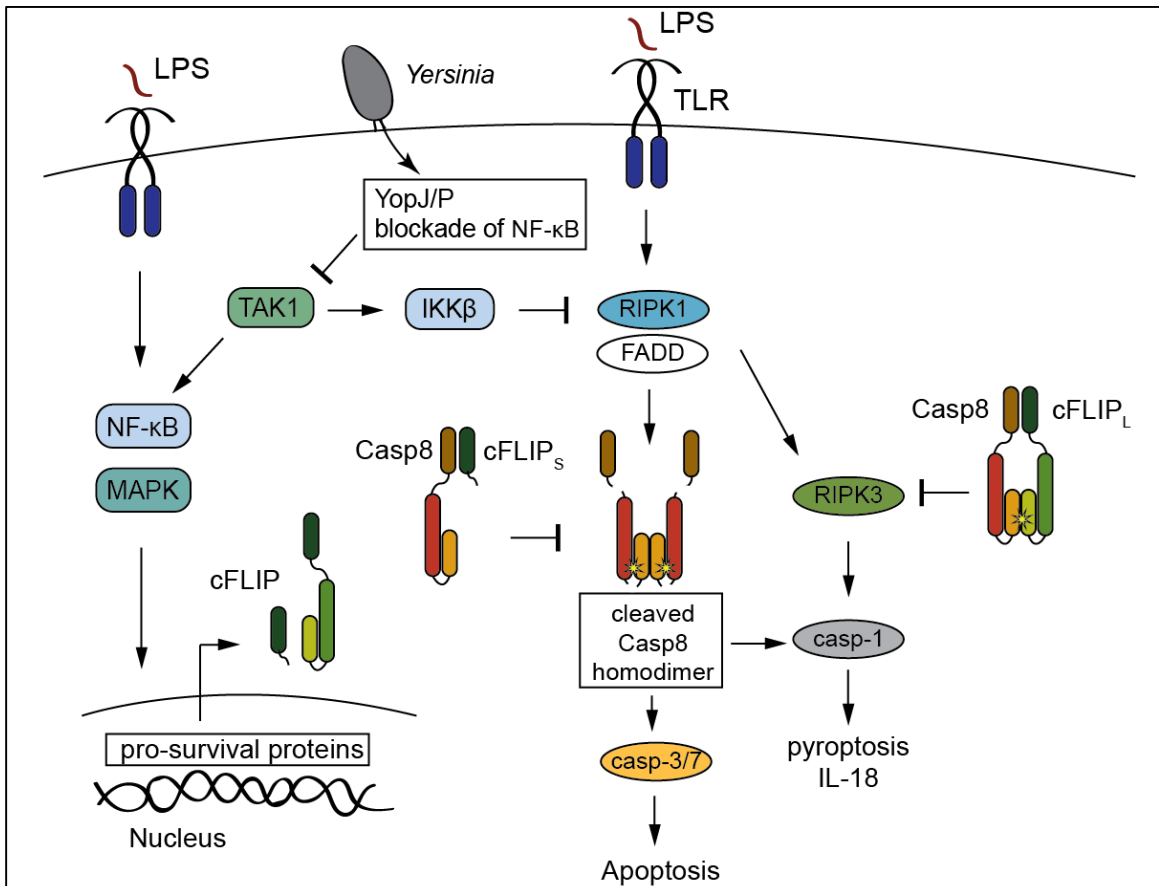


**Figure 33. Inhibition of NF-κB signaling activates inflammatory caspase-8-dependent cell death.** *Yersinia* YopJ blocks NF-κB and MAPK signaling, resulting in lower levels of pro-survival proteins such as cFLIP. cFLIP<sub>s</sub>/casp8 dimers are thought to sterically block caspase-8 homodimerization and apoptosis. In addition, cFLIP<sub>L</sub>-casp8 dimers actively inhibit RIPK3 necrosis. Lower levels of cFLIP can derepress necrosis and potentiate apoptosis. Caspase-8 is required for caspase-1 processing, but in the absence of caspase-8, RIPK3 can activate caspase-1 cleavage. YopJ may activate caspase-8 via RIPK1 and FADD. Since YopJ inhibits TAK1 and subsequently IKKβ activity, RIPK1 is no longer phosphorylated. Unphosphorylated RIPK1 promotes RIPK1-dependent apoptosis and necrosis.

TLR4- and TRIF-deficient macrophages not completely protected from *Yersinia*-induced cell death, suggesting another receptor likely contributes to cell death (16, 123). Since TNFR1 also activates caspase-8-, RIPK1- and RIPK3-dependent cell death (233), TNFR1 presents a likely candidate as a second death receptor that mediates *Yersinia*-induced cell death in macrophages. Indeed, *Tnfr<sup>-/-</sup>* BMDMs are partially protected and *Trif<sup>-/-</sup>Tnfr<sup>-/-</sup>* BMDMs are completely resistant to *Yersinia*-induced cell death (Lance Peterson, manuscript submitted). Intriguingly, while YopJ prevents NF- $\kappa$ B and MAPK signaling, *Yersinia*-infected BMDMs express and secrete small amounts of TNF that collaborates with the cell-intrinsic activities of intracellular YopJ to activate cell death (Lance Peterson, submitted).

Murine infections with YopP-expressing *Yersinia*, a hypercytotoxic variant of YopJ, displayed enhanced bacterial clearance compared to YopJ-expressing *Yersinia* (89, 99). To test whether *Yersinia*-induced cell death impacts immune responses *in vivo*, I infected *Ripk3<sup>-/-</sup>Casp8<sup>-/-</sup>* mice, whose cells were unable to undergo cell death in response to *Yersinia* infection. These mice suffered from high morbidity and mortality rates after *Yersinia* infection, and had defective cytokine production. Notably, cytokine responses were partly restored in *Ripk3<sup>-/-</sup>Casp8<sup>-/-</sup>* mice that were infected with YopJ-deficient *Yersinia*, which does not induce cell death. These findings imply that cell death may contribute to protective immune responses. However, given the recent studies implying that caspase-8 regulates innate cytokine production (123, 124, 173, 179), I considered the possibility that caspase-8 may play a cell-intrinsic role in cytokine generation independently of cell death. Indeed, using mixed bone marrow chimeras, I found that there was a smaller proportion of *Ripk3<sup>-/-</sup>Casp8<sup>-/-</sup>* cells producing inflammatory cytokines compared to *Ripk3<sup>-/-</sup>* cells in the same mouse. Concomitantly, *Ripk3<sup>-/-</sup>Casp8<sup>-/-</sup>* cells generated lower amounts of cytokine per cell compared to *Ripk3<sup>-/-</sup>* cells within the

same mouse, suggesting that *Ripk3<sup>-/-</sup>Casp8<sup>-/-</sup>* cells have a cell-intrinsic defect in cytokine production. Therefore, to specifically examine the role of cell death on immune responses *in vivo*, we need to turn to a system that is not confounded by cell-intrinsic effects on cytokine generation.

RIPK1 has been shown to trigger formation of complex IIb containing RIPK1, FADD and caspase-8 that activates apoptosis, as well as the RIPK1/RIPK3/MLKL necrosome that initiates necroptosis. I have demonstrated that RIPK1 and RIPK1 kinase activity are both required for *Yersinia*-induced cell death. As a key regulator of cell death pathways, RIPK1 positions itself as a promising target to test the role of cell death *in vivo* (Lance Peterson, unpublished). However, *Ripk1<sup>-/-</sup>* mice are post-natal lethal (251), because, paradoxically, RIPK1 blocks certain forms of caspase-8- and RIPK3-dependent cell death (29, 31) (252). Interestingly, RIPK1 kinase activity is dispensable for viability and homeostasis as *Ripk1<sup>kd/kd</sup>* (RIPK1 kinase dead K45A) mice are viable and healthy (253). Utilizing a combination of mixed bone marrow chimeras and murine infections with hypo- versus hypercytotoxic *Yersinia*, we can assess the impact of cell death on inflammation (Lance Peterson, unpublished).

A major gap in knowledge lies in our understanding of which cell types need to die and where immunogenic cell death needs to take place to be beneficial to the host. One approach to address this question would be a system in which specific cell types are made resistant to *Yersinia*-induced cell death. For instance, generating mixed bone marrow chimeras from *Ripk1<sup>kd/kd</sup>* mice and *Ccr2<sup>-/-</sup>* mice, would test the role of monocyte cell death *in vivo*, as all monocytes would be resistant to *Yersinia*-induced cell death. A limitation to this system is that the mixed environment of other immune cells may also contribute to any role of *Ccr2*-dependent monocytic responses. A combination of

reporter strains of mice, labeled bacteria and intravital imaging could be utilized to investigate the effect of cell death on the local cellular environment.

What is the purpose of a system that is set up to respond to microbial agents by either undergoing immunogenic cell death or gene expression of inflammatory mediators? When innate cells encounter microbial products, there are a series of checkpoints that determine whether a cell dies, or activates gene expression. I propose that one major checkpoint occurs along the steps of the NF- $\kappa$ B and MAPK pathways. Ligation of TLRs activates NF- $\kappa$ B and MAPK signaling and when these pathways proceed unimpeded, transcription factors activate cytokine expression. Blocking these pathways, by a bacterial product such as YopJ, raises an alarm within the cell to increase the inflammatory output. One mechanism that can induce inflammation but simultaneously override microbial blockade of inflammatory pathways is the activation of regulated cell death. But, cell death cannot be the default pathway in response to TLR ligation because it comes at a high cost – the life of a cell. Dead cells must be replaced to maintain homeostasis and some cells, such as monocyte-derived macrophages are much easier to replace than others, for instance memory T or B cells. Therefore, cell death amplifies inflammation and serves as an alternative strategy for immune defense, when classical signaling pathways are inhibited.

Caspases control cell death and survival programs. However, some caspases have also been shown to have non-apoptotic roles. Caspase-8 has been recently implicated in TLR signaling, but how caspase-8 promotes gene expression is unknown. I demonstrated that caspase-8 has a cell-intrinsic role in inflammatory gene expression downstream of both MyD88- and TRIF-dependent TLR signaling. Importantly, the enzymatic but not self-cleavage activity of caspase-8 is necessary for optimal cytokine

production. These data attribute a novel function to caspase-8 in control of inflammatory gene expression independent of its role in cell death.

Death receptor signaling induces caspase-8 homodimerization and self-cleavage, releasing the p10 and p20 subunits that subsequently form tetramers. These self-processing events stabilize active caspase-8 under cellular conditions, resulting in cleavage of apoptotic substrates. Caspase-8 can also form heterodimers with its catalytically dead homolog cFLIP. Caspase-8/cFLIP heterodimers have catalytic activity and inhibit apoptosis and programmed necrosis, but the self-cleavage of caspase-8 is not required for these functions. To test whether the self-cleavage activity of caspase-8 is necessary for gene expression, we generated *Casp8<sup>DA/DA</sup>* knock-in mice using CRISPR/Cas9. These mice have a mutation in aspartate 387 to alanine (D387A, also called *Casp8<sup>DA</sup>*) which ablates caspase-8 self-processing activity. In response to PAMP stimulation, *Casp8<sup>DA/DA</sup>* macrophages produce equivalent levels of cytokines as WT macrophages, suggesting that caspase-8 cleavage is not required for gene expression. Since the self-cleavage activity of caspase-8 is required for the apoptotic functions of the caspase-8 homodimer, but not the caspase-8/cFLIP heterodimer, these data implicate a novel function for the caspase-8/cFLIP heterodimer in gene expression (Figure 20).

Further experiments will need to specifically test whether the caspase-8/cFLIP heterodimer mediates gene expression. Unfortunately, cFLIP-deficient mice are embryonic lethal and are only viable when bred to *Ripk3<sup>-/-</sup>Casp8<sup>-/-</sup>* mice (160, 254). A mutation in human cFLIP, Q390D, prevents caspase-8/cFLIP dimerization (163). While this residue is conserved in murine cFLIP, whether Q390D in murine cFLIP will interfere with dimerization needs to be determined. Since the cFLIP/caspase-8 heterodimer inhibits both caspase-8-dependent apoptosis and RIPK3-dependent necrosis, these experiments will need to be performed on a *Ripk3<sup>-/-</sup>Casp8<sup>DA/DA</sup>* background: cFLIP can



be mutated in immortalized *Ripk3<sup>-/-</sup>Casp8<sup>DA/DA</sup>* BMDMs, or a novel knock-in mouse can be generated using CRISPR/Cas9 to test whether blocking cFLIP dimerization with caspase-8 affects gene expression.

A second approach to abrogate the caspase-8/cFLIP heterodimer, would be to use siRNA against cFLIP to knock down cFLIP in *Ripk3<sup>-/-</sup>Casp8<sup>DA/DA</sup>* cells. As cFLIP-deficiency potentiates RIPK3-necrosis, these experiments will again need to be done in RIPK3-deficient cells or in the presence of RIPK3 kinase inhibitors. The viral serpin protease CrmA preferentially inhibits the activity of caspase-8 homodimers compared to caspase-8/cFLIP heterodimers (26, 255). Ectopic expression of CrmA in fibroblasts potently blocks caspase-8-induced apoptosis without potentiating RIPK3-dependent necrosis (26). A third approach to test whether caspase-8/cFLIP heterodimers or caspase-8 homodimers regulate gene expression, would be to either ectopically express CrmA in B6 BMDMs or infect cells with CrmA-sufficient or -deficient pox virus, to specifically target caspase-8 homodimers. Since high levels of CrmA will inhibit caspase-8/cFLIP heterodimers, the concentration of CrmA or virus-expressing CrmA will need to be titrated to achieve minimal targeting of caspase-8 heterodimers.

Another system that could be potentially useful to tease apart the roles of caspase-8-containing complexes would be a drug-inducible fusion protein dimerization system (20, 148). In these studies, the pro-domains of caspase-8 were replaced with the FK506 binding proteins (FKBP), which bind rapamycin and analogous drugs with high affinity, and cFLIP was linked to FKBP12 rapamycin binding (FRB). These two distinct domains allow for homodimerization or heterodimerization. Unfortunately, these experiments generate superphysiological amounts of homodimers and heterodimers that result in cell death (20, 148). Low doses of drug may have low cytotoxicity and thus make it possible to test the role of homodimers versus heterodimers in gene regulation.

My studies have shown that caspase-8 is involved in TLR, but not TNFR signaling in macrophages. Interestingly, caspase-8 does not associate with the myddosome, a macromolecular complex that activates multiple signaling cascades in response to MyD88-dependent TLR activation (6, 7). Caspase-8-deficient cells also have no defect in myddosome formation. These data suggest that caspase-8 likely functions downstream of the myddosome to regulate gene expression. Whether caspase-8 promotes NF- $\kappa$ B signaling is unresolved as studies have arrived at opposite conclusions (166-175). Notably, we have demonstrated that caspase-8 does not affect early NF- $\kappa$ B or MAPK signaling events in macrophages, implying caspase-8 plays a role in a distinct pathway or affects late NF- $\kappa$ B and MAPK signaling. How TLR signaling activates caspase-8 remains a major gap in the field.

Mass spectrometry-based proteomics to detect specific binding partners can be employed to address how caspase-8 may be activated in response to TLR ligation (256). Briefly, proteins in TLR-stimulated versus unstimulated *Ripk3<sup>-/-</sup>Casp8<sup>-/-</sup>* BMDMs can be differentially labelled using stable isotope labelling of amino acids in cell culture (SILAC). Cell lysates are combined at a 1:1 ratio and affinity-purified with caspase-8 death effector domain (DED) GST fusion proteins followed by liquid chromatography-tandem mass spectrometry (LC-MS/MS). Proteins that interact with the bait in a stimulation-dependent manner will have more intense peaks and can be distinguished from background binding proteins, which are exemplified by their 1:1 ratio between unstimulated and stimulated states. A caveat to this approach is that it assumes that the mechanism by which TLRs engage caspase-8 involves interactions with the DED of caspase-8. One argument in favor of this is that *Ripk3<sup>-/-</sup>Fadd<sup>-/-</sup>* BMDMs have a similar cytokine profile as *Ripk3<sup>-/-</sup>Casp8<sup>-/-</sup>* BMDMs in response to TLR ligation, suggesting that a complex containing caspase-8 and FADD (which interact via DEDs) likely mediates gene

expression. FADD also contains a death domain (DD), that may be important for linking caspase-8 to known TLR signaling proteins. Peptides identified by this screen will need to be validated by i) confirming that multiple peptides of the same protein are enriched, ii) conducting affinity purification with the DED of FADD, as this should reveal common candidates, iii) conducting affinity purification with other fragments of caspase-8 or cFLIP that may be involved in signaling, iv) affinity purification with the DD of FADD and v) co-immunoprecipitation of candidate proteins with caspase-8 or FADD. Proteins with weak interactions may not be detected, however this approach should reveal candidates that are capable of binding caspase-8 and can be validated by other techniques such as co-immunoprecipitation.

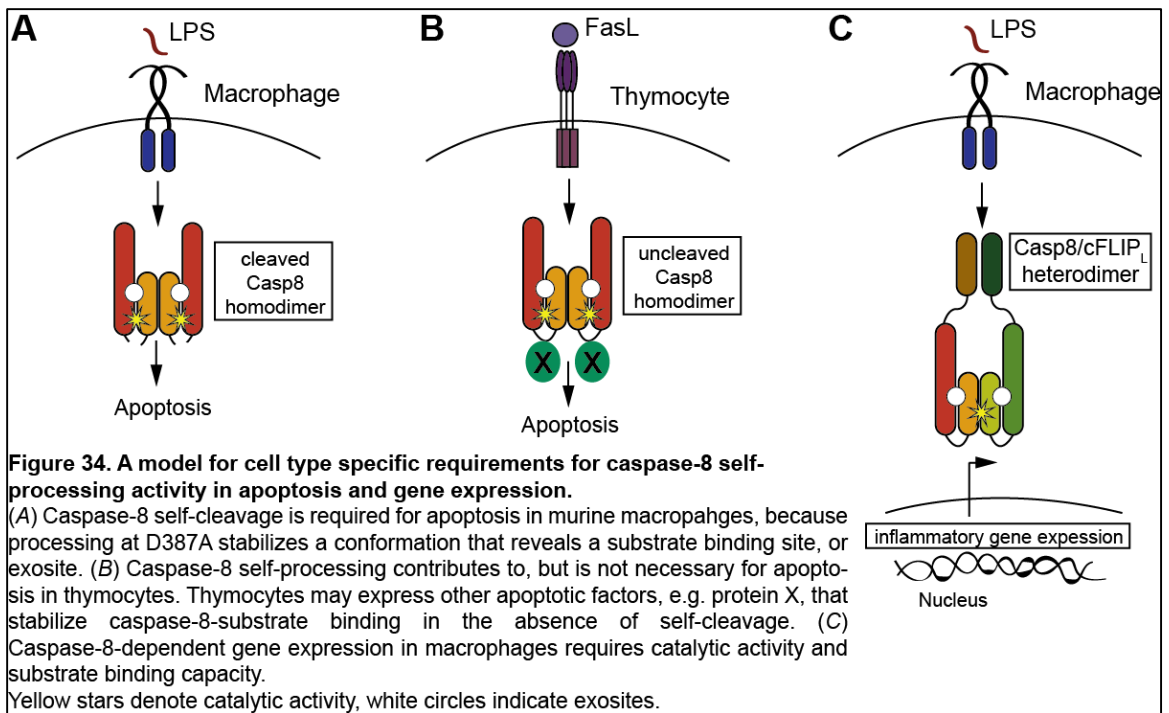
As the enzymatic activity of caspase-8 is necessary for optimal cytokine responses, we favor a model where caspase-8 cleaves some protein(s) X that subsequently regulate(s) gene expression. On the other hand, enzymatically active caspase-8 may adopt a conformation that allows it to act as a signaling platform. Unfortunately, there are no hard and fast rules that define “substrates” versus “non-substrates”, only “poor”, “intermediate” and “good” substrates. A peptide with the sequence  $P_4-P_3-P_2-P_1-P_1'$ , with  $P_1-P_1'$  as a scissile bond, is a good caspase substrate if, first, the  $P_1$  residue is asparagine; second, the  $P_1'$  residue is a neutral amino acid, such as glycine, alanine or serine; third, residues  $P_4-P_3-P_2$  interact favorably with the catalytic groove (this depends on the caspase); fourth, the substrate cleavage site  $P_4-P_1'$  is exposed to the aqueous environment; fifth, substrates and caspases must colocalize (257, 258). Finally, high cleavage site specificity is often insufficient for proteolysis. Many enzymes including caspase-8 have exosites, that serve as substrate binding sites and are distinct from the catalytic site (259). Much less is known about caspase exosites, but

some of our preliminary data, discussed in more detail below, suggest that caspase-8 may have one exosite in its p10 subunit.

When caspase-8 is activated by dimerization and cleavage, p10<sub>2</sub>-p20<sub>2</sub> tetramers bind and process apoptotic substrates. The catalytic cysteine at residue 360 is necessary for proteolytic activity, and an aspartate at residue 387 is critical for self-cleavage between the p20 and p10 subunits. But the residues required for substrate binding (exosites) are not well-defined. Interestingly, thymocytes from BAC-transgenic mice expressing murine caspase-8 D387A undergo delayed Fas-induced apoptosis and caspase-3 activation, suggesting that self-processing of caspase-8 contributes to, but is not necessary for apoptosis in thymocytes ((242) and unpublished data). However, abrogating self-cleavage activity in human caspase-8, through mutations at complementary as well as additional residues, demonstrated that caspase-8 self-processing was required for caspase-8 activation in cells (20). One interpretation of these data is that murine caspase-8 may have additional unknown aspartate residues that undergo self-cleavage and that cleavage at those residues is sufficient for apoptotic activity. Alternatively, cleavage at D387A of murine caspase-8, may allow accessibility to a substrate binding site and this conformation is stabilized by cell type-specific factors (Figure 34).

To address whether caspase-8 undergoes self-processing at additional aspartate residues, we generated macrophage cell-lines that have three mutations in caspase-8 D387A, D397A and D400A, termed *Casp8*<sup>D3A</sup>. Macrophages that express *Casp8*<sup>D3A</sup> do not undergo caspase-8 processing and have no detectible caspase-8 activity in response to *Yersinia* infection (123). However, BMDMs from *Casp8*<sup>DA</sup> mice (expressing caspase-8 D387A) also do not undergo caspase-8 processing or apoptosis, raising the possibility that mutations D397A and D400A do not alter protein function. To determine

the role of caspase-8 self cleavage *in vivo* and whether *Casp8*<sup>D3A</sup> functions differently from *Casp8*<sup>DA</sup>, we generated *Casp8*<sup>D3A</sup> knock-in mice and compared them to *Casp8*<sup>DA</sup> mice (unpublished). Intriguingly, while *Casp8*<sup>DA/DA</sup> mice are viable and healthy, *Casp8*<sup>D3A/D3A</sup> mice are not viable. Litters from *Casp8*<sup>D3A/+</sup> x *Casp8*<sup>D3A/+</sup> crosses bear no *Casp8*<sup>D3A/D3A</sup> homozygous pups, but instead only wild type and heterozygous animals at ratios of 1:2. Since active caspase-8 protects mice from RIPK3-mediated lethal inflammation during embryonic development, *Casp8*<sup>D3A/D3A</sup> mice are likely susceptible for the same reasons. Therefore, I hypothesize D397 and D400 are critical residues for substrate binding and indirectly regulate catalytic activity.



My work has demonstrated that caspase-8 regulates gene expression at the transcriptional level. Whether caspase-8 regulates chromatin accessibility to transcription factor binding in a manner similar to priming with IFN $\gamma$  or RNA polymerase II elongation, is an open question (260). To assess whether caspase-8 controls genome-wide chromatin accessibility, we can perform assay for transposase accessible

chromatin with high-throughput sequencing (ATAC-seq) for open vs closed chromatin regions (261). Regions that are identified as less accessible in RIPK3/caspase-8-deficient macrophages compared to wild type macrophages will be validated with ChIP-qPCR against transcription factors or histone modifications. Poorly accessible promoters may display less H3K4me3 and closed enhancers may depict lower levels of H3K4me1. These regions may be associated with repressive chromatin marks such as H3K27me3 or H3K20me3. These experiments would indirectly test whether caspase-8-deficiency is associated with altered histone demethylase, methylase, deacetylase or acetylase activity.

Since caspase-8 controls gene transcription, caspase-8 could regulate RNA polymerase II (Pol II) elongation. Pol II is differentially phosphorylated and phosphorylation at serine 2 (S2) releases Pol II from pausing. The complex P-TEFb, which consists of cdk9 and a cyclin T, phosphorylates Pol II S2 and other proteins required for elongation. Caspase-8 could regulate the formation or recruitment of P-TEFb to Pol II via the cleavage of unknown substrates.

Caspase-8 may stabilize interactions between transcription factors. For instance, I $\kappa$ B $\beta$  stabilizes cRel:p65 dimer formation, which is required for optimal transcription of a subset of LPS-responsive genes including *Tnf*, *Il1a* and *Il12b* (262). Even-though cRel and p65 ChIP at the *Tnf* promoter was unaffected in I $\kappa$ B $\beta$ -deficient macrophages, transcription of *Tnf* was significantly reduced. It is plausible that caspase-8 controls gene expression via stabilizing dimerization of NF- $\kappa$ B subunits.

The mechanism by which TLRs activate caspase-8 remains elusive. In T cells, the paracaspase, MALT1, associates with caspase-8 and cFLIP to regulate T cell activation (263). MALT1 contains a death domain and a paracaspase domain. Therefore, it is conceivable that MALT1 serves as the link between TLRs and caspase-8

activation. TNFR1-associated death domain protein (TRADD) facilitates formation of a signaling complex at TNFR1 and TLR4 through homotypic interaction motifs (264). Thus, TRADD may activate caspase-8 in response to TLR stimulation. Indeed, TRADD-deficient macrophages produce lower amounts of IL-6 and TNF in response to LPS.

An important area that requires further study is understanding how caspase-8 serves to modulate only 8% of the LPS response. Caspase-8 may behave as an intermediate tier or stimulus-specific transcription factor, whose chromatin binding is regulated by pioneer or lineage determining transcription factors, similar to JunB (265, 266). JunB-deficient macrophages have defects in M1 and M2 polarization and associated cytokine production (267, 268). Interestingly, I found that RIPK3/caspase-8-deficient macrophages express lower levels of *Junb* transcript compared to *Ripk3*<sup>-/-</sup> BMDMs in response to LPS stimulation. However, these differences at the mRNA level did not translate to differences in JunB protein as measured by western blotting (unpublished). Nevertheless, GSEA analysis that compared a JunB-dependent LPS responsive gene set with a rank-ordered list of caspase-8-dependent genes (from our RNA-seq) revealed significant correlation and enrichment of caspase-8-dependent genes in the JunB gene set (unpublished). Thus, it is possible that caspase-8 regulates JunB expression and that small differences (that may not be detectable by western blotting), together with differences in other regulators, have a cumulative effect on gene expression.

To further understand the basis for the specificity of caspase-8-dependent gene expression, I chose to model these data on the theory of scale-free networks (Figure 35). Scale-free networks are characterized by nodes and hubs (269, 270). Nodes are defined as elements that have interactions or edges with other elements within the network. There is an inverse correlation between the frequency of a node being within a

network and the number of node edges. Nodes with a large number of edges are known as hubs and disruptions at hubs, but not at nodes, significantly impact the network. As biological systems are not binary in nature, I hypothesize that there is a hierarchy to network hubs; major hubs function as on/off switches, while intermediate hubs serve as an analog dial to fine tune responses. I propose that caspase-8 acts as an intermediate signaling hub modulating multiple nodes that each affect distinct aspects of TLR signaling. Since caspase-8-deficient cells are capable of producing a low level of cytokines and only 8% of the LPS response is impacted, caspase-8 is not a major hub. Proteins upstream in signaling pathways, such as TRIF or MyD88 would be classified as major hubs, as they are required for signal transduction. Finally, scale-free networks highlight the robustness of biological networks. Disturbing one node such as STAT5A or IRF1 may not have a significant impact on cytokine production (unpublished), but removing a hub, such as caspase-8, substantially alters signaling outputs.

To conclude, my studies have shed light on the mechanisms by which the gram-negative pathogen *Yersinia* induces cell death and caspase-1 activation in macrophages. I have used *Yersinia* as a model to elucidate the impact of cell death on immune responses *in vivo*. These data suggest that inflammatory cell death may be an effective host defense response to pathogens that actively subvert immune signaling. I have also investigated the non-apoptotic function of caspase-8 and have ascribed a novel role for caspase-8 enzymatic activity in regulating inflammatory gene expression. Caspase-8 positions itself as an important signaling hub that likely fine tunes innate immune responses, ensuring that anti-pathogen responses are appropriately regulated. As many of the pathways and proteins I examined are conserved in humans, my work may offer rational strategies for therapeutics that target autoimmunity, inflammatory and infectious disease, and cancer.



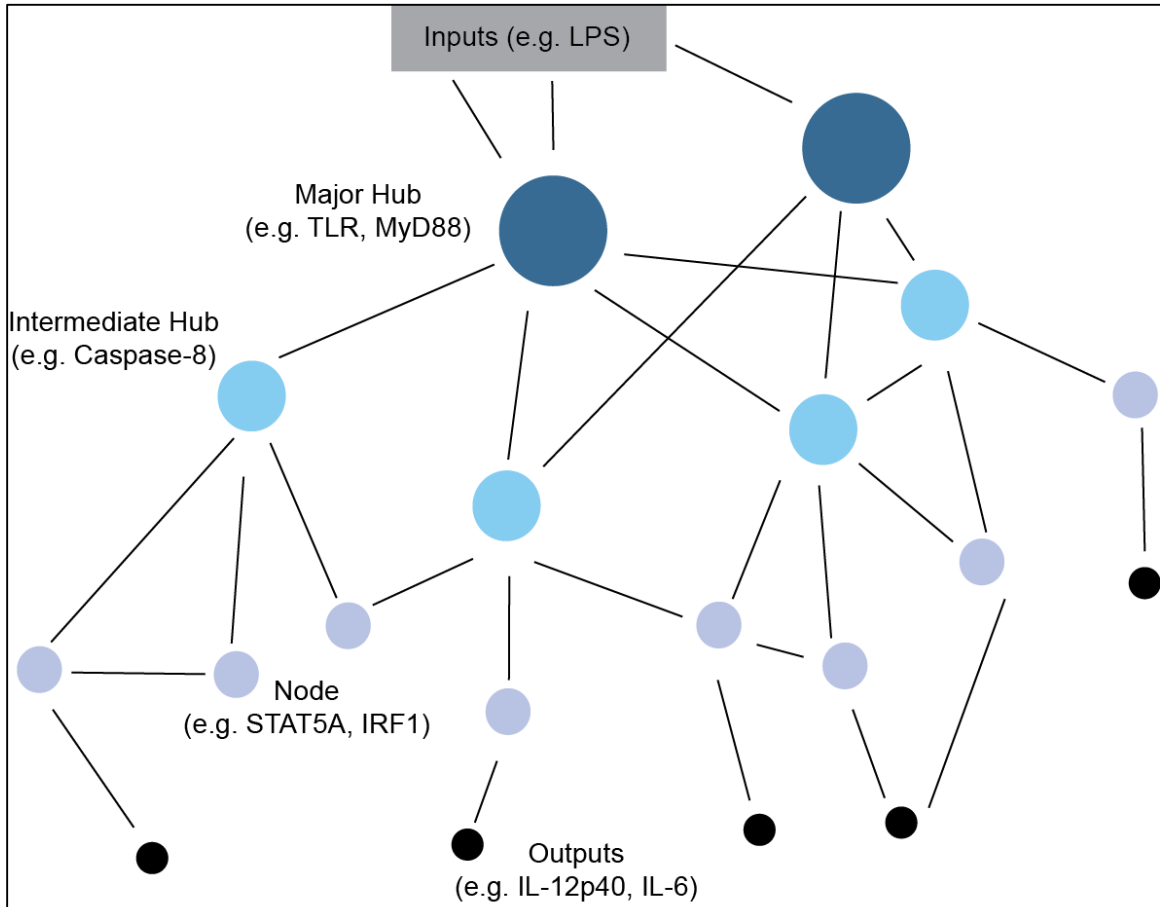


**Figure 35. Biological networks show properties of scale-free networks.**

Biological networks are robust and respond appropriately to changing environments. Scale-free networks are characterized by nodes, elements in the networks that have interactions with other elements, and hubs. Hubs are a type of node that has more outputs than inputs and perturbation of a hub disrupts the network. On the other hand, modulating a single node has little to no effect on the network, making scale-free networks robust. Here, I propose that there are several classes of hubs; major hubs are necessary for relaying inputs to outputs, while intermediate hubs serve to fine-tune responses. For instance, I hypothesize that caspase-8 is one such intermediate hub, as deficiency in caspase-8 results in reduced levels in a specific subset of TLR-dependent outputs. Whereas MyD88 is a major hub, because MyD88 is absolutely required for signal transduction of multiple inputs.

## VI. APPENDIX I SUPPLEMENTARY CODE

This appendix contains all the code used to analyze the RNA-seq data in this thesis. Briefly, B6, *Ripk3*<sup>-/-</sup> and *Ripk3*<sup>-/-</sup>*Casp8*<sup>-/-</sup> BMDMs were stimulated with LPS for 6hrs or left untreated. RNA was isolated using the RNeasy Mini Kit (Qiagen) and processed as per manufacturer's instructions. mRNA-seq libraries were prepared using the TruSeq Stranded Total RNA LT Kit with Ribo-Zero Gold, according to the manufacturer's instructions. Samples were run on Illumina NextSeq 500 to generate between 151 base-pair, paired-end reads with a Q30 score of ~80%, resulting in 25-50 million fragments/sample. All data processing and analyses were carried out using the R programming language (Version 3.2.2) and the RStudio interface (Version 0.99.489), and can be reproduced using this supplementary code file.

### R Packages

These are the R/Bioconductor packages that were used for this analysis

```
library(Rsubread)
library(limma)
library(edgeR)
library(ShortRead)
library(org.Mm.eg.db)
library(AnnotationDbi)
library(WGCNA)
library(ggplot2)
library(reshape2)
library(dplyr)
library(ggvis)
library(Biobase)
library(RColorBrewer)
library(gplots)
```

This dynamic html summary report was compiled in Rmarkdown using the following packages:

```
library(rmarkdown)
library(knitr)
library(devtools)
```

## Set-up and QC

To start off, I read in a file that describes the design of the study. This file sets treatment groups, replicates, sample names and more

```
targets <- readTargets("Igor_Ripk3_BMMC_studyDesign_RNAseq.txt",
row.names=NULL) targets.mod <- targets[1:12,]
myGroups <- factor(paste(targets.mod$genotype, targets.mod$treatment,
sep=".")) sampleLabels <- paste(targets.mod$genotype,
targets.mod$treatment, targets.mod$rep, sep=".") design <-
model.matrix(~0+myGroups)
```

Then I read in my raw data. Fastq files were previously aligned to the mouse genome Mus\_musculus.GRCm38 to generate BAM files. Reads were then aligned to exons and compiled in a digital gene expression (DGE) list.

```
load("DGElist")
myEnsemblIDs <- DGEList$genes$GeneID
```

Normalize unfiltered data based on mean-variance relationship and generate log2 counts per million (CPM) and reads per kilobase per million (RPKM)

```
load("DGElist")
myEnsemblIDs <- DGEList$genes$GeneID

normData.unfiltered <- voom(DGEList, design,
plot=FALSE) exprs.unfiltered <-
normData.unfiltered$E
exprs.matrix.unfiltered <-
as.matrix(exprs.unfiltered) rpkm.unfiltered <-
rpkm(DGEList, DGEList$genes$Length)
```

Filter data to only keep those genes that had >10 reads per million mapped reads in atleast two libraries.

```
load("DGElist")
myEnsemblIDs <- DGEList$genes$GeneID

normData.unfiltered <- voom(DGEList, design,
plot=FALSE) exprs.unfiltered <-
normData.unfiltered$E
exprs.matrix.unfiltered <-
as.matrix(exprs.unfiltered) rpkm.unfiltered
<- rpkm(DGEList, DGEList$genes$Length)
```

```

cpm.matrix.filtered <- rowSums(cpm(DGEList)
> 10) >= 2 DGEList.filtered<-
DGEList[cpm.matrix.filtered,]
rpkm.filtered <- rpkm(DGEList.filtered,
DGEList.filtered$genes$Length) rpkm.filtered <-
log2(rpkm.filtered + 1)
normData <- voom(DGEList.filtered, design,
plot=FALSE) exprs <- normData$E
exprs.matrix.filtered <- as.matrix(exprs)

```

Annotate expression data using the updated mouse database, insert EntrezIDs and filter out genes on X and Y chromosome as mixed-sex BMDMs were used.

```

load("DGEList")
myEnsemblIDs <- DGEList$genes$GeneID

normData.unfiltered<- voom(DGEList, design,
plot=FALSE) exprs.unfiltered <-
normData.unfiltered$E
exprs.matrix.unfiltered <-
as.matrix(exprs.unfiltered) rpkm.unfiltered <-
rpkm(DGEList, DGEList$genes$Length)

```

```

cpm.matrix.filtered <- rowSums(cpm(DGEList)
> 10) >= 2 DGEList.filtered<-
DGEList[cpm.matrix.filtered,]
rpkm.filtered <- rpkm(DGEList.filtered,
DGEList.filtered$genes$Length) rpkm.filtered <-
log2(rpkm.filtered + 1)
normData <- voom(DGEList.filtered, design,
plot=FALSE) exprs <- normData$E
exprs.matrix.filtered <- as.matrix(exprs)

```

```

columns(org.Mm.eg.db) keytypes(org.Mm.eg.db)
myAnnot.unfiltered <- AnnotationDbi::select(org.Mm.eg.db,
keys=rownames(exprs.matrix.unfiltered), keytype="ENSEMBL",
columns=c("ENTREZID", "GENENAME", "SYMBOL", "CHR"))
myAnnot.filtered <- AnnotationDbi::select(org.Mm.eg.db,
keys=rownames(exprs.matrix.filtered), keytype="ENSEMBL",
columns=c("ENTREZID", "GENENAME", "SYMBOL", "CHR"))
resultTable.unfiltered <- merge(myAnnot.unfiltered,
exprs.matrix.unfiltered, by.x="ENSEMBL", by.y=0) resultTable.filtered <-
merge(myAnnot.filtered, exprs.matrix.filtered, by.x="ENSEMBL", by.y=0)
head(resultTable.unfiltered)
dim(resultTable.unfiltered) dim(resultTable.filtered)

```

```

#add more appropriate sample names as column headers
colnames(resultTable.unfiltered)<-c("Ensembl", "Entrez", "Name", "Symbol", "Chr", sampleLabels)
colnames(resultTable.filtered)<-c("Ensembl", "Entrez", "Name", "Symbol", "Chr", sampleLabels)
#now write these annotated datasets out
write.table(resultTable.unfiltered, "normalizedUnfilteredRNAseq.txt", sep="\t", quote=FALSE)
write.table(resultTable.filtered, "normalizedFilteredRNAseq.txt", sep="\t", quote=FALSE)
head(resultTable.unfiltered)
head(resultTable.filtered)
#remove all genes on X and Y chromosomes using dplyr filter function as mixed sex BMDMs were used
class(resultTable.filtered) dim(resultTable.filtered)
myDataX.filter <- resultTable.filtered%>%
filter(Chr!="X") head(myDataX.filter)
myDataXY.filter <- myDataX.filter%>%
filter(Chr!="Y") head(myDataXY.filter) dim(myDataXY.filter)
write.table(myDataXY.filter, "normalizedFilteredXYRNAseq.txt", sep="\t", quote=FALSE)

```

Since RNA-seq may bring up multiple gene segments per gene ID, collapse expression data so that each gene corresponds to one set of values.

```

dupFiltered <- unique(myDataXY.filter$Symbol)
myIDs <- rownames(myDataXY.filter)
mySymbols <- myDataXY.filter[,4]
head(myDataXY.filter)
resultTable <- myDataXY.filter[,-1:-5]
head(resultTable)
myCollapsed <- collapseRows(resultTable, mySymbols, myIDs, method = "MaxMean")
myCollapsed <- myCollapsed$datETcollapsed
write.table(myCollapsed, "Collapsed.txt", sep="\t", quote=FALSE)
dim(myCollapsed)

```

## Exploratory Analysis

Here, I plot a cluster dendrogram that groups samples based on similarity

```

sampleLabels <- paste(targets$genotype, targets$treatment, sep=".")
distance <- dist(t(exprs.matrix.filtered), method="maximum")
clusters <- hclust(distance, method = "complete")
plot(clusters, label = sampleLabels, hang = -1)

```

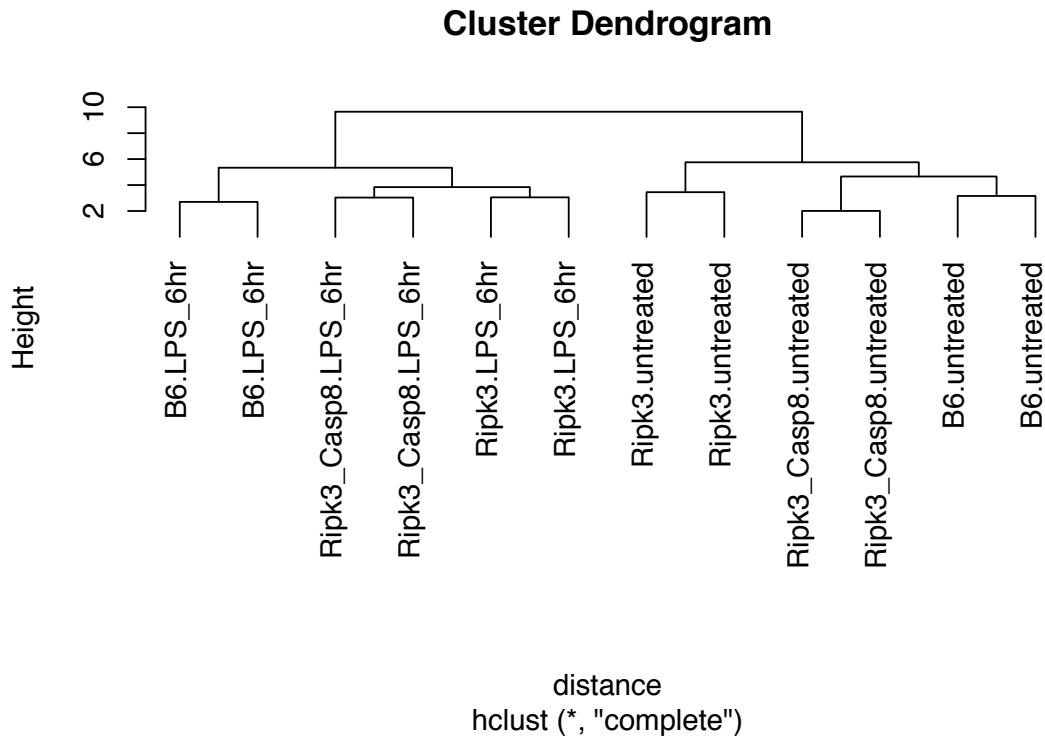


Figure 1: Samples group by genotype and treatment.

Principal component analysis of these data portrays variables that account for most of the variation in the data

Figure 2: LPS accounts for over 95% of the variance.

```
pca.res <- prcomp(t(exprs.matrix.filtered), scale.=F, retx=T)
ls(pca.res)
summary(pca.res)
head(pca.res$rotation)
head(pca.res$x)
plot(pca.res, las=1)
```

## pca.res



```
pc.var<-pca.res$sdev^2
pc.per<-round(pc.var/sum(pc.var)*100, 1)
pc.per
```

Now we can visualize how the samples contribute to PC1 and PC2

```
pc.var<-pca.res$sdev^2
pc.per<-round(pc.var/sum(pc.var)*100, 1)
pc.per
```

```
data.frame <- as.data.frame(pca.res$x) ggplot(data.frame,aes(x=PC1,y=PC2,
color=myGroups))+
geom_point(size=5) +
scale_colour_manual(values=c("#000000", "#AAAAAA", "#E36B09", "#FFCC66", "#297A18",
"#6EF054"))+
theme(legend.position="right", legend.key=element_rect(fill=NA))+
#remove axis ticks and tick text
theme(axis.ticks = element_blank(),axis.text = element_blank())+
#change background and gridlines
theme(panel.background=element_rect(fill=NA,colour="black"), panel.grid.major =
element_line(colour = NA), panel.grid.minor=element_line(colour=NA))
```

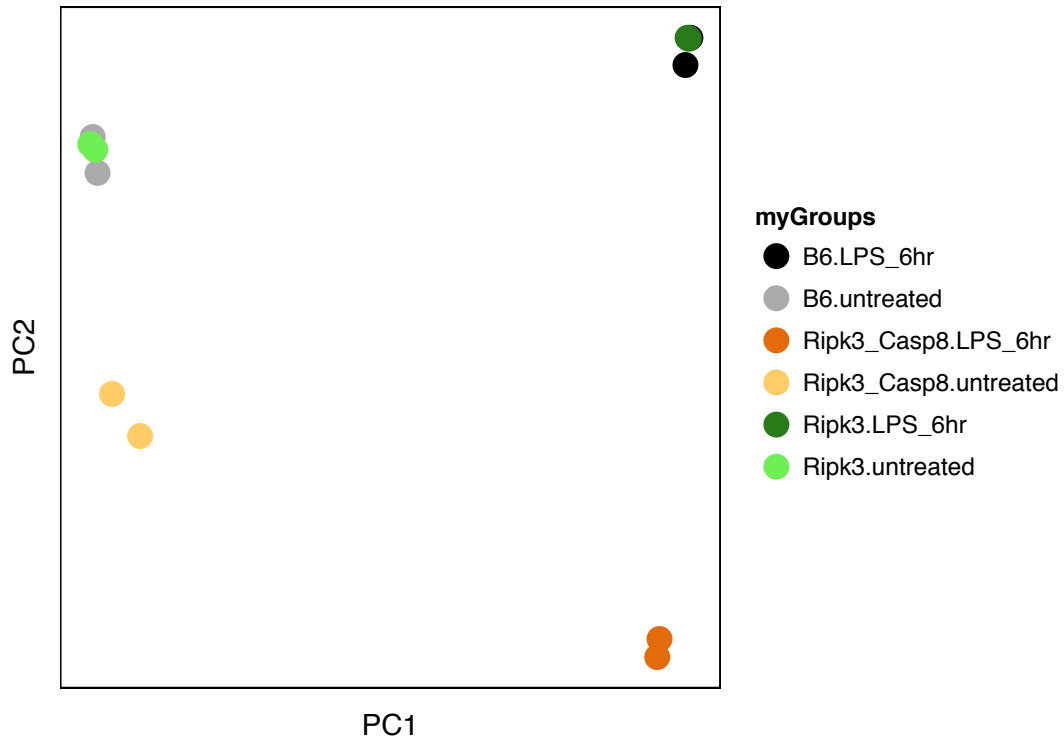


Figure 3: LPS-treatment contributes to the largest variation between samples (96%), where B6 and *Ripk3*<sup>-/-</sup> cluster together and are separated from the corresponding *Ripk3*<sup>-/-</sup>*Casp8*<sup>-/-</sup> samples.

## Identification of Differentially Expressed Genes

I fit a linear model to the data and set up contrast matrices of the analyses I'm interested in.

```
fit <- lmFit(myCollapsed, design)
# set up a contrast matrix comparing UT and LPS in B6 BMDMs = "LPS-responsive genes"
contrast.matrix.UT.LPS.B6 <- makeContrasts(B6UT.v.B6LPS=B6.LPS_6hr-B6.untreated,
levels=design)
# extract the linear model fit for the contrast matrix that you just defined above
fitsUT.LPS.B6 <- contrasts.fit(fit, contrast.matrix.UT.LPS.B6)
# get bayesian stats for your linear model fit
ebFitUT.LPS.B6 <- eBayes(fitsUT.LPS.B6)
```

Here, I pull out probeIDs from all genes in the Venn diagram and combine them with expression data into one file.



```

# use the 'decideTests' function to show Venn diagram for all diffexp genes
resultsUT.LPS.B6 <- decideTests(ebFitUT.LPS.B6, method="global",
                                adjust.method="BH", p.value=0.05, lfc=0.59)
diffProbesUT.LPS.B6 <- which(resultsUT.LPS.B6[,1] !=0)
myEset.ALL <- new("ExpressionSet", exprs = myCollapsed)
# retrieve expression data for the probes from above and export into excel table
diffDataUT.LPS.B6 <- myEset.ALL[resultsUT.LPS.B6[,1] !=0]
diffDataUT.LPS.B6 <- exprs(diffDataUT.LPS.B6)
write.table(cbind(diffProbesUT.LPS.B6, diffDataUT.LPS.B6),
             "DiffGenesUTvsLPSB6.xls", sep="\t", quote=FALSE)

```

Now, use LPS-responsive genes (diffDataUT.LPS.B6) as input gene list to determine which genes are caspase-8 and/or RIPK3-dependent.

```

fit <- lmFit(diffDataUT.LPS.B6, design)
# set up contrast matrices based on the pairwise comparisons of interest
contrast.matrix.LPS.ofB6LPSR3 <- makeContrasts(R3.v.B6=Ripk3.LPS_6hr-B6.LPS_6hr,
levels=design) contrast.matrix.LPS.ofB6LPSR3C8 <- makeContrasts(R3C8.v.R3=
Ripk3_Casp8.LPS_6hr-Ripk3.LPS_6hr,
R3C8.v.B6=Ripk3_Casp8.LPS_6hr-B6.LPS_6hr, levels=design)

# extract the linear model fit for the contrast matrix that you just defined above
fitsLPS.ofB6LPSR3 <- contrasts.fit(fit, contrast.matrix.LPS.ofB6LPSR3) fitsLPS.ofB6LPSR3C8 <- contrasts.fit(fit,
contrast.matrix.LPS.ofB6LPSR3C8)

# get bayesian stats for your linear model fit
ebFitLPS.ofB6LPSR3 <- eBayes(fitsLPS.ofB6LPSR3) ebFitLPS.ofB6LPSR3C8 <- eBayes(fitsLPS.ofB6LPSR3C8)

resultsLPS.ofB6LPSR3 <- decideTests(ebFitLPS.ofB6LPSR3, method="global",
adjust.method="BH", p.value=0.05, lfc=0.59) resultsLPS.ofB6LPSR3C8 <-
decideTests(ebFitLPS.ofB6LPSR3C8, method="global",
adjust.method="BH", p.value=0.05, lfc=0.59)

diffProbesLPS.ofB6LPSR3 <- which(resultsLPS.ofB6LPSR3[,1] !=0)
diffProbesLPS.ofB6LPSR3C8 <- which(resultsLPS.ofB6LPSR3C8[,1] !=0 |
resultsLPS.ofB6LPSR3C8[,2] !=0)

library(Biobase)
myEset.ALL <- new("ExpressionSet", exprs = diffDataUT.LPS.B6)

# retrieve expression data for the probes from above
diffData.LPS.ofB6LPSR3 <- myEset.ALL[diffProbesLPS.ofB6LPSR3,1] !=0]
diffData.LPS.ofB6LPSR3C8 <- myEset.ALL[diffProbesLPS.ofB6LPSR3C8[,1] !=0 |
diffProbesLPS.ofB6LPSR3C8[,2] !=0]

# pull the expression data back out of the eset object
diffData.LPS.ofB6LPSR3 <- exprs(diffData.LPS.ofB6LPSR3)
diffData.LPS.ofB6LPSR3C8 <- exprs(diffData.LPS.ofB6LPSR3C8)

```

```

#combineprobeIDs,genesymbolsandexpressiondatafordifferentiallyexpressedgenesintoone
file
# 62 genes of 6379 were RIPK3-dependent:
write.table(cbind(diffProbesLPS.ofB6LPSR3, diffData.LPS.ofB6LPSR3),
"DiffGenesLPSofB6.B6vsR3.xls", sep="\t", quote=FALSE)
# 527 genes of 6379 were RIPK3/caspase-8-dependent, 8.3%, Fig3C:
write.table(cbind(diffProbesLPS.ofB6LPSR3C8, diffData.LPS.ofB6LPSR3C8),
"DiffGenesLPSofB6.vsR3C8.xls", sep="\t", quote=FALSE)

```

Determine the overlap between RIPK3 and RIPK3/Caspase-8-dependent genes.

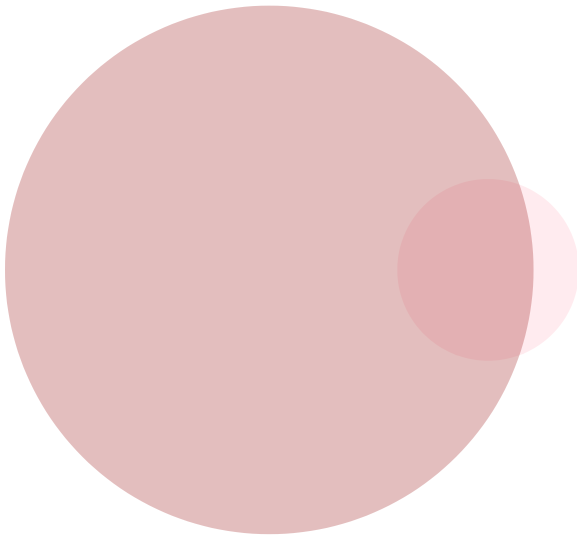
```

#load gene sets of interest. (diffData.LPS.ofB6LPSR3C8), (diffData.LPS.ofB6LPSR3)
R3C8.LPSgene.symbols <- row.names(diffData.LPS.ofB6LPSR3C8)
R3.LPSgene.symbols <- row.names(diffData.LPS.ofB6LPSR3)

#now determine shared genes between R3C8 LPS and R3 LPS treatment
LPS.sharedR3.R3C8 <- intersect(R3C8.LPSgene.symbols, R3.LPSgene.symbols)
LPS.R3C8only <- setdiff(R3C8.LPSgene.symbols, R3.LPSgene.symbols)
LPS.R3only <- setdiff(R3.LPSgene.symbols, R3C8.LPSgene.symbols)
# 48 shared genes
write.table(LPS.sharedR3.R3C8, "LPS.sharedbetweenR3.R3C8.xls", sep="\t",
quote=FALSE)
# 479 genes only RIPK3/caspase-8-dependent
write.table(LPS.R3C8only, "LPS.onlyR3C8notR3.xls", sep="\t", quote=FALSE)
# 14 genes only RIPK3-dependent
write.table(LPS.R3only, "LPS.onlyR3notR3C8.xls", sep="\t", quote=FALSE)

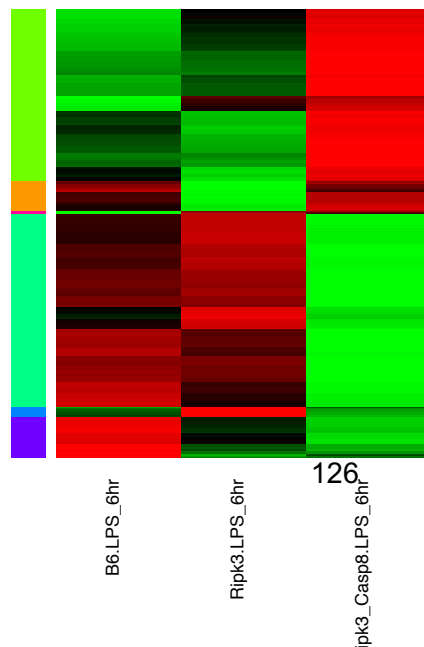
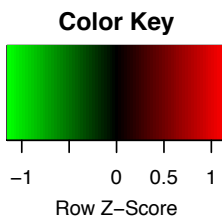
#plot venn diagram showing genes that are shared/unique. Where A=LPS only, B=UT
only
require(venneuler)
vLPSR3.R3C8 <- venneuler(c(A=14, B=479, "A&B"=48))
vLPSR3.R3C8$labels <- rep("", length(vLPSR3.R3C8$labels)) plot(vLPSR3.R3C8,
col=c("pink", "brown"))

```

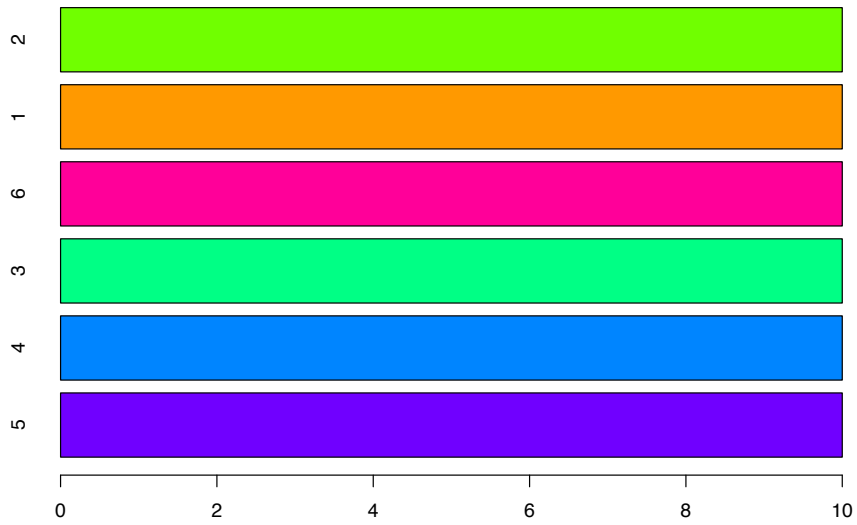


**Generate heatmap of caspase-8-dependent genes regulated by LPS treatment.**

```
mycl <- cutree(hr, k=6)
mycolhc <- rainbow(length(unique(mycl)), start=0.1, end=0.9)
mycolhc <- mycolhc[as.vector(mycl)]
myheatcol <- greenred(75)
heatmap.2(diffData.LPS.subset.AVG, Rowv=as.dendrogram(hr), Colv=NA,
          col=myheatcol, scale="row", labRow=NA,
          density.info="none", trace="none", RowSideColors=mycolhc,
          cexRow=1, cexCol=1, margins=c(12,25), key=T)
```



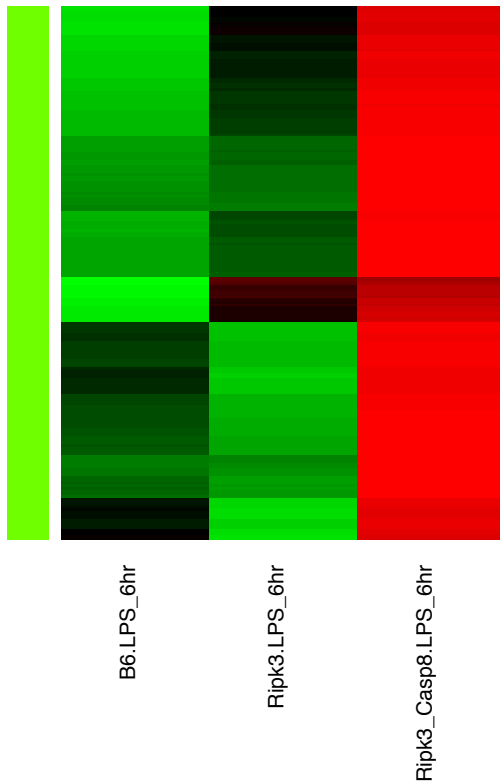
```
#now find out what your clusters are  
names(mycolhc) <- names(mycl)  
barplot(rep(10, max(mycl)),  
        col=unique(mycolhc[hr$labels[hr$order]]),  
        horiz=T, names=unique(mycl[hr$order]), margins=c(12,25))
```



```

#The numbers next to the color boxes correspond to the cluster numbers in
'mycl'.
#clusters 2,1,6,3,4,5 from top down for diffData.LPS.ofB6LPSR3C8.AVG
#select sub-clusters of co-regulated transcripts for downstream analysis
c(2)=cluster 1
clid <- c(2)
ysub <- diffData.LPS.subset.AVG[names(mycl[mycl%in%clid]),]
hrsub <- hclust(as.dist(1-cor(t(ysub), method="pearson")), method="average")
clusterIDs <- data.frame(Labels=rev(hrsub$labels[hrsub$order]))
clusterIDs <- as.vector(t(clusterIDs))
heatmap.2(ysub, Rowv=as.dendrogram(hrsub), Colv=NA, labRow=NA,
           col=myheatcol, scale="row", density.info="none",
           trace="none", RowSideColors=mycolhc[mycl%in%clid],
           margins=c(12,25), cexCol=1)

```

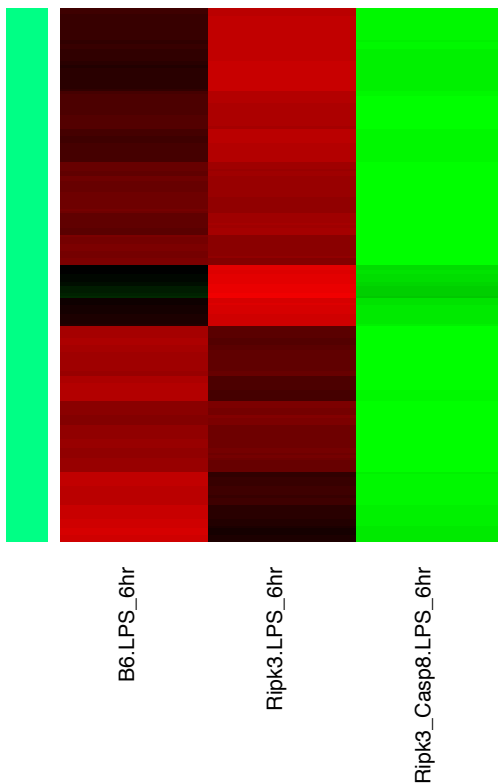


```

#retrieve gene symbols for selected cluster for downstream applications
(i.e. GO enrichment in DAVID)
write.table(clusterIDs,"LPSinducedR3C8.cluster1.xls",sep="t",quote=FALSE)

#select sub-clusters of co-regulated transcripts for downstream
analysis c(3)=cluster 2
clid <- c(3)
ysub <- diffData.LPS.subset.AVG[names(mycl[mycl%in%clid]),]
hrsub<-hclust(as.dist(1-cor(t(ysub),method="pearson")),method="average") clusterIDs<-
data.frame(Labels=rev(hrsub$labels[hrsub$order]))
clusterIDs <- as.vector(t(clusterIDs))
heatmap.2(ysub,Rowv=as.dendrogram(hrsub),Colv=NA,labRow=NA,col=myheatcol,
scale="row", density.info="none", trace="none", RowSideColors=mycolhc[mycl%in%clid],
margins=c(12,25),cexCol=1)

```



```
#retrieve gene symbols for selected cluster for downstream applications
(i.e. GO enrichment in DAVID)
write.table(clusterIDs, "LPSinducedR3C8.cluster2.xls", sep="t", quote=FALSE)
```

## Generate heatmap of subset of cluster 2.

```
#read in your data from a text file that contains genes symbols as rows,
and samples as columns.
#This file MUST be a dataframe, NOT a data matrix myDiffGenes.LPS<-
read.delim("LPS.Cluster2.txt",header=TRUE) head(myDiffGenes.LPS)
colnames(myDiffGenes.LPS)
#use the dplyr 'mutate' command to get averages and fold changes for all
your replicates
myDiffGenes.LPS <-mutate(myDiffGenes.LPS,
B6.untreated.AVG = (B6.untreated.1 + B6.untreated.2)/2, Ripk3.untreated.AVG=
(Ripk3.untreated.1+Ripk3.untreated.2)/2,
Ripk3_Casp8.untreated.AVG=(Ripk3_Casp8.untreated.1+Ripk3_Casp8.untreated.2)/2,
B6.LPS_6hr.AVG = (B6.LPS_6hr.1 + B6.LPS_6hr.2)/2,
Ripk3.LPS_6hr.AVG = (Ripk3.LPS_6hr.1 + Ripk3.LPS_6hr.2)/2, Ripk3_Casp8.LPS_6hr.AVG=
(Ripk3_Casp8.LPS_6hr.1+Ripk3_Casp8.LPS_6hr.2)/2,
LogFC.B6.LPS_6hr.vs.B6.untreated = (B6.LPS_6hr.AVG - B6.untreated.AVG),
LogFC.Ripk3.LPS_6hr.vs.Ripk3.untreated=(Ripk3.LPS_6hr.AVG-Ripk3.untreated.AVG),
LogFC.Ripk3_Casp8.LPS_6hr.vs.Ripk3_Casp8.untreated =
(Ripk3_Casp8.LPS_6hr.AVG - Ripk3_Casp8.untreated.AVG),
LogFC.Ripk3.LPS_6hr.vs.B6.LPS_6hr=(Ripk3.LPS_6hr.AVG-B6.LPS_6hr.AVG),
LogFC.Ripk3_Casp8.LPS_6hr.vs.Ripk3.LPS_6hr =
(Ripk3_Casp8.LPS_6hr.AVG - Ripk3.LPS_6hr.AVG),
LogFC.Ripk3_Casp8.LPS_6hr.vs.B6.LPS_6hr=(Ripk3_Casp8.LPS_6hr.AVG-B6.LPS_6hr.AVG),
LogFC.Ripk3_Casp8.untreated.vs.Ripk3.untreated =
(Ripk3_Casp8.untreated.AVG - Ripk3.untreated.AVG), LogFC.Ripk3.untreated.vs.B6.untreated
=(Ripk3.untreated.AVG-B6.untreated.AVG), LogFC.Ripk3_Casp8.untreated.vs.B6.untreated =
(Ripk3_Casp8.untreated.AVG - B6.untreated.AVG), FC.Ripk3_Casp8.LPS_6hr.vs.Ripk3.LPS_6hr=
(-2^(-LogFC.Ripk3_Casp8.LPS_6hr.vs.Ripk3.LPS_6hr)),
FC.Ripk3_Casp8.LPS_6hr.vs.Ripk3_Casp8.untreated =
(2^(LogFC.Ripk3_Casp8.LPS_6hr.vs.Ripk3_Casp8.untreated)),
FC.Ripk3.LPS_6hr.vs.Ripk3.untreated = (2^(LogFC.Ripk3.LPS_6hr.vs.Ripk3.untreated)))

head(myDiffGenes.LPS)
#use dplyr "arrange" and "select" functions to sort by LogFC column of
interest (arrange)
myDiffGenes.LPS <- myDiffGenes.LPS%>%
arrange(desc(LogFC.Ripk3_Casp8.LPS_6hr.vs.Ripk3.LPS_6hr)) head(myDiffGenes.LPS)
write.table(myDiffGenes.LPS, "myGOcluster2.xls", sep="t", quote=FALSE)

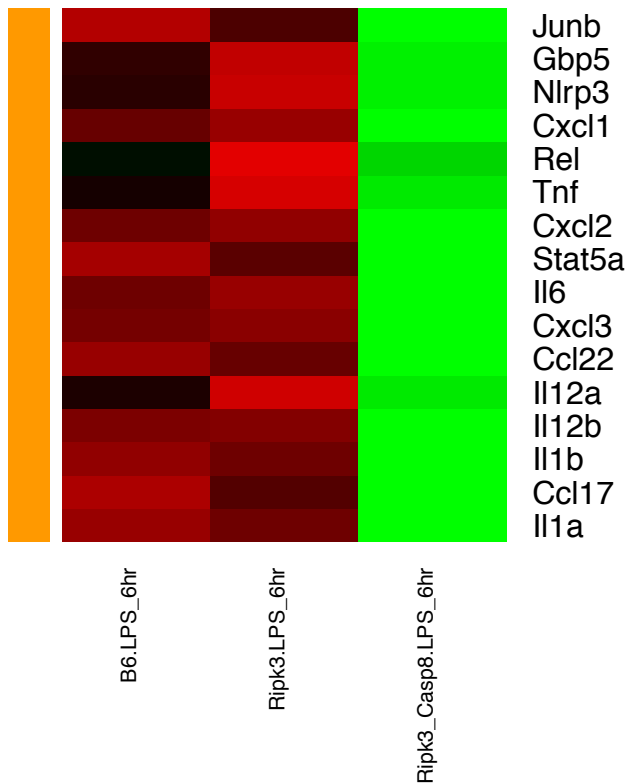
#Generate heatmap of Cluster2 subset
mySelectedHeatmap <- read.delim("LPS.Cluster2.heatmap.txt", sep="t", stringsAsFactors=
FALSE,header=TRUE,row.names=1)
head(mySelectedHeatmap) dim(mySelectedHeatmap) colnames(mySelectedHeatmap)<-
myGroups
```

```

mySelectedHeatmap.AVG<-avearrays(mySelectedHeatmap,
ID=colnames(mySelectedHeatmap))
head(mySelectedHeatmap.AVG) dim(mySelectedHeatmap.AVG)
mySelectedHeatmap.AVG <- mySelectedHeatmap.AVG[,c(4,5,6)] mySelectedHeatmap<-
as.matrix(mySelectedHeatmap.AVG)

hr <- hclust(as.dist(1-cor(t(mySelectedHeatmap), method="pearson")), method="average") hc <-
hclust(as.dist(1-cor(mySelectedHeatmap, method="spearman")), method="complete")
dim(mySelectedHeatmap)
mycl <- cutree(hr,k=1)
mycolhc <- rainbow(length(unique(mycl)), start=0.1, end=0.9) mycolhc <-
mycolhc[as.vector(mycl)]
myheatcol <- greenred(75)
#Rowv=NA maintains the order of the rows you have in your data table.
heatmap.2(mySelectedHeatmap,Rowv=NA,Colv=NA,col=myheatcol, scale="row",
density.info="none", trace="none", RowSideColors=mycolhc, labRow=NULL,
cexRow=1.5, cexCol=1, margins=c(12,25),key=T)

```





## All analyses were carried out on the following system:

```
sessionInfo()
```

```
R version 3.2.2 (2015-08-14) Platform: x86_64-apple-darwin13.4.0
(64-bit) Running under: OS X 10.10.5 (Yosemite)
locale: [1] en_US.UTF-8/en_US.UTF-8/en_US.UTF-8/C/en_US.UTF-
8/en_US.UTF-8 attached base packages: [1] stats4 parallel stats
graphics grDevices utils datasets [8] methods base other attached
packages: [1] venneuler_1.1-0 rJava_0.9-7
[3] devtools_1.9.1 knitr_1.12
[5] rmarkdown_0.9.2 gplots_2.17.0
[7] RColorBrewer_1.1-2 ggvis_0.4.2
[9] dplyr_0.4.3 reshape2_1.4.1
[11] ggplot2_1.0.1 WGCNA_1.48
[13] fastcluster_1.1.16 dynamicTreeCut_1.62
[15] org.Mm.eg.db_3.2.3 RSQLite_1.0.0
[17] DBI_0.3.1 AnnotationDbi_1.32.0
[19] ShortRead_1.28.0 GenomicAlignments_1.6.1
[21] SummarizedExperiment_1.0.1 Biobase_2.30.0
[23] Rsamtools_1.22.0 GenomicRanges_1.22.1
[25] GenomeInfoDb_1.6.1 Biostrings_2.38.2
[27] XVector_0.10.0 IRanges_2.4.5
[29] S4Vectors_0.8.4 BiocParallel_1.4.0
[31] BiocGenerics_0.16.1 edgeR_3.12.0
[33] limma_3.26.3 Rsubread_1.20.2
loaded via a namespace (and not attached):
[1] splines_3.2.2 foreach_1.4.3 gtools_3.5.0
[4] Formula_1.2-1 shiny_0.12.2 assertthat_0.1
[7] latticeExtra_0.6-26 yaml_2.1.13 impute_1.44.0
[10] lattice_0.20-33 digest_0.6.8 colorspace_1.2-6
[13] htmltools_0.2.6 httpuv_1.3.3 preprocessCore_1.32.0
[16] plyr_1.8.3 zlibbioc_1.16.0 xtable_1.8-0
[19] GO.db_3.2.2 scales_0.3.0 gdata_2.17.0
[22] lazyeval_0.1.10 nnet_7.3-11 proto_0.3-10
[25] survival_2.38-3 magrittr_1.5 mime_0.4
[28] memoise_0.2.1 evaluate_0.8 doParallel_1.0.10
[31] MASS_7.3-45 hwriter_1.3.2 foreign_0.8-66
[34] tools_3.2.2 formatR_1.2.1 matrixStats_0.15.0
[37] stringr_1.0.0 munsell_0.4.2 cluster_2.0.3
[40] lambda.r_1.1.7 caTools_1.17.1 futile.logger_1.4.1
[43] grid_3.2.2 iterators_1.0.8 labeling_0.3
[46] bitops_1.0-6 gtable_0.1.2 codetools_0.2-14
[49] R6_2.1.1 gridExtra_2.0.0 Hmisc_3.17-0
[52] futile.options_1.0.0 KernSmooth_2.23-15 stringi_1.0-1
[55] Rcpp_0.12.2 rpart_4.1-10 acepack_1.3-3.3
```

## VIII. BIBLIOGRAPHY

1. Philip NH & Brodsky IE (2012) Cell death programs in Yersinia immunity and pathogenesis. *Front Cell Infect Microbiol* 2:149.
2. Janeway CA, Jr. & Medzhitov R (2002) Innate immune recognition. *Annu Rev Immunol* 20:197-216.
3. Iwasaki A & Medzhitov R (2010) Regulation of adaptive immunity by the innate immune system. *Science* 327(5963):291-295.
4. Kagan JC & Barton GM (2015) Emerging principles governing signal transduction by pattern-recognition receptors. *Cold Spring Harb Perspect Biol* 7(3):a016253.
5. Kagan JC, *et al.* (2008) TRAM couples endocytosis of Toll-like receptor 4 to the induction of interferon-beta. *Nat Immunol* 9(4):361-368.
6. Lin SC, Lo YC, & Wu H (2010) Helical assembly in the MyD88-IRAK4-IRAK2 complex in TLR/IL-1R signalling. *Nature* 465(7300):885-890.
7. Motshwene PG, *et al.* (2009) An oligomeric signaling platform formed by the Toll-like receptor signal transducers MyD88 and IRAK-4. *J Biol Chem* 284(37):25404-25411.
8. Green DR, Ferguson T, Zitvogel L, & Kroemer G (2009) Immunogenic and tolerogenic cell death. *Nat Rev Immunol* 9(5):353-363.
9. Kono H & Rock KL (2008) How dying cells alert the immune system to danger. *Nat Rev Immunol* 8(4):279-289.
10. Kroemer G, Galluzzi L, Kepp O, & Zitvogel L (2013) Immunogenic cell death in cancer therapy. *Annu Rev Immunol* 31:51-72.
11. Zitvogel L, Kepp O, & Kroemer G (2010) Decoding cell death signals in inflammation and immunity. *Cell* 140(6):798-804.
12. Torchinsky MB, Garaude J, Martin AP, & Blander JM (2009) Innate immune recognition of infected apoptotic cells directs T(H)17 cell differentiation. *Nature* 458(7234):78-82.
13. Green DR & Llambi F (2015) Cell Death Signaling. *Cold Spring Harb Perspect Biol* 7(12).
14. Haase R, *et al.* (2003) A dominant role of Toll-like receptor 4 in the signaling of apoptosis in bacteria-faced macrophages. *J Immunol* 171(8):4294-4303.
15. Ruckdeschel K, *et al.* (2004) Signaling of apoptosis through TLRs critically involves toll/IL-1 receptor domain-containing adapter inducing IFN-beta, but not MyD88, in bacteria-infected murine macrophages. *J Immunol* 173(5):3320-3328.
16. Zhang Y & Bliska JB (2003) Role of Toll-like receptor signaling in the apoptotic response of macrophages to Yersinia infection. *Infect Immun* 71(3):1513-1519.
17. Kaiser WJ & Offermann MK (2005) Apoptosis induced by the toll-like receptor adaptor TRIF is dependent on its receptor interacting protein homotypic interaction motif. *J Immunol* 174(8):4942-4952.
18. Chan FK, Luz NF, & Moriwaki K (2015) Programmed necrosis in the cross talk of cell death and inflammation. *Annu Rev Immunol* 33:79-106.
19. Weinlich R & Green DR (2014) The two faces of receptor interacting protein kinase-1. *Mol Cell* 56(4):469-480.
20. Oberst A, *et al.* (2010) Inducible dimerization and inducible cleavage reveal a requirement for both processes in caspase-8 activation. *J Biol Chem* 285(22):16632-16642.

21. Kantari C & Walczak H (2011) Caspase-8 and bid: caught in the act between death receptors and mitochondria. *Biochim Biophys Acta* 1813(4):558-563.
22. Feoktistova M, *et al.* (2011) cIAPs block Ripoptosome formation, a RIP1/caspase-8 containing intracellular cell death complex differentially regulated by cFLIP isoforms. *Mol Cell* 43(3):449-463.
23. He S, Liang Y, Shao F, & Wang X (2011) Toll-like receptors activate programmed necrosis in macrophages through a receptor-interacting kinase-3-mediated pathway. *Proc Natl Acad Sci U S A* 108(50):20054-20059.
24. Kaiser WJ, *et al.* (2013) Toll-like receptor 3-mediated necrosis via TRIF, RIP3, and MLKL. *J Biol Chem* 288(43):31268-31279.
25. Kaiser WJ, *et al.* (2011) RIP3 mediates the embryonic lethality of caspase-8-deficient mice. *Nature* 471(7338):368-372.
26. Oberst A, *et al.* (2011) Catalytic activity of the caspase-8-FLIP(L) complex inhibits RIPK3-dependent necrosis. *Nature* 471(7338):363-367.
27. Yeh WC, *et al.* (1998) FADD: essential for embryo development and signaling from some, but not all, inducers of apoptosis. *Science* 279(5358):1954-1958.
28. Kang TB, *et al.* (2004) Caspase-8 serves both apoptotic and nonapoptotic roles. *J Immunol* 173(5):2976-2984.
29. Dillon CP, *et al.* (2014) RIPK1 blocks early postnatal lethality mediated by caspase-8 and RIPK3. *Cell* 157(5):1189-1202.
30. Gunther C, *et al.* (2011) Caspase-8 regulates TNF-alpha-induced epithelial necroptosis and terminal ileitis. *Nature* 477(7364):335-339.
31. Rickard JA, *et al.* (2014) RIPK1 regulates RIPK3-MLKL-driven systemic inflammation and emergency hematopoiesis. *Cell* 157(5):1175-1188.
32. Welz PS, *et al.* (2011) FADD prevents RIP3-mediated epithelial cell necrosis and chronic intestinal inflammation. *Nature* 477(7364):330-334.
33. Murphy JM, *et al.* (2013) The pseudokinase MLKL mediates necroptosis via a molecular switch mechanism. *Immunity* 39(3):443-453.
34. Sun L, *et al.* (2012) Mixed lineage kinase domain-like protein mediates necrosis signaling downstream of RIP3 kinase. *Cell* 148(1-2):213-227.
35. Wu J, *et al.* (2013) Mkl1 knockout mice demonstrate the indispensable role of Mkl1 in necroptosis. *Cell Res* 23(8):994-1006.
36. Dondelinger Y, *et al.* (2014) MLKL compromises plasma membrane integrity by binding to phosphatidylinositol phosphates. *Cell Rep* 7(4):971-981.
37. Quarato G, *et al.* (2016) Sequential Engagement of Distinct MLKL Phosphatidylinositol-Binding Sites Executes Necroptosis. *Mol Cell* 61(4):589-601.
38. Wang H, *et al.* (2014) Mixed lineage kinase domain-like protein MLKL causes necrotic membrane disruption upon phosphorylation by RIP3. *Mol Cell* 54(1):133-146.
39. Cai Z, *et al.* (2014) Plasma membrane translocation of trimerized MLKL protein is required for TNF-induced necroptosis. *Nat Cell Biol* 16(1):55-65.
40. Chen X, *et al.* (2014) Translocation of mixed lineage kinase domain-like protein to plasma membrane leads to necrotic cell death. *Cell Res* 24(1):105-121.
41. Lamkanfi M & Dixit VM (2014) Mechanisms and functions of inflammasomes. *Cell* 157(5):1013-1022.
42. Vanaja SK, Rathinam VA, & Fitzgerald KA (2015) Mechanisms of inflammasome activation: recent advances and novel insights. *Trends Cell Biol* 25(5):308-315.
43. Davis BK, Wen H, & Ting JP (2011) The inflammasome NLRs in immunity, inflammation, and associated diseases. *Annu Rev Immunol* 29:707-735.

44. Achoui Y, *et al.* (2013) Caspase-11 protects against bacteria that escape the vacuole. *Science* 339(6122):975-978.
45. Hornung V, *et al.* (2009) AIM2 recognizes cytosolic dsDNA and forms a caspase-1-activating inflammasome with ASC. *Nature* 458(7237):514-518.
46. Kayagaki N, *et al.* (2011) Non-canonical inflammasome activation targets caspase-11. *Nature* 479(7371):117-121.
47. Mariathasan S, *et al.* (2004) Differential activation of the inflammasome by caspase-1 adaptors ASC and Ipaf. *Nature* 430(6996):213-218.
48. Martinon F, Petrilli V, Mayor A, Tardivel A, & Tschopp J (2006) Gout-associated uric acid crystals activate the NALP3 inflammasome. *Nature* 440(7081):237-241.
49. Amer A, *et al.* (2006) Regulation of Legionella phagosome maturation and infection through flagellin and host Ipaf. *J Biol Chem* 281(46):35217-35223.
50. Franchi L, *et al.* (2006) Cytosolic flagellin requires Ipaf for activation of caspase-1 and interleukin 1beta in salmonella-infected macrophages. *Nat Immunol* 7(6):576-582.
51. Miao EA, *et al.* (2006) Cytoplasmic flagellin activates caspase-1 and secretion of interleukin 1beta via Ipaf. *Nat Immunol* 7(6):569-575.
52. Miao EA, *et al.* (2010) Innate immune detection of the type III secretion apparatus through the NLRC4 inflammasome. *Proc Natl Acad Sci U S A* 107(7):3076-3080.
53. Chavarria-Smith J & Vance RE (2015) The NLRP1 inflammasomes. *Immunol Rev* 265(1):22-34.
54. Boyden ED & Dietrich WF (2006) Nalp1b controls mouse macrophage susceptibility to anthrax lethal toxin. *Nat Genet* 38(2):240-244.
55. Zamboni DS & Lima-Junior DS (2015) Inflammasomes in host response to protozoan parasites. *Immunol Rev* 265(1):156-171.
56. Rathinam VA, *et al.* (2010) The AIM2 inflammasome is essential for host defense against cytosolic bacteria and DNA viruses. *Nat Immunol* 11(5):395-402.
57. Ataide MA, *et al.* (2014) Malaria-induced NLRP12/NLRP3-dependent caspase-1 activation mediates inflammation and hypersensitivity to bacterial superinfection. *PLoS Pathog* 10(1):e1003885.
58. Elinav E, *et al.* (2011) NLRP6 inflammasome regulates colonic microbial ecology and risk for colitis. *Cell* 145(5):745-757.
59. Normand S, *et al.* (2011) Nod-like receptor pyrin domain-containing protein 6 (NLRP6) controls epithelial self-renewal and colorectal carcinogenesis upon injury. *Proc Natl Acad Sci U S A* 108(23):9601-9606.
60. Vladimer GI, *et al.* (2012) The NLRP12 inflammasome recognizes Yersinia pestis. *Immunity* 37(1):96-107.
61. Wlodarska M, *et al.* (2014) NLRP6 inflammasome orchestrates the colonic host-microbial interface by regulating goblet cell mucus secretion. *Cell* 156(5):1045-1059.
62. Gurung P, *et al.* (2012) Toll or interleukin-1 receptor (TIR) domain-containing adaptor inducing interferon-beta (TRIF)-mediated caspase-11 protease production integrates Toll-like receptor 4 (TLR4) protein- and Nlrp3 inflammasome-mediated host defense against enteropathogens. *J Biol Chem* 287(41):34474-34483.
63. Wang S, *et al.* (1998) Murine caspase-11, an ICE-interacting protease, is essential for the activation of ICE. *Cell* 92(4):501-509.

64. Hagar JA, Powell DA, Aachoui Y, Ernst RK, & Miao EA (2013) Cytoplasmic LPS activates caspase-11: implications in TLR4-independent endotoxic shock. *Science* 341(6151):1250-1253.
65. Kayagaki N, *et al.* (2013) Noncanonical inflammasome activation by intracellular LPS independent of TLR4. *Science* 341(6151):1246-1249.
66. Broz P, *et al.* (2012) Caspase-11 increases susceptibility to Salmonella infection in the absence of caspase-1. *Nature* 490(7419):288-291.
67. Case CL, *et al.* (2013) Caspase-11 stimulates rapid flagellin-independent pyroptosis in response to Legionella pneumophila. *Proc Natl Acad Sci U S A* 110(5):1851-1856.
68. Casson CN, *et al.* (2013) Caspase-11 activation in response to bacterial secretion systems that access the host cytosol. *PLoS Pathog* 9(6):e1003400.
69. Rathinam VA, *et al.* (2012) TRIF licenses caspase-11-dependent NLRP3 inflammasome activation by gram-negative bacteria. *Cell* 150(3):606-619.
70. Coll NS, Epple P, & Dangl JL (2011) Programmed cell death in the plant immune system. *Cell Death Differ* 18(8):1247-1256.
71. Kepp O, *et al.* (2009) Disruption of the PP1/GADD34 complex induces calreticulin exposure. *Cell Cycle* 8(23):3971-3977.
72. Obeid M, *et al.* (2007) Calreticulin exposure dictates the immunogenicity of cancer cell death. *Nat Med* 13(1):54-61.
73. Ahrens S, *et al.* (2012) F-actin is an evolutionarily conserved damage-associated molecular pattern recognized by DNGR-1, a receptor for dead cells. *Immunity* 36(4):635-645.
74. Sancho D, *et al.* (2009) Identification of a dendritic cell receptor that couples sensing of necrosis to immunity. *Nature* 458(7240):899-903.
75. Apetoh L, *et al.* (2007) Toll-like receptor 4-dependent contribution of the immune system to anticancer chemotherapy and radiotherapy. *Nat Med* 13(9):1050-1059.
76. O'Connor W, Jr., *et al.* (2009) A protective function for interleukin 17A in T cell-mediated intestinal inflammation. *Nat Immunol* 10(6):603-609.
77. Sonnenberg GF, *et al.* (2010) Pathological versus protective functions of IL-22 in airway inflammation are regulated by IL-17A. *J Exp Med* 207(6):1293-1305.
78. Ye P, *et al.* (2001) Requirement of interleukin 17 receptor signaling for lung CXC chemokine and granulocyte colony-stimulating factor expression, neutrophil recruitment, and host defense. *J Exp Med* 194(4):519-527.
79. Miao EA, *et al.* (2010) Caspase-1-induced pyroptosis is an innate immune effector mechanism against intracellular bacteria. *Nat Immunol* 11(12):1136-1142.
80. Brydges SD, *et al.* (2013) Divergence of IL-1, IL-18, and cell death in NLRP3 inflammasomopathies. *J Clin Invest* 123(11):4695-4705.
81. Upton JW, Kaiser WJ, & Mocarski ES (2010) Virus inhibition of RIP3-dependent necrosis. *Cell Host Microbe* 7(4):302-313.
82. Inoue M, Williams KL, Gunn MD, & Shinohara ML (2012) NLRP3 inflammasome induces chemotactic immune cell migration to the CNS in experimental autoimmune encephalomyelitis. *Proc Natl Acad Sci U S A* 109(26):10480-10485.
83. Yatim N, *et al.* (2015) RIPK1 and NF-kappaB signaling in dying cells determines cross-priming of CD8(+) T cells. *Science* 350(6258):328-334.
84. Viboud G & Bliska JB (2005) Yersinia outer proteins: role in modulation of host cell signaling responses and pathogenesis. *Annu Rev Microbiol* 59:69-89.
85. Cornelis GR (2006) The type III secretion injectisome. *Nat Rev Microbiol* 4(11):811-825.

86. Mills SD, *et al.* (1997) *Yersinia enterocolitica* induces apoptosis in macrophages by a process requiring functional type III secretion and translocation mechanisms and involving YopP, presumably acting as an effector protein. *Proc Natl Acad Sci U S A* 94(23):12638-12643.
87. Monack DM, Meccas J, Ghori N, & Falkow S (1997) *Yersinia* signals macrophages to undergo apoptosis and YopJ is necessary for this cell death. *Proc Natl Acad Sci U S A* 94(19):10385-10390.
88. Ruckdeschel K, *et al.* (1998) *Yersinia enterocolitica* impairs activation of transcription factor NF-kappaB: involvement in the induction of programmed cell death and in the suppression of the macrophage tumor necrosis factor alpha production. *J Exp Med* 187(7):1069-1079.
89. Brodsky IE & Medzhitov R (2008) Reduced secretion of YopJ by *Yersinia* limits in vivo cell death but enhances bacterial virulence. *PLoS Pathog* 4(5):e1000067.
90. Ruckdeschel K, Richter K, Mannel O, & Heesemann J (2001) Arginine-143 of *Yersinia enterocolitica* YopP crucially determines isotype-related NF-kappaB suppression and apoptosis induction in macrophages. *Infect Immun* 69(12):7652-7662.
91. Zauberman A, *et al.* (2006) Interaction of *Yersinia pestis* with macrophages: limitations in YopJ-dependent apoptosis. *Infect Immun* 74(6):3239-3250.
92. Zheng Y, *et al.* (2011) A *Yersinia* effector with enhanced inhibitory activity on the NF-kappaB pathway activates the NLRP3/ASC/caspase-1 inflammasome in macrophages. *PLoS Pathog* 7(4):e1002026.
93. Bergsbaken T & Cookson BT (2007) Macrophage activation redirects yersinia-infected host cell death from apoptosis to caspase-1-dependent pyroptosis. *PLoS Pathog* 3(11):e161.
94. Ruckdeschel K, *et al.* (2001) *Yersinia* outer protein P of *Yersinia enterocolitica* simultaneously blocks the nuclear factor-kappa B pathway and exploits lipopolysaccharide signaling to trigger apoptosis in macrophages. *J Immunol* 166(3):1823-1831.
95. Ruckdeschel K, *et al.* (1997) Interaction of *Yersinia enterocolitica* with macrophages leads to macrophage cell death through apoptosis. *Infect Immun* 65(11):4813-4821.
96. Zheng Y, Lilo S, Mena P, & Bliska JB (2012) YopJ-induced caspase-1 activation in *Yersinia*-infected macrophages: independent of apoptosis, linked to necrosis, dispensable for innate host defense. *PLoS One* 7(4):e36019.
97. Monack DM, Meccas J, Bouley D, & Falkow S (1998) *Yersinia*-induced apoptosis in vivo aids in the establishment of a systemic infection of mice. *J Exp Med* 188(11):2127-2137.
98. Bergman MA, Loomis WP, Meccas J, Starnbach MN, & Isberg RR (2009) CD8(+) T cells restrict *Yersinia pseudotuberculosis* infection: bypass of anti-phagocytosis by targeting antigen-presenting cells. *PLoS Pathog* 5(9):e1000573.
99. Zauberman A, *et al.* (2009) *Yersinia pestis* endowed with increased cytotoxicity is avirulent in a bubonic plague model and induces rapid protection against pneumonic plague. *PLoS One* 4(6):e5938.
100. Grabenstein JP, Marceau M, Pujol C, Simonet M, & Bliska JB (2004) The response regulator PhoP of *Yersinia pseudotuberculosis* is important for replication in macrophages and for virulence. *Infect Immun* 72(9):4973-4984.
101. Heath WR & Carbone FR (2001) Cross-presentation, dendritic cells, tolerance and immunity. *Annu Rev Immunol* 19:47-64.

102. Orth K, *et al.* (2000) Disruption of signaling by Yersinia effector YopJ, a ubiquitin-like protein protease. *Science* 290(5496):1594-1597.
103. Palmer LE, Pancetti AR, Greenberg S, & Bliska JB (1999) YopJ of Yersinia spp. is sufficient to cause downregulation of multiple mitogen-activated protein kinases in eukaryotic cells. *Infect Immun* 67(2):708-716.
104. Sweet CR, Conlon J, Golenbock DT, Goguen J, & Silverman N (2007) YopJ targets TRAF proteins to inhibit TLR-mediated NF-kappaB, MAPK and IRF3 signal transduction. *Cell Microbiol* 9(11):2700-2715.
105. Zhou H, *et al.* (2005) Yersinia virulence factor YopJ acts as a deubiquitinase to inhibit NF-kappa B activation. *J Exp Med* 202(10):1327-1332.
106. Mittal R, Peak-Chew SY, & McMahon HT (2006) Acetylation of MEK2 and I kappa B kinase (IKK) activation loop residues by YopJ inhibits signaling. *Proc Natl Acad Sci U S A* 103(49):18574-18579.
107. Mukherjee S, *et al.* (2006) Yersinia YopJ acetylates and inhibits kinase activation by blocking phosphorylation. *Science* 312(5777):1211-1214.
108. Paquette N, *et al.* (2012) Serine/threonine acetylation of TGFbeta-activated kinase (TAK1) by Yersinia pestis YopJ inhibits innate immune signaling. *Proc Natl Acad Sci U S A* 109(31):12710-12715.
109. Zhang Y, Ting AT, Marcu KB, & Bliska JB (2005) Inhibition of MAPK and NF-kappa B pathways is necessary for rapid apoptosis in macrophages infected with Yersinia. *J Immunol* 174(12):7939-7949.
110. Grobner S, *et al.* (2007) Catalytically active Yersinia outer protein P induces cleavage of RIP and caspase-8 at the level of the DISC independently of death receptors in dendritic cells. *Apoptosis* 12(10):1813-1825.
111. Denecker G, *et al.* (2001) Yersinia enterocolitica YopP-induced apoptosis of macrophages involves the apoptotic signaling cascade upstream of bid. *J Biol Chem* 276(23):19706-19714.
112. Grobner S, *et al.* (2006) Yersinia YopP-induced apoptotic cell death in murine dendritic cells is partially independent from action of caspases and exhibits necrosis-like features. *Apoptosis* 11(11):1959-1968.
113. Vance RE, Isberg RR, & Portnoy DA (2009) Patterns of pathogenesis: discrimination of pathogenic and nonpathogenic microbes by the innate immune system. *Cell Host Microbe* 6(1):10-21.
114. Schroder K & Tschopp J (2010) The inflammasomes. *Cell* 140(6):821-832.
115. Brodsky IE, *et al.* (2010) A Yersinia effector protein promotes virulence by preventing inflammasome recognition of the type III secretion system. *Cell Host Microbe* 7(5):376-387.
116. Bauernfeind FG, *et al.* (2009) Cutting edge: NF-kappaB activating pattern recognition and cytokine receptors license NLRP3 inflammasome activation by regulating NLRP3 expression. *J Immunol* 183(2):787-791.
117. Ratner D, *et al.* (2016) Manipulation of IL-1beta and IL-18 production by Yersinia pestis effectors YopJ and YopM and redundant impact on virulence. *J Biol Chem*.
118. Schoberle TJ, Chung LK, McPhee JB, Bogin B, & Bliska JB (2016) Uncovering an Important Role for YopJ in the Inhibition of Caspase-1 in Activated Macrophages and Promoting Yersinia pseudotuberculosis Virulence. *Infect Immun*.
119. Chung LK, *et al.* (2014) IQGAP1 is important for activation of caspase-1 in macrophages and is targeted by Yersinia pestis type III effector YopM. *MBio* 5(4):e01402-01414.

120. LaRock CN & Cookson BT (2012) The Yersinia virulence effector YopM binds caspase-1 to arrest inflammasome assembly and processing. *Cell Host Microbe* 12(6):799-805.
121. Lilo S, Zheng Y, & Bliska JB (2008) Caspase-1 activation in macrophages infected with Yersinia pestis KIM requires the type III secretion system effector YopJ. *Infect Immun* 76(9):3911-3923.
122. Greten FR, *et al.* (2007) NF-kappaB is a negative regulator of IL-1beta secretion as revealed by genetic and pharmacological inhibition of IKKbeta. *Cell* 130(5):918-931.
123. Philip NH, *et al.* (2014) Caspase-8 mediates caspase-1 processing and innate immune defense in response to bacterial blockade of NF-kappaB and MAPK signaling. *Proc Natl Acad Sci U S A* 111(20):7385-7390.
124. Weng D, *et al.* (2014) Caspase-8 and RIP kinases regulate bacteria-induced innate immune responses and cell death. *Proc Natl Acad Sci U S A* 111(20):7391-7396.
125. Broz P, von Moltke J, Jones JW, Vance RE, & Monack DM (2010) Differential requirement for Caspase-1 autoproteolysis in pathogen-induced cell death and cytokine processing. *Cell Host Microbe* 8(6):471-483.
126. Sander LE, *et al.* (2011) Detection of prokaryotic mRNA signifies microbial viability and promotes immunity. *Nature* 474(7351):385-389.
127. Jung C, *et al.* (2012) Yersinia pseudotuberculosis disrupts intestinal barrier integrity through hematopoietic TLR-2 signaling. *J Clin Invest* 122(6):2239-2251.
128. Meinzer U, *et al.* (2012) Yersinia pseudotuberculosis effector YopJ subverts the Nod2/RICK/TAK1 pathway and activates caspase-1 to induce intestinal barrier dysfunction. *Cell Host Microbe* 11(4):337-351.
129. Lemaitre N, Sebbane F, Long D, & Hinnebusch BJ (2006) Yersinia pestis YopJ suppresses tumor necrosis factor alpha induction and contributes to apoptosis of immune cells in the lymph node but is not required for virulence in a rat model of bubonic plague. *Infect Immun* 74(9):5126-5131.
130. Lathem WW, Price PA, Miller VL, & Goldman WE (2007) A plasminogen-activating protease specifically controls the development of primary pneumonic plague. *Science* 315(5811):509-513.
131. Dessein R, *et al.* (2009) Toll-like receptor 2 is critical for induction of Reg3 beta expression and intestinal clearance of Yersinia pseudotuberculosis. *Gut* 58(6):771-776.
132. Dube PH, Revell PA, Chaplin DD, Lorenz RG, & Miller VL (2001) A role for IL-1 alpha in inducing pathologic inflammation during bacterial infection. *Proc Natl Acad Sci U S A* 98(19):10880-10885.
133. Cerretti DP, *et al.* (1992) Molecular cloning of the interleukin-1 beta converting enzyme. *Science* 256(5053):97-100.
134. Thornberry NA, *et al.* (1992) A novel heterodimeric cysteine protease is required for interleukin-1 beta processing in monocytes. *Nature* 356(6372):768-774.
135. Yuan J, Shaham S, Ledoux S, Ellis HM, & Horvitz HR (1993) The C. elegans cell death gene ced-3 encodes a protein similar to mammalian interleukin-1 beta-converting enzyme. *Cell* 75(4):641-652.
136. van Raam BJ & Salvesen GS (2012) Proliferative versus apoptotic functions of caspase-8 Hetero or homo: the caspase-8 dimer controls cell fate. *Biochim Biophys Acta* 1824(1):113-122.



137. Eckhart L, *et al.* (2008) Identification of novel mammalian caspases reveals an important role of gene loss in shaping the human caspase repertoire. *Mol Biol Evol* 25(5):831-841.
138. Wachmann K, *et al.* (2010) Activation and specificity of human caspase-10. *Biochemistry* 49(38):8307-8315.
139. Chang DW, Xing Z, Capacio VL, Peter ME, & Yang X (2003) Interdimer processing mechanism of procaspase-8 activation. *EMBO J* 22(16):4132-4142.
140. Hoffmann JC, Pappa A, Krammer PH, & Lavrik IN (2009) A new C-terminal cleavage product of procaspase-8, p30, defines an alternative pathway of procaspase-8 activation. *Mol Cell Biol* 29(16):4431-4440.
141. Boatright KM, *et al.* (2003) A unified model for apical caspase activation. *Mol Cell* 11(2):529-541.
142. Pop C, Fitzgerald P, Green DR, & Salvesen GS (2007) Role of proteolysis in caspase-8 activation and stabilization. *Biochemistry* 46(14):4398-4407.
143. Murphy BM, Creagh EM, & Martin SJ (2004) Interchain proteolysis, in the absence of a dimerization stimulus, can initiate apoptosis-associated caspase-8 activation. *J Biol Chem* 279(35):36916-36922.
144. Sohn D, Schulze-Osthoff K, & Janicke RU (2005) Caspase-8 can be activated by interchain proteolysis without receptor-triggered dimerization during drug-induced apoptosis. *J Biol Chem* 280(7):5267-5273.
145. Cowling V & Downward J (2002) Caspase-6 is the direct activator of caspase-8 in the cytochrome c-induced apoptosis pathway: absolute requirement for removal of caspase-6 prodomain. *Cell Death Differ* 9(10):1046-1056.
146. Medema JP, *et al.* (1997) Cleavage of FLICE (caspase-8) by granzyme B during cytotoxic T lymphocyte-induced apoptosis. *Eur J Immunol* 27(12):3492-3498.
147. Hughes MA, *et al.* (2009) Reconstitution of the death-inducing signaling complex reveals a substrate switch that determines CD95-mediated death or survival. *Mol Cell* 35(3):265-279.
148. Pop C, *et al.* (2011) FLIP(L) induces caspase 8 activity in the absence of interdomain caspase 8 cleavage and alters substrate specificity. *Biochem J* 433(3):447-457.
149. Bertin J, *et al.* (1997) Death effector domain-containing herpesvirus and poxvirus proteins inhibit both Fas- and TNFR1-induced apoptosis. *Proc Natl Acad Sci U S A* 94(4):1172-1176.
150. Goltsev YV, *et al.* (1997) CASH, a novel caspase homologue with death effector domains. *J Biol Chem* 272(32):19641-19644.
151. Han DK, *et al.* (1997) MRIT, a novel death-effector domain-containing protein, interacts with caspases and BclXL and initiates cell death. *Proc Natl Acad Sci U S A* 94(21):11333-11338.
152. Hu S, Vincenz C, Ni J, Gentz R, & Dixit VM (1997) I-FLICE, a novel inhibitor of tumor necrosis factor receptor-1- and CD-95-induced apoptosis. *J Biol Chem* 272(28):17255-17257.
153. Inohara N, Koseki T, Hu Y, Chen S, & Nunez G (1997) CLARP, a death effector domain-containing protein interacts with caspase-8 and regulates apoptosis. *Proc Natl Acad Sci U S A* 94(20):10717-10722.
154. Irmeler M, *et al.* (1997) Inhibition of death receptor signals by cellular FLIP. *Nature* 388(6638):190-195.
155. Rasper DM, *et al.* (1998) Cell death attenuation by 'Usurpin', a mammalian DED-caspase homologue that precludes caspase-8 recruitment and activation by the CD-95 (Fas, APO-1) receptor complex. *Cell Death Differ* 5(4):271-288.

156. Srinivasula SM, *et al.* (1997) FLAME-1, a novel FADD-like anti-apoptotic molecule that regulates Fas/TNFR1-induced apoptosis. *J Biol Chem* 272(30):18542-18545.
157. Thome M, *et al.* (1997) Viral FLICE-inhibitory proteins (FLIPs) prevent apoptosis induced by death receptors. *Nature* 386(6624):517-521.
158. Varfolomeev EE, *et al.* (1998) Targeted disruption of the mouse Caspase 8 gene ablates cell death induction by the TNF receptors, Fas/Apo1, and DR3 and is lethal prenatally. *Immunity* 9(2):267-276.
159. Yeh WC, *et al.* (2000) Requirement for Casper (c-FLIP) in regulation of death receptor-induced apoptosis and embryonic development. *Immunity* 12(6):633-642.
160. Dillon CP, *et al.* (2012) Survival function of the FADD-CASPASE-8-cFLIP(L) complex. *Cell Rep* 1(5):401-407.
161. Tschopp J, Thome M, Hofmann K, & Meink E (1998) The fight of viruses against apoptosis. *Curr Opin Genet Dev* 8(1):82-87.
162. Boatright KM, Deis C, Denault JB, Sutherlin DP, & Salvesen GS (2004) Activation of caspases-8 and -10 by FLIP(L). *Biochem J* 382(Pt 2):651-657.
163. Micheau O, *et al.* (2002) The long form of FLIP is an activator of caspase-8 at the Fas death-inducing signaling complex. *J Biol Chem* 277(47):45162-45171.
164. Yu JW, Jeffrey PD, & Shi Y (2009) Mechanism of procaspase-8 activation by c-FLIPL. *Proc Natl Acad Sci U S A* 106(20):8169-8174.
165. Stoven S, *et al.* (2003) Caspase-mediated processing of the Drosophila NF-kappaB factor Relish. *Proc Natl Acad Sci U S A* 100(10):5991-5996.
166. Dohrman A, *et al.* (2005) Cellular FLIP (long form) regulates CD8+ T cell activation through caspase-8-dependent NF-kappa B activation. *J Immunol* 174(9):5270-5278.
167. Golks A, Brenner D, Krammer PH, & Lavrik IN (2006) The c-FLIP-NH2 terminus (p22-FLIP) induces NF-kappaB activation. *J Exp Med* 203(5):1295-1305.
168. Kataoka T, *et al.* (2000) The caspase-8 inhibitor FLIP promotes activation of NF-kappaB and Erk signaling pathways. *Curr Biol* 10(11):640-648.
169. Koenig A, *et al.* (2014) The c-FLIPL cleavage product p43FLIP promotes activation of extracellular signal-regulated kinase (ERK), nuclear factor kappaB (NF-kappaB), and caspase-8 and T cell survival. *J Biol Chem* 289(2):1183-1191.
170. Lemmers B, *et al.* (2007) Essential role for caspase-8 in Toll-like receptors and NFkappaB signaling. *J Biol Chem* 282(10):7416-7423.
171. Rathore N, Matta H, & Chaudhary PM (2004) An evolutionary conserved pathway of nuclear factor-kappaB activation involving caspase-mediated cleavage and N-end rule pathway-mediated degradation of IkappaBalpha. *J Biol Chem* 279(38):39358-39365.
172. Su H, *et al.* (2005) Requirement for caspase-8 in NF-kappaB activation by antigen receptor. *Science* 307(5714):1465-1468.
173. Allam R, *et al.* (2014) Mitochondrial apoptosis is dispensable for NLRP3 inflammasome activation but non-apoptotic caspase-8 is required for inflammasome priming. *EMBO Rep* 15(9):982-990.
174. Beisner DR, Ch'en IL, Kolla RV, Hoffmann A, & Hedrick SM (2005) Cutting edge: innate immunity conferred by B cells is regulated by caspase-8. *J Immunol* 175(6):3469-3473.
175. Ch'en IL, *et al.* (2008) Antigen-mediated T cell expansion regulated by parallel pathways of death. *Proc Natl Acad Sci U S A* 105(45):17463-17468.

176. Carlile GW, Smith DH, & Wiedmann M (2004) Caspase-3 has a nonapoptotic function in erythroid maturation. *Blood* 103(11):4310-4316.
177. Fernando P, Kelly JF, Balazsi K, Slack RS, & Megeney LA (2002) Caspase 3 activity is required for skeletal muscle differentiation. *Proc Natl Acad Sci U S A* 99(17):11025-11030.
178. Oomman S, Strahlendorf H, Dertien J, & Strahlendorf J (2006) Bergmann glia utilize active caspase-3 for differentiation. *Brain Res* 1078(1):19-34.
179. Gurung P, *et al.* (2014) FADD and caspase-8 mediate priming and activation of the canonical and noncanonical Nlrp3 inflammasomes. *J Immunol* 192(4):1835-1846.
180. Man SM, *et al.* (2013) Salmonella infection induces recruitment of Caspase-8 to the inflammasome to modulate IL-1beta production. *J Immunol* 191(10):5239-5246.
181. Rajput A, *et al.* (2011) RIG-I RNA helicase activation of IRF3 transcription factor is negatively regulated by caspase-8-mediated cleavage of the RIP1 protein. *Immunity* 34(3):340-351.
182. Shenderov K, *et al.* (2014) Cutting edge: Endoplasmic reticulum stress licenses macrophages to produce mature IL-1beta in response to TLR4 stimulation through a caspase-8- and TRIF-dependent pathway. *J Immunol* 192(5):2029-2033.
183. Lakhani SA, *et al.* (2006) Caspases 3 and 7: key mediators of mitochondrial events of apoptosis. *Science* 311(5762):847-851.
184. Rongvaux A, *et al.* (2014) Apoptotic caspases prevent the induction of type I interferons by mitochondrial DNA. *Cell* 159(7):1563-1577.
185. Henao-Mejia J, *et al.* (2016) Generation of Genetically Modified Mice Using the CRISPR-Cas9 Genome-Editing System. *Cold Spring Harb Protoc* 2016(2):pdb prot090704.
186. Tapia K, *et al.* (2013) Defective viral genomes arising in vivo provide critical danger signals for the triggering of lung antiviral immunity. *PLoS Pathog* 9(10):e1003703.
187. Edmonson MN, *et al.* (2011) Bambino: a variant detector and alignment viewer for next-generation sequencing data in the SAM/BAM format. *Bioinformatics* 27(6):865-866.
188. Keane TM, *et al.* (2011) Mouse genomic variation and its effect on phenotypes and gene regulation. *Nature* 477(7364):289-294.
189. Zhang J, *et al.* (2012) The genetic basis of early T-cell precursor acute lymphoblastic leukaemia. *Nature* 481(7380):157-163.
190. Benavente CA, *et al.* (2013) Cross-species genomic and epigenomic landscape of retinoblastoma. *Oncotarget* 4(6):844-859.
191. Ghosn EE, *et al.* (2010) Two physically, functionally, and developmentally distinct peritoneal macrophage subsets. *Proc Natl Acad Sci U S A* 107(6):2568-2573.
192. Yount JS, Kraus TA, Horvath CM, Moran TM, & Lopez CB (2006) A novel role for viral-defective interfering particles in enhancing dendritic cell maturation. *J Immunol* 177(7):4503-4513.
193. Black DS & Bliska JB (1997) Identification of p130Cas as a substrate of Yersinia YopH (Yop51), a bacterial protein tyrosine phosphatase that translocates into mammalian cells and targets focal adhesions. *EMBO J* 16(10):2730-2744.
194. Simonet M & Falkow S (1992) Invasin expression in Yersinia pseudotuberculosis. *Infect Immun* 60(10):4414-4417.

195. Zhang Y, Murtha J, Roberts MA, Siegel RM, & Bliska JB (2008) Type III secretion decreases bacterial and host survival following phagocytosis of *Yersinia pseudotuberculosis* by macrophages. *Infect Immun* 76(9):4299-4310.
196. Portnoy DA, Wolf-Watz H, Bolin I, Beeder AB, & Falkow S (1984) Characterization of common virulence plasmids in *Yersinia* species and their role in the expression of outer membrane proteins. *Infect Immun* 43(1):108-114.
197. Hoiseth SK & Stocker BA (1981) Aromatic-dependent *Salmonella typhimurium* are non-virulent and effective as live vaccines. *Nature* 291(5812):238-239.
198. Blasi E, *et al.* (1985) Selective immortalization of murine macrophages from fresh bone marrow by a raf/myc recombinant murine retrovirus. *Nature* 318(6047):667-670.
199. Ramirez-Carrozzi VR, *et al.* (2009) A unifying model for the selective regulation of inducible transcription by CpG islands and nucleosome remodeling. *Cell* 138(1):114-128.
200. Sun Y, *et al.* (2015) Immunostimulatory Defective Viral Genomes from Respiratory Syncytial Virus Promote a Strong Innate Antiviral Response during Infection in Mice and Humans. *PLoS Pathog* 11(9):e1005122.
201. Shi W (2015) A Bioconductor R pipeline for analysis of RNA-seq data.
202. Liao Y, Smyth GK, & Shi W (2013) The Subread aligner: fast, accurate and scalable read mapping by seed-and-vote. *Nucleic Acids Res* 41(10):e108.
203. Liao Y, Smyth GK, & Shi W (2014) featureCounts: an efficient general purpose program for assigning sequence reads to genomic features. *Bioinformatics* 30(7):923-930.
204. Law CW, Chen Y, Shi W, & Smyth GK (2014) voom: Precision weights unlock linear model analysis tools for RNA-seq read counts. *Genome Biol* 15(2):R29.
205. Ritchie ME, *et al.* (2015) limma powers differential expression analyses for RNA-sequencing and microarray studies. *Nucleic Acids Res* 43(7):e47.
206. Huang da W, Sherman BT, & Lempicki RA (2009) Systematic and integrative analysis of large gene lists using DAVID bioinformatics resources. *Nat Protoc* 4(1):44-57.
207. Huang da W, Sherman BT, & Lempicki RA (2009) Bioinformatics enrichment tools: paths toward the comprehensive functional analysis of large gene lists. *Nucleic Acids Res* 37(1):1-13.
208. Mootha VK, *et al.* (2003) PGC-1 $\alpha$ -responsive genes involved in oxidative phosphorylation are coordinately downregulated in human diabetes. *Nat Genet* 34(3):267-273.
209. Subramanian A, *et al.* (2005) Gene set enrichment analysis: a knowledge-based approach for interpreting genome-wide expression profiles. *Proc Natl Acad Sci U S A* 102(43):15545-15550.
210. Medzhitov R (2007) Recognition of microorganisms and activation of the immune response. *Nature* 449(7164):819-826.
211. Broz P & Monack DM (2013) Newly described pattern recognition receptors team up against intracellular pathogens. *Nat Rev Immunol* 13(8):551-565.
212. Orth K, *et al.* (1999) Inhibition of the mitogen-activated protein kinase kinase superfamily by a *Yersinia* effector. *Science* 285(5435):1920-1923.
213. Palmer LE, Hobbie S, Galan JE, & Bliska JB (1998) YopJ of *Yersinia pseudotuberculosis* is required for the inhibition of macrophage TNF- $\alpha$  production and downregulation of the MAP kinases p38 and JNK. *Mol Microbiol* 27(5):953-965.

214. Muzio M, *et al.* (1996) FLICE, a novel FADD-homologous ICE/CED-3-like protease, is recruited to the CD95 (Fas/APO-1) death--inducing signaling complex. *Cell* 85(6):817-827.
215. Vandenabeele P, Declercq W, Van Herreweghe F, & Vanden Berghe T (2010) The role of the kinases RIP1 and RIP3 in TNF-induced necrosis. *Sci Signal* 3(115):re4.
216. Feoktistova M, Geserick P, Panayotova-Dimitrova D, & Leverkus M (2012) Pick your poison: the Ripoptosome, a cell death platform regulating apoptosis and necroptosis. *Cell Cycle* 11(3):460-467.
217. Green DR, Oberst A, Dillon CP, Weinlich R, & Salvesen GS (2011) RIPK-dependent necrosis and its regulation by caspases: a mystery in five acts. *Mol Cell* 44(1):9-16.
218. Degterev A, *et al.* (2008) Identification of RIP1 kinase as a specific cellular target of necrostatins. *Nat Chem Biol* 4(5):313-321.
219. Kang TB, Yang SH, Toth B, Kovalenko A, & Wallach D (2013) Caspase-8 blocks kinase RIPK3-mediated activation of the NLRP3 inflammasome. *Immunity* 38(1):27-40.
220. Vince JE, *et al.* (2012) Inhibitor of apoptosis proteins limit RIP3 kinase-dependent interleukin-1 activation. *Immunity* 36(2):215-227.
221. Antonopoulos C, El Sanadi C, Kaiser WJ, Mocarski ES, & Dubyak GR (2013) Proapoptotic chemotherapeutic drugs induce noncanonical processing and release of IL-1beta via caspase-8 in dendritic cells. *J Immunol* 191(9):4789-4803.
222. McPhee JB, Mena P, Zhang Y, & Bliska JB (2012) Interleukin-10 induction is an important virulence function of the *Yersinia pseudotuberculosis* type III effector YopM. *Infect Immun* 80(7):2519-2527.
223. Bossaller L, *et al.* (2012) Cutting edge: FAS (CD95) mediates noncanonical IL-1beta and IL-18 maturation via caspase-8 in an RIP3-independent manner. *J Immunol* 189(12):5508-5512.
224. Park JM, *et al.* (2005) Signaling pathways and genes that inhibit pathogen-induced macrophage apoptosis--CREB and NF-kappaB as key regulators. *Immunity* 23(3):319-329.
225. Chun HJ, *et al.* (2002) Pleiotropic defects in lymphocyte activation caused by caspase-8 mutations lead to human immunodeficiency. *Nature* 419(6905):395-399.
226. Su HC & Lenardo MJ (2008) Genetic defects of apoptosis and primary immunodeficiency. *Immunol Allergy Clin North Am* 28(2):329-351, ix.
227. Bolze A, *et al.* (2010) Whole-exome-sequencing-based discovery of human FADD deficiency. *Am J Hum Genet* 87(6):873-881.
228. Ch'en IL, Tsau JS, Molkentin JD, Komatsu M, & Hedrick SM (2011) Mechanisms of necroptosis in T cells. *J Exp Med* 208(4):633-641.
229. Dondelinger Y, *et al.* (2015) NF-kappaB-Independent Role of IKKalpha/IKKbeta in Preventing RIPK1 Kinase-Dependent Apoptotic and Necroptotic Cell Death during TNF Signaling. *Mol Cell* 60(1):63-76.
230. Salmena L, *et al.* (2003) Essential role for caspase 8 in T-cell homeostasis and T-cell-mediated immunity. *Genes Dev* 17(7):883-895.
231. Ramirez-Carrozzi VR, *et al.* (2006) Selective and antagonistic functions of SWI/SNF and Mi-2beta nucleosome remodeling complexes during an inflammatory response. *Genes Dev* 20(3):282-296.
232. Besnault-Mascard L, *et al.* (2005) Caspase-8 sumoylation is associated with nuclear localization. *Oncogene* 24(20):3268-3273.

233. Oberst A & Green DR (2011) It cuts both ways: reconciling the dual roles of caspase 8 in cell death and survival. *Nat Rev Mol Cell Biol* 12(11):757-763.
234. Kato H, *et al.* (2005) Cell type-specific involvement of RIG-I in antiviral response. *Immunity* 23(1):19-28.
235. Yount JS, Gitlin L, Moran TM, & Lopez CB (2008) MDA5 participates in the detection of paramyxovirus infection and is essential for the early activation of dendritic cells in response to Sendai Virus defective interfering particles. *J Immunol* 180(7):4910-4918.
236. Mandal P, *et al.* (2014) RIP3 induces apoptosis independent of pronecrotic kinase activity. *Mol Cell* 56(4):481-495.
237. Newton K, *et al.* (2014) Activity of protein kinase RIPK3 determines whether cells die by necroptosis or apoptosis. *Science* 343(6177):1357-1360.
238. Remijnen Q, *et al.* (2014) Depletion of RIPK3 or MLKL blocks TNF-driven necroptosis and switches towards a delayed RIPK1 kinase-dependent apoptosis. *Cell Death Dis* 5:e1004.
239. Donepudi M, Mac Sweeney A, Briand C, & Grutter MG (2003) Insights into the regulatory mechanism for caspase-8 activation. *Mol Cell* 11(2):543-549.
240. Zhang DW, *et al.* (2009) RIP3, an energy metabolism regulator that switches TNF-induced cell death from apoptosis to necrosis. *Science* 325(5938):332-336.
241. Wu YT, *et al.* (2011) zVAD-induced necroptosis in L929 cells depends on autocrine production of TNF $\alpha$  mediated by the PKC-MAPKs-AP-1 pathway. *Cell Death Differ* 18(1):26-37.
242. Kang TB, *et al.* (2008) Mutation of a self-processing site in caspase-8 compromises its apoptotic but not its nonapoptotic functions in bacterial artificial chromosome-transgenic mice. *J Immunol* 181(4):2522-2532.
243. Gringhuis SI, *et al.* (2012) Dectin-1 is an extracellular pathogen sensor for the induction and processing of IL-1 $\beta$  via a noncanonical caspase-8 inflammasome. *Nat Immunol* 13(3):246-254.
244. Maelfait J, *et al.* (2008) Stimulation of Toll-like receptor 3 and 4 induces interleukin-1 $\beta$  maturation by caspase-8. *J Exp Med* 205(9):1967-1973.
245. Moriwaki K, *et al.* (2014) The necroptosis adaptor RIPK3 promotes injury-induced cytokine expression and tissue repair. *Immunity* 41(4):567-578.
246. Cuda CM, *et al.* (2014) Caspase-8 acts as a molecular rheostat to limit RIPK1- and MyD88-mediated dendritic cell activation. *J Immunol* 192(12):5548-5560.
247. Cuda CM, *et al.* (2015) Conditional deletion of caspase-8 in macrophages alters macrophage activation in a RIPK-dependent manner. *Arthritis Res Ther* 17:291.
248. Nilsen NJ, *et al.* (2015) A role for the adaptor proteins TRAM and TRIF in toll-like receptor 2 signaling. *J Biol Chem* 290(6):3209-3222.
249. Wang L, Du F, & Wang X (2008) TNF- $\alpha$  induces two distinct caspase-8 activation pathways. *Cell* 133(4):693-703.
250. Feng S, *et al.* (2007) Cleavage of RIP3 inactivates its caspase-independent apoptosis pathway by removal of kinase domain. *Cell Signal* 19(10):2056-2067.
251. Kelliher MA, *et al.* (1998) The death domain kinase RIP mediates the TNF-induced NF- $\kappa$ B signal. *Immunity* 8(3):297-303.
252. Takahashi N, *et al.* (2014) RIPK1 ensures intestinal homeostasis by protecting the epithelium against apoptosis. *Nature* 513(7516):95-99.
253. Berger SB, *et al.* (2014) Cutting Edge: RIP1 kinase activity is dispensable for normal development but is a key regulator of inflammation in SHARPIN-deficient mice. *J Immunol* 192(12):5476-5480.

254. Weinlich R, *et al.* (2013) Protective roles for caspase-8 and cFLIP in adult homeostasis. *Cell Rep* 5(2):340-348.
255. Zhou Q, *et al.* (1997) Target protease specificity of the viral serpin CrmA. Analysis of five caspases. *J Biol Chem* 272(12):7797-7800.
256. Blagoev B, *et al.* (2003) A proteomics strategy to elucidate functional protein-protein interactions applied to EGF signaling. *Nat Biotechnol* 21(3):315-318.
257. Pop C & Salvesen GS (2009) Human caspases: activation, specificity, and regulation. *J Biol Chem* 284(33):21777-21781.
258. Timmer JC & Salvesen GS (2007) Caspase substrates. *Cell Death Differ* 14(1):66-72.
259. Xu G, *et al.* (2001) Covalent inhibition revealed by the crystal structure of the caspase-8/p35 complex. *Nature* 410(6827):494-497.
260. Qiao Y, *et al.* (2013) Synergistic activation of inflammatory cytokine genes by interferon-gamma-induced chromatin remodeling and toll-like receptor signaling. *Immunity* 39(3):454-469.
261. Buenrostro JD, Wu B, Chang HY, & Greenleaf WJ (2015) ATAC-seq: A Method for Assaying Chromatin Accessibility Genome-Wide. *Curr Protoc Mol Biol* 109:21 29 21-29.
262. Rao P, *et al.* (2010) IkappaBbeta acts to inhibit and activate gene expression during the inflammatory response. *Nature* 466(7310):1115-1119.
263. Kawadler H, Gantz MA, Riley JL, & Yang X (2008) The paracaspase MALT1 controls caspase-8 activation during lymphocyte proliferation. *Mol Cell* 31(3):415-421.
264. Chen NJ, *et al.* (2008) Beyond tumor necrosis factor receptor: TRADD signaling in toll-like receptors. *Proc Natl Acad Sci U S A* 105(34):12429-12434.
265. Smale ST & Natoli G (2014) Transcriptional control of inflammatory responses. *Cold Spring Harb Perspect Biol* 6(11):a016261.
266. Smale ST, Tarakhovsky A, & Natoli G (2014) Chromatin contributions to the regulation of innate immunity. *Annu Rev Immunol* 32:489-511.
267. Fontana MF, *et al.* (2015) Myeloid expression of the AP-1 transcription factor JUNB modulates outcomes of type 1 and type 2 parasitic infections. *Parasite Immunol* 37(9):470-478.
268. Fontana MF, *et al.* (2015) JUNB is a key transcriptional modulator of macrophage activation. *J Immunol* 194(1):177-186.
269. Albert R (2005) Scale-free networks in cell biology. *J Cell Sci* 118(Pt 21):4947-4957.
270. Brodsky IE & Medzhitov R (2009) Targeting of immune signalling networks by bacterial pathogens. *Nat Cell Biol* 11(5):521-526.